

Role of Spo13 in regulating meiotic chromosome segregation in yeast

Dissertation zur Erlangung des Doktorgrades der
Naturwissenschaften (Dr. rer. nat.)
an der Fakultät für Biologie der
Ludwig-Maximilians-Universität München



Vorgelegt von Julie ROJAS
Geboren am 22.06.1990 in Marseille, France
München 27. Mai, 2019

Eidesstattliche Erklärung

Hiermit erkläre ich an Eides statt, dass ich die vorliegende Dissertation selbstständig und ohne unerlaubte Hilfe angefertigt habe. Ich habe weder anderweitig versucht, eine Dissertation einzureichen oder eine Doktorprüfung durchzuführen, noch habe ich diese Dissertation oder Teile derselben einer anderen Prüfungskommission vorgelegt.

München, den 27. May, 2019

Julie Rojas (Unterschrift)

Promotionsgesuch eingereicht: 22.01.2019
Tag der mündlichen Prüfung: 24.05.2019
Erstgutachter: Prof. Dr. Barbara Conradt
Zweitgutachter: Prof. Dr. Peter Becker

Abstract

During the mitotic cell cycle, DNA replication and chromosome segregation strictly alternate in order to maintain a constant ploidy. Meiosis, on the other hand, is a special form of cell division that is characterized by a single round of DNA replication followed by two consecutive nuclear divisions. In order to understand how these two divisions are implemented, mutants that undergo a single meiotic division are of special interest. The *spo13* mutant undergoes a single nuclear division, during which it segregates a mixture of homologous chromosomes and sister chromatids. The Spo13 protein has been implicated in both the monopolar attachment of sister chromatids at meiosis I and the protection of centromeric cohesin until the second meiotic division. However, we showed that *SPO13* deletion cells were delayed in metaphase I by the spindle assembly checkpoint (SAC). In this work, we re-investigated the involvement of Spo13 for monopolar attachment and centromeric cohesin protection while taking into account the delay at metaphase I. We found that, while Spo13 is directly required for monopolar attachment, it is not directly involved in centromeric cohesin protection. Indeed, the premature loss of centromeric cohesin in *spo13Δ* cells is due to their delay in metaphase I, and shortening this delay restores centromeric cohesin protection. Furthermore, we found that Spo13, together with the polo-like kinase, prevents the activation of APC/C^{Ama1} in meiosis I by phosphorylating the B-type cyclin, Clb1. Spo13 is therefore required for coordinating the APC/C activity with meiosis I-specific events.

Contents

Eidesstattliche Erklärung	iii
Abstract	v
1 Introduction	1
1.1 Overview of the mitotic cell cycle	1
1.2 The cell cycle oscillator: Cdk1 against the APC/C	2
1.2.1 The timely synthesis and destruction of cyclins order cell cycle events	4
1.2.2 APC/C activation triggers the segregation of chromosomes and the exit from mitosis	4
1.3 The Spindle Assembly Checkpoint	5
1.3.1 The SAC sensory apparatus is located at kinetochores	6
1.3.2 Formation of a SAC effector	8
1.3.3 Chromosome passenger complex (CPC): the tension sensor of the SAC	9
1.4 Overview of the meiotic program	9
1.4.1 Meiosis in budding yeast	11
1.5 Bi-orientation of homologous chromosomes in meiosis I	11
1.5.1 The budding yeast monopolin complex	13
1.6 The chromosomes pairing machinery	13
1.6.1 Cohesin structure	14
1.6.2 Cohesin cleavage	15
1.6.3 The centromeric protection machinery	16
1.7 The M phase cyclins and APC/C regulation in meiosis	18
1.7.1 Cdc20 and Ama1 regulate APC/C activity in meiosis	18
1.7.2 How to make two successive waves of Cdk1 activity?	19
1.8 Spo13 is essential for the proper completion of meiosis	20
1.8.1 Spo13 is required for monopolar attachment	21
1.8.2 Spo13 has been linked to the maintenance of centromeric cohesin protection	22

1.8.3	How does Spo13 insure the completion of the two meiotic division?	22
1.8.4	Spo13 homologs: Moa1 and Meikin	23
2	Results	25
2.1	Metaphase I is prolonged in absence of Spo13	25
2.2	SAC activity delays anaphase onset in <i>spo13Δ</i>	27
2.2.1	A SAC activity assay for time-lapse microscopy	27
2.2.2	SAC activity in metaphase I is prolonged in the <i>spo13</i> mutant	31
2.2.3	Improving bi-orientation in <i>spo13Δ</i> cells partially rescues meiosis II	35
2.2.4	Bi-orientation of sister kinetochores in meiosis I does not trigger a strong SAC response	39
2.3	Characterization of the <i>spo13Δ mad2Δ</i> mutant	40
2.3.1	Spo13 is directly involved in monopolar attachment	42
2.3.2	<i>spo13Δ mad2Δ</i> strain does not display centromeric protection defect	42
2.3.3	Conclusion	52
2.4	Spo13 inhibits APC/ C^{Ama1} in metaphase I	55
2.4.1	Spo13 deletion enables Ama1 to induce nuclear division in the absence of Cdc20	55
2.4.2	The nuclear division in <i>spo13</i> mutant seems to be triggered by the two APC/C coactivator, Cdc20 and Ama1	55
2.4.3	The <i>CLB1</i> deletion also enables Ama1 to induce nuclear division in the absence of Cdc20	58
2.4.4	Clb1 directly interacts with Ama1, independently of the interaction of Ama1 with the APC/C	58
2.4.5	The Spo13-Cdc5 complex phosphorylates Clb1	60
2.4.6	Clb1 phosphorylation mapping	61
2.4.7	Clb1 non-phosphorylatable mutant fails to inhibit APC/ C^{Ama1}	63
3	Discussion	69
3.1	Spo13 is directly required for monopolar attachment but not for centromeric cohesin protection	70
3.2	<i>spo13</i> mutant's SAC response is triggered by a mixture of monopolar and bipolar attachment	74
3.3	The SAC-dependent metaphase I delay alone does not recapitulate <i>spo13Δ</i> phenotype	74
3.4	Spo13-Cdc5 and Clb1-Cdk1 inhibit APC/ C^{Ama1} in metaphase I . . .	75

3.5	Concluding remarks	79
4	Materials and Methods	81
4.1	Yeast Strains	81
4.1.1	Construction of plasmids and yeast strains	81
4.2	Meiotic time course	88
4.3	TCA extraction	89
4.4	Western Blotting and protein detection	89
4.5	Immuno-fluorescence	91
4.6	Immuno-precipitation	92
4.7	Affinity-enrichment mass spectrometry of Clb1-GFP	93
4.7.1	Large-scale meiotic culture	93
4.7.2	Immuno-precipitation for mass spectrometry	94
4.8	Mass spectrometry: protein enrichment and post transcriptional modifications analysis	96
4.8.1	Raw data processing	96
4.8.2	Data analysis	96
4.9	Live-cell imaging	98
4.9.1	Image acquisition	98
4.9.2	Data Analysis and figures	98
	Bibliography	101
	Contributions	121
	Acknowledgements	123

List of Figures

1	The mitotic cell cycle	3
2	M-phase cyclins-Cdk1 and APC/C activity in mitosis	6
3	Model of SAC and CPC mechanisms	7
4	The meiotic program	12
5	Reconstitution on the monopolin complex structure, adapted from Corbett et al. (Corbett and Harrison, 2012)	14
6	Structure of the cohesin complex and models of chromosomes binding, adapted from Nasmyth and Haering, 2009.	15
7	Model for a differential cohesin cleavage at anaphase I	17
8	Cdk1-Cyclin B and APC/C activity in meiosis	19
9	<i>spo13Δ</i> cells are delayed in metaphase I.	26
10	<i>spo13Δ</i> cells accumulates M-phase proteins normally but undergo a single nuclear division.	28
11	The <i>MAD2</i> deletion restores the entry into meiosis II in <i>spo13Δ</i> cells.	29
12	Formation of Mad2 foci depends on Mad1.	30
13	Mad2 foci persist longer in metaphase I in the absence of Spo11.	32
14	The phospho-mimic Rec8 mutant <i>rec8-18D</i> causes prolonged per- sistence of Mad2 at kinetochores in meiosis II.	33
15	Mad2 foci persist longer in <i>spo13Δ</i> than in wild-type cells.	34
16	Mad2 foci persist longer in monopolin mutants than in the wild-type.	36
17	The <i>MAM1</i> deletion partially rescues entry into meiosis II in <i>spo13Δ</i> cells.	37
18	<i>spo13Δ spo11Δ mam1Δ</i> cells fully rescue SPBs re-duplication.	38
19	Improving sister chromatids bi-orientation in <i>spo13Δ</i> cells reduces the timing of Mad2 clusters.	41
20	<i>spo13Δ mad2Δ</i> cells have a monopolar attachment defect.	43
21	Comparison of monopolar attachment defect in <i>spo13Δ mad2Δ</i> and <i>mam1Δ mad2Δ</i> cells.	44
22	<i>mam1Δ</i> cells bi-orient sister kinetochores in meiosis I.	45
23	Mam1-GFP does not localize to kinetochores in <i>spo13Δ mad2Δ</i> cells.	46

24	Shugoshin depletion rescues the first nuclear division in <i>spo13Δ spo11Δ mad2Δ</i> cells.	48
25	The <i>rec8-18D</i> mutation restores the first nuclear division in <i>spo13Δ spo11Δ mad2Δ</i> cells.	49
26	Rec8 is degraded in two steps in wild-type cells, <i>mad2Δ</i> and <i>spo13Δ mad2Δ</i> cells, while being degraded in a single step in the <i>spo13Δ</i> single mutant.	50
27	Rec8 is degraded in two steps in <i>spo13Δ mad2Δ</i> cells, whereas it is degraded in a single step in <i>CLB2p-SGO1 spo13Δ mad2Δ</i> cells.	51
28	Rts1 localization in <i>spo13Δ</i> and <i>spo13Δ mad2Δ</i> cells.	53
29	APC/C ^{Ama1} triggers a meiotic division in <i>spo13Δ SCC1p-CDC20</i>	56
30	Cdh1 does not trigger the APC/C activation in <i>spo13Δ SCC1p-CDC20</i>	57
31	APC/C activation in <i>spo13Δ</i> can be triggered by Cdc20 or Ama1.	59
32	Clb1 interacts with myc9-Ama1 and with Ama1-myc9.	60
33	Clb1 modification depends on Spo13 and Cdc5.	61
34	Cdc5-myc15 interacts with Clb1-ha3, this interaction is not affected by the deletion of <i>SPO13</i>	62
35	Several phosphorylation sites were identified in the N-terminus of <i>CLB1</i>	64
36	Clb1 phosphorylations are enriched in the wild-type compare to <i>spo13Δ</i> or Cdc5 depletion strains.	65
37	<i>clb1-6A clb2Δ</i> haploids are viable.	66
38	APC/C ^{Ama1} triggers a meiotic division in <i>clb1-6A SCC1p-CDC20</i>	67
39	Model for Spo13 function in meiosis I	80

List of Tables

1	<i>S. cerevisiae</i> SK1 strains used in this study	82
2	Antibodies specifications and incubation time.	90

List of Abbreviations

AE-MS	A ffinity E nrichment - M ass S pectrometry
APC/C	A naphase P romoting C omplex/ C yclosome
CENP-C	C ENtrome r e P rotein C
CPC	C hromosomal P assenger C omplex
DHJ	D ouble H olliday J unction
DNA	D eoxyribo N ucleic A cid
DSB	D ouble S trand B reak
FDR	F alse D iscovery R ate
GFP	G reen F luorescent P rotein
IF	I mmuno F luorescence
KMN	K NL-1/ M is12/ N dc80 complex
LC-MS/MS	L iquid C hromatography tandem M ass S pectrometry
LFQ	L abel F ree Q uantification
MCC	M itotic C heckpoint C omplex
OD	O ptical D ensity
PBD	P olo B ox D omain
RFP	R ed F luorescent P rotein
SAC	S pindle A ssembly C heckpoint
SDS	S odium D odecyl S ulfate
SPM	S Porulation M edia
TCA	T ri- C hloroacetic A cid
YEPA	Y east E xtract P eptone A Acetate
YPD	Y east extract P eptone D extrose
YPG	Y east extract P eptone G lycerol

To my family

1 Introduction

Most eukaryotic organisms can undergo two types of cell division: mitosis and meiosis. In mitotic cells, DNA replication is followed by a single round of chromosome segregation during which sister chromatids are pulled apart, generating two daughter cells which contain the same number of chromosomes as the mother cells (Figure 1). In contrast to mitosis, meiosis is characterized by a single round of DNA replication followed by two rounds of chromosomes segregation, thereby halving the number of chromosomes (Figure 4) (Petronczki et al., 2003). The meiotic program is essential for sexual reproduction. Indeed, without the capacity to halve the chromosome number, fertilization would result in doubling the number of chromosomes of zygotes in each generation. Error in chromosome segregation during meiosis causes aneuploidy that leads to spontaneous abortion or severe birth defects in humans (Hassold and Hunt, 2001). Hence, a better understanding of the meiotic program could help to improve human reproductive health. Meiosis requires both cell cycle regulators and meiosis-specific proteins that mediate processes that are unique to meiosis (Marston and Amon, 2004). Therefore, I will first describe the mitotic cell cycle before focusing on meiosis. Both parts will have a strong emphasis on the mechanisms found in budding yeast, many of which are evolutionarily conserved.

1.1. Overview of the mitotic cell cycle

Mitosis generates two genetically identical daughter cells containing the same number of chromosomes by alternating between DNA replication and chromosome segregation (Figure 1). As DNA is replicated, sister chromatids are linked together by ring-shaped complexes, called cohesins (Uhlmann and Nasmyth, 1998). Once replication is completed, cells enter metaphase during which sister chromatids are progressively captured by the microtubules of the mitotic spindle. The microtubules attach to chromatids through large protein complexes, called kinetochores, that assemble on centromeric DNA. The sister kinetochores of each chromatid pair attach microtubules emanating from opposite poles so that each daughter cell inherits one copy of each chromosome. Since sister chromatids are physically bound together, the attachment of sister chromatids to opposite poles

of the spindle creates tension, while attachment to the same spindle pole does not. This tension stabilizes microtubule-kinetochores attachments, while attachments that lack tension are quickly dissolved (Nicklas, 1997). Once all chromosomes are properly attached, cells enter anaphase: the cohesin complexes holding sister chromatids together are cleaved, allowing chromatids to segregate to opposite poles of the cell. The spindle is then disassembled and cells exit mitosis to enter the next G1 phase. As cells exit from mitosis, they undergo cytokinesis, forming two separate daughter cells with the same number of chromosomes (Lindon, 2008).

1.2. The cell cycle oscillator: Cdk1 against the APC/C

The cell cycle control system is composed of a series of biochemical switches that trigger cell cycle events in the correct order (Morgan, 2006). The central components of this system are the cyclin-dependent kinases (Cdks) and their regulators (Nasmyth, 1996). Cdks are proline-directed kinases that phosphorylate serine or threonine in S/T-P motifs (Langan et al., 1989; Shenoy et al., 1989). As cells progress through the cell cycle, rapid changes in the enzymatic activities of the Cdks leads to changes in the phosphorylation state of their substrates (reviewed in Bloom and Cross, 2007). These phosphorylations can either activate or inhibit the proteins targeted, thereby controlling several aspects of the cell cycle. The cell cycle can, therefore, be understood as an oscillator between high and low levels of Cdk activity (Nasmyth, 1996). Although higher eukaryotes possess several Cdks, the cell cycle of budding yeast is controlled by a single Cdk, Cdc28, which is the equivalent of Cdk1 in other organisms (reviewed in Bloom and Cross, 2007). For more clarity, we will use the denomination Cdk1 instead of Cdc28 throughout this work. The levels of Cdk1 remains constant through the cell cycle. Cells are, therefore, using several mechanisms to modulate Cdk1's enzymatic activity. As their name suggests, Cdk activity requires the binding of co-activators, named cyclins, that are essential for Cdk catalytic activity. As a result, the main level of control for Cdk1 activity is the regulation of the timely accumulation and destruction of different cyclins. Changes in cyclins gene synthesis and destruction by proteolysis is, therefore, central to the establishment of the cell cycle oscillator (Nasmyth, 1996).

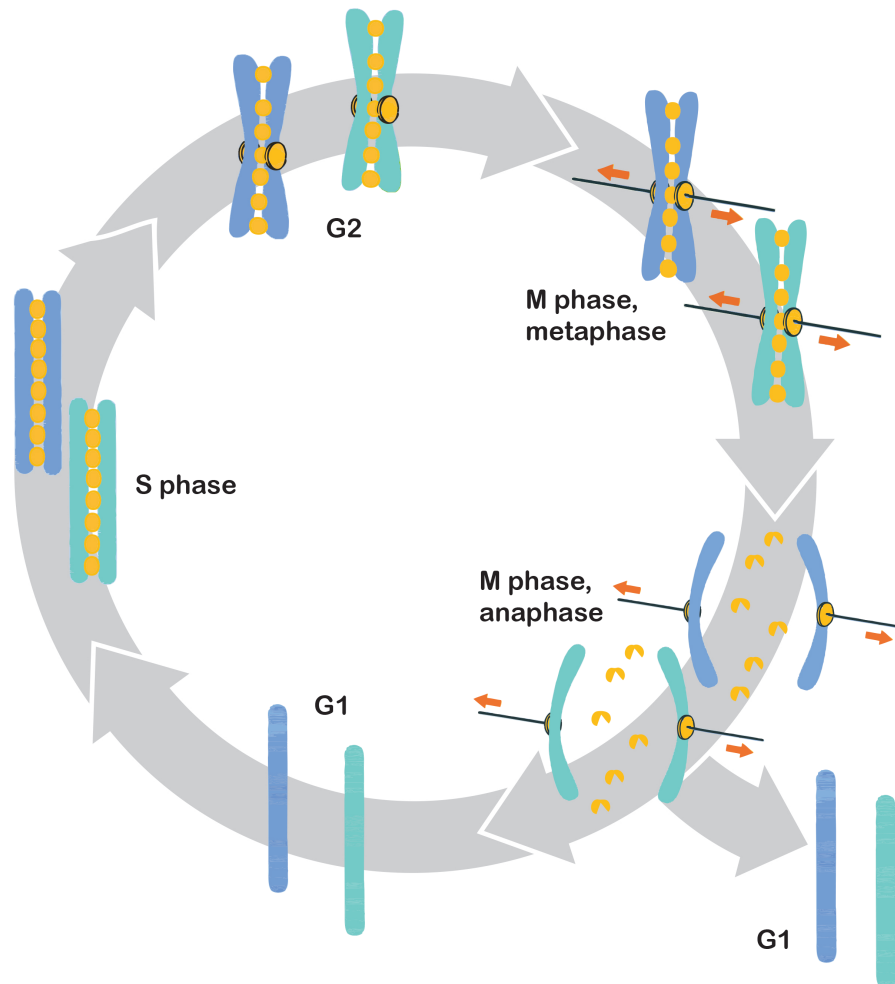


Figure 1: The mitotic cell cycle

Proliferating cells replicate their genomic DNA during S-phase, transforming each chromosome into two sister chromatids held together by cohesin complexes (yellow balls). As cells enter metaphase, sister kinetochores are attached to opposite poles of the spindle. When all kinetochores are attached and under tension, cells enter anaphase. The cohesin complexes are cleaved and sister chromatids segregate to opposite spindle poles. The resulting daughter cells have identical copies of the original genetic information and can enter a new cycle.

1.2.1. The timely synthesis and destruction of cyclins order cell cycle events

Several types of cyclins are expressed and destroyed at different stages of the cell cycle. Each cyclin type shows affinity for a different set of substrates and directs the Cdk1 kinase activity to different targets and cellular locations (reviewed in Bloom and Cross, 2007). Cyclins can be divided into four classes, based on their time of expression and on their functions. The G1 cyclins (Cln3 in yeast, cyclin D in vertebrates) coordinate cell growth with entry into a new cell cycle. The G1/S cyclins are expressed in late G1 and initiate the entry into the cell cycle and to start S-phase by alleviating the inhibition against S cyclins-Cdk activity. The S phase cyclins trigger DNA replication. The M-phase cyclins are Clb1, Clb2, Clb3 and Clb4 in budding yeast (cyclin B in vertebrates, Bloom and Cross, 2007). Their levels rise at metaphase onset and are targeted for degradation by the APC/C at the onset of anaphase I (Zachariae and Nasmyth, 1999). M phase cyclins roles are partially redundant and the deletion of a single cyclin has moderate effects on the cell cycle (Fitch et al., 1992). In mitosis, the main cyclin is Clb2. Indeed, Clb2 alone is able to compensate for the loss of all the other M cyclins and to direct cells through mitosis (Fitch et al., 1992). The cyclins B - Cdk1 complexes (Clbs-Cdk1) drive the assembly of the mitotic spindle and the bipolar attachment of sister chromatids. At anaphase onset, the ubiquitin-ligase, APC/C^{Cdc20}, triggers the degradation of M-phase proteins such as cyclins B and the polo-like kinase, Cdc5. Furthermore, to complete anaphase, Clbs-Cdk1 kinase activity must be turned off. At anaphase onset, the Cdc14 phosphatase is released from the nucleolus where it is held inactive for most of the cell cycle. Once released, it directly targets Clbs-Cdk1 substrates and de-phosphorylates them. Two pathways, the FEAR and the MEN networks, trigger the release of Cdc14 (Jaspersen et al., 1999; Visintin et al., 1998; Rock and Amon, 2009). These two pathways are indirectly activated by APC/C^{Cdc20}.

1.2.2. APC/C activation triggers the segregation of chromosomes and the exit from mitosis

The Anaphase-promoting complex/cyclosome (APC/C) is a large, multisubunit, ubiquitin-ligase that directs its substrates for degradation by the 26S proteasome through the addition of a polyubiquitin chain (Peters, 2006). Its activity must also be tightly regulated during the cell cycle (Figure 2). Similar to Cdk1, the levels of APC/C core components are constant through the cell cycle. Its activity is mostly

regulated by the availability of its co-activators. The mitotic cell cycle is regulated by two APC/C co-activators, Cdc20 and Cdh1, that dictate the substrate specificity and the timing of APC/C activation (Pesin and Orr-Weaver, 2008; Schwab et al., 1997; Visintin et al., 1997). Cdc20 is present during M-phase but is strongly inhibited by the spindle assembly checkpoint (SAC) until all chromosomes are correctly attached. Meanwhile, Clbs-Cdk1 prepares the onset of anaphase by phosphorylating the APC/C. Indeed, the modification of the APC/C mediated by Clbs-Cdk1 is crucial for its activity (Rudner and Murray, 2000; Rahal and Amon, 2008). Once cells are ready to segregate chromosomes, the SAC is silenced and the APC/C^{Cdc20} targets the separase inhibitor called securin (Pds1 in yeast), the mitotic cyclins and other M-phase proteins for degradation (Zachariae and Nasmyth, 1999). Therefore, APC/C^{Cdc20} causes the separation of sister chromatids, since the degradation of securin permits the separase protease to cleave the cohesin complexes that hold sister chromatids together (Uhlmann et al., 1999; Hauf et al., 2001; Uhlmann et al., 2000). APC/C^{Cdh1} activity is regulated by protein levels as well as phosphorylation of the Cdh1 activator (Pesin and Orr-Weaver, 2008). From S-phase to M-phase, S-phase cyclin and M-phase cyclins, together with Cdk1, phosphorylates Cdh1 to prevent its binding to the APC/C (Zachariae et al., 1998; Jaspersen et al., 1999). This system ensures the sequential activation of APC/C^{Cdc20} and APC/C^{Cdh1}. First, APC/C^{Cdc20} degrades the cyclins and promotes the release of the Cdc14 phosphatase. Cdc14 then removes the phosphorylations from Clbs-Cdk1, relieving the inhibitory phosphorylation on Cdh1 (Jaspersen et al., 1999; Visintin et al., 1998; Anghileri et al., 1999). APC/C^{Cdh1} finally triggers the exit from mitosis.

1.3. The Spindle Assembly Checkpoint

In mitosis, kinetochore-microtubule attachments are monitored by the spindle assembly checkpoint (SAC, Figure 3). The purpose of this checkpoint is to sense the presence of unattached kinetochores and to inhibit APC/C^{Cdc20} until all chromosomes have been properly attached (Musacchio and Hardwick, 2002; Hwang et al., 1998; Kim et al., 1998). An elegant set of experiments in vertebrate cells showed that the strength of the SAC inhibitory power depends on the number of unattached chromosomes and that a single unattached kinetochore is sufficient to delay anaphase onset (Rieder et al., 1994; Rieder et al., 1995). Hence, the SAC plays a crucial role in coordinating the proper attachment of chromosomes with the onset of anaphase. Although most studies on SAC regulation focused on mitosis, several studies performed in different model organisms suggest that the

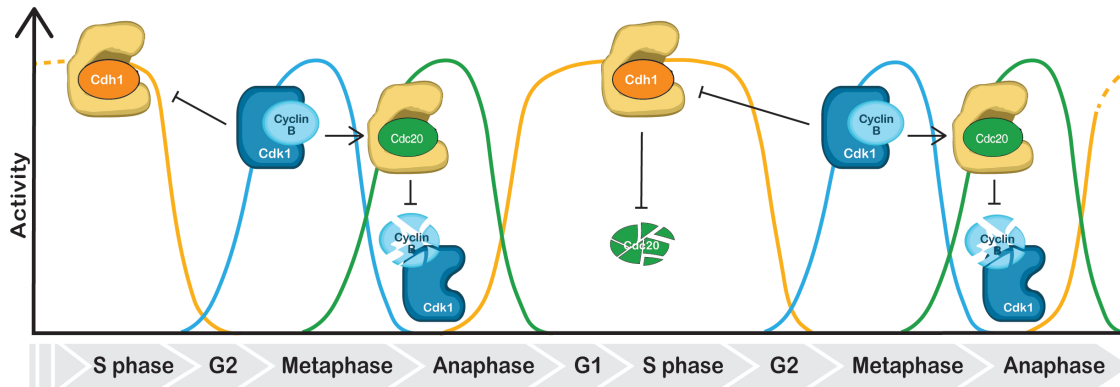


Figure 2: M-phase cyclins-Cdk1 and APC/C activity in mitosis

During G1, APC/C^{Cdh1} activity is high and prevent the accumulation of M-phase cyclin. As cells go to S-phase, the S-phase cyclins (not depicted), that are not susceptible to APC/C^{Cdh1} targeting for degradation, inhibits APC/C^{Cdh1}. Cyclins B start to accumulate as cells enter metaphase, creating a high Clbs-Cdk1 kinase activity phase. APC/C phosphorylation by Clbs-Cdk1 is required for the subsequent activation of the APC/C^{Cdc20}. Clbs-Cdk1 also phosphorylates Cdh1, thus keeping APC/C^{Cdh1} inactive through M-phase. At anaphase onset, APC/C^{Cdc20} triggers the degradation of cyclins B. Cdk1 is therefore inactivated, allowing the relieve of APC/C^{Cdh1} inhibition and, subsequently, the exit form M-phase and entry into G1 (Marston and Amon, 2004).

SAC plays a similar role in meiosis (Sun and Kim, 2011; Shonn et al., 2000). Yeast cells that undergo meiosis with a defective SAC are subjected to an abnormal level of chromosomes mis-segregation and, consequently, to low spore viability (Shonn et al., 2000). The SAC proteins were initially discovered in 1991, in budding yeast (*Saccharomyces cerevisiae*) by two genetic screens searching for mutants that would bypass the metaphase arrest triggered by poisons, such as nocodazole, causing the disassembly of the spindle (Hoyt et al., 1991; Li and Murray, 1991). The genes identified include: *MAD1*, *MAD2*, *MAD3* (for Mitotic Arrest Deficient) and *BUB1* and *BUB3* (for Budding Uninhibited by Benzimidazole). The components of the SAC are conserved among all eukaryotes. The Mps1 kinase and the Aurora B kinase (Ipl1 in budding yeast) were also identified as essential components of the checkpoint (Weiss and Winey, 1996; Hardwick et al., 1996; Biggins and Murray, 2001; Kallio et al., 2002; Ditchfield et al., 2003). Although Aurora B does not seem to trigger a SAC arrest in case of unattached kinetochores, it plays an essential role in correcting tensionless attachments (Biggins and Murray, 2001; Tanaka et al., 2002; Hauf et al., 2003).

1.3.1. The SAC sensory apparatus is located at kinetochores

At metaphase onset, the SAC proteins localize at kinetochores (Cleveland et al., 2003; Maiato et al., 2004). Aurora B recruits Mps1 to kinetochores (Vigneron et al.,

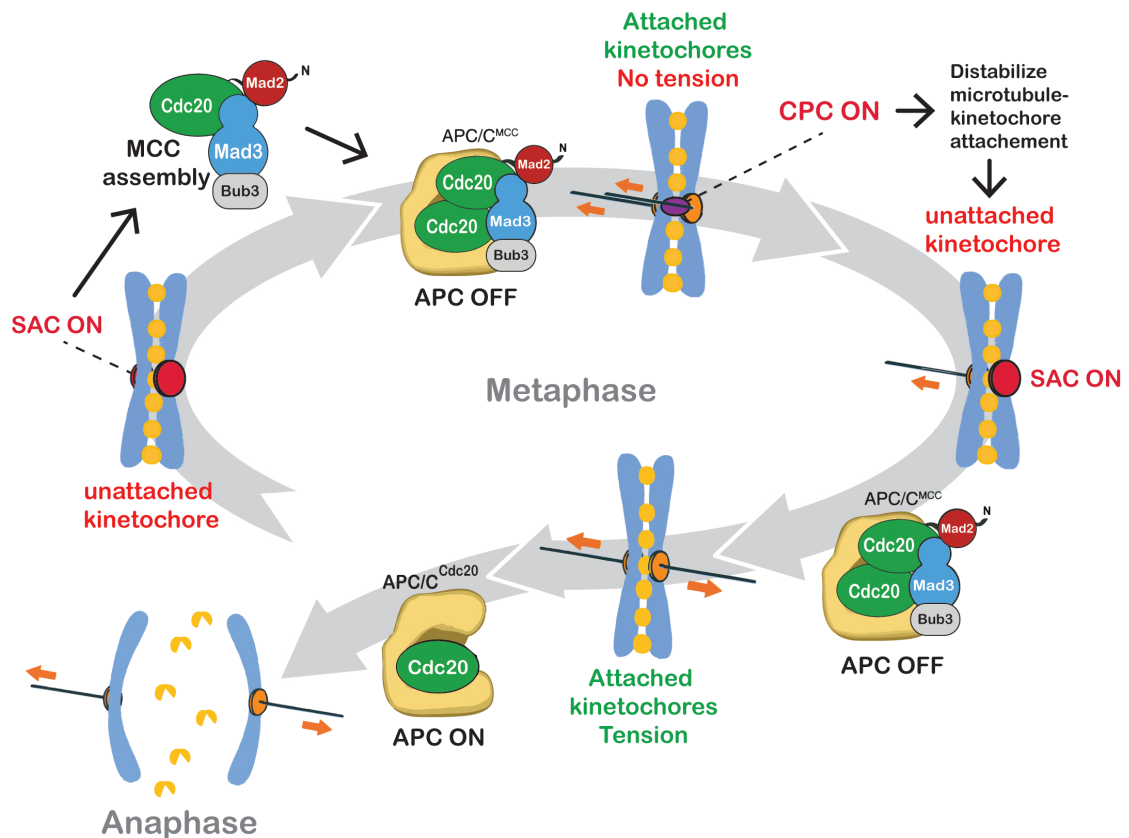


Figure 3: Model of SAC and CPC mechanisms

The SAC is present and active on unattached kinetochores and forms an APC/C inhibitor, the mitotic checkpoint complex (MCC), that inhibits the anaphase onset and arrests the cell in metaphase until all the chromosomes are properly attached. The chromosome passenger complex (CPC) senses the lack of tension and destabilizes the faulty microtubule-kinetochore attachment. Once all kinetochores are attached to microtubules and under tension, the SAC is silenced, allowing APC/C^{Cdc20} to trigger the onset of anaphase.

2004). Mps1 is then recruiting Mad1 that, in turn, binds to Mad2 (Abrieu et al., 2001; Chen et al., 1998). Certain SAC proteins, such as Bub1, Bub3, Mad1, Mad2 and Mad3 are removed from kinetochores upon attachment to microtubules (Chen et al., 1996; Waters et al., 1998; Skoufias et al., 2001; Abrieu et al., 2001; Campbell and Hardwick, 2003; Taylor et al., 2001). The removal of Mad1 and Mad2 from kinetochores, and therefore the inactivation of the SAC, depends on microtubule-kinetochore attachment and, most likely, on the tension generated, (Skoufias et al., 2001; Waters et al., 1998; Howell et al., 2001). The pool of SAC proteins concentrated at unattached kinetochores catalyses the formation of the SAC inhibitory complex, called the mitotic checkpoint complex (MCC), whose role is to maintain APC/C^{Cdc20} in an inactive state (reviewed in Musacchio and Salmon, 2007).

1.3.2. Formation of a SAC effector

The Mad2 protein can be found in two different conformations (Luo and Yu, 2008; Mapelli and Musacchio, 2007). The most abundant form is referred to as Open-Mad2 (O-Mad2) and corresponds to "free" Mad2 (De Antoni et al., 2005; Shah et al., 2004; Vink et al., 2006; Howell et al., 2004). When bound to Mad1, Mad2 adopts a conformation known as closed-Mad2 (C-Mad2). The Mad1:C-Mad2 complex acts as a catalyst for the conformational change of O-Mad2 to C-Mad2 and its subsequent binding to Cdc20 (Luo et al., 2002; Luo et al., 2004; Sironi et al., 2002). This mechanism for the formation of Cdc20:C-Mad2 complex is called the Mad2 template model (reviewed in Musacchio and Salmon, 2007). Although the dimerization of Cdc20 with Mad2 can occur without any catalyst, Mad1:C-Mad2 complexes at unattached kinetochores drastically increase the rate of the Mad2:Cdc20 dimerization and is believed to determine the rate of MCC assembly (Musacchio and Salmon, 2007; De Antoni et al., 2005; Simonetta et al., 2009). The recruitment of Mad3 and Bub3 to Mad2-C:Cdc20 forms a potent inhibitor of the APC/C^{Cdc20}, the MCC (Figure 3) (Musacchio and Salmon, 2007; Fang et al., 1998; Sudakin et al., 2001; Wassmann and Benezra, 1998; Hardwick et al., 2000). The MCC directly binds to the APC/C (Kallio et al., 1998; Wassmann and Benezra, 1998; Burton and Solomon, 2007; Braunstein et al., 2007; Sczaniecka et al., 2008). Structural studies show that the MCC:APC/C complex contains two Cdc20 subunits and locks the APC/C substrate-binding pocket in a "closed" state, thereby preventing the binding and ubiquitinylation of APC/C^{Cdc20} substrates (Herzog et al., 2009; Chang et al., 2014; Chang et al., 2015; Chao et al., 2012). Hence, the MCC inhibits the APC/C by acting as a pseudo-substrate (reviewed in Musacchio, 2015).

1.3.3. Chromosome passenger complex (CPC): the tension sensor of the SAC

Microtubule–kinetochore attachments that lack tension are destabilized, while attachments that generate tension between bi-orientated sister kinetochores are stabilized (Nicklas, 1997; Nicklas et al., 2001). The destabilization of erroneous microtubules-kinetochores attachments depends on the chromosome passenger complex (CPC, Figure 3) (Carmena et al., 2012; Hauf et al., 2003; Lampson et al., 2004; Tanaka et al., 2002). Once the CPC has severed the microtubule-kinetochore attachment, the SAC machinery produces MCC complexes to inhibit APC/C^{Cdc20}. The CPC is composed of the Aurora B kinase (Ip11 in *S. cerevisiae*) and of three regulatory and targeting components INCENP (Sli15 in *S. cerevisiae*), survivin (Bir1 in *S. cerevisiae*) and borealin (Nbl1 in *S. cerevisiae*) (Waal et al., 2012; Kelly and Funabiki, 2009; Ruchaud et al., 2007). The CPC localizes at kinetochores during early metaphase and re-localizes to spindles at anaphase (Carmena et al., 2012). Aurora B phosphorylates several substrates within the outer kinetochore to destabilize microtubule-kinetochore attachments that do not generate tension (Carmena et al., 2012; Welburn et al., 2010; Liu et al., 2010; DeLuca et al., 2011; Salimian et al., 2011). Microtubules bind to the kinetochore through an interaction with the KNL-1/Mis12/Ndc80 complex (KMN) network (Cheeseman et al., 2006). Aurora B controls the stability of the kinetochore-microtubule attachment by phosphorylating KMN subunits, such as Ndc80. De-phosphorylation of Aurora B substrates is required for stabilization of proper kinetochore-microtubule attachments. An attractive model proposes that tension-mediated stretching of centromeric chromatin shifts the Aurora B substrates away from the kinase at the inner centromere and towards the PP1 and PP2A phosphatases that are localized at the kinetochore (Carmena et al., 2012; Tanaka et al., 2002; Maresca and Salmon, 2010; Lampson and Cheeseman, 2011).

1.4. Overview of the meiotic program

Meiosis is characterized by a single round of DNA replication followed by two rounds of chromosomes segregation (Figure 4). Several meiosis-specific processes need to be implemented in order to faithfully segregate DNA for both meiotic divisions (Marston and Amon, 2004).

1. As mitosis, meiosis begins with the replication of DNA, during which cohesin complexes are loaded onto DNA to tether sister chromatids together. While

mitotic cells soon enter M-phase, meiotic cells enter a long prophase period during which meiotic recombination occurs. Recombination permits the exchange of DNA segments between paternal and maternal chromosomes, generating genetic diversity. More importantly, some of these recombination events result in crossovers that physically link homologous chromosomes. This feature is indispensable for the correct segregation of homologous chromosomes during the first meiotic division (Nicklas and Ward, 1994).

2. The first meiotic division is unique as homologous chromosomes are bi-oriented and segregated, while the second meiotic division resembles mitosis as chromatids are pulled apart (Petronczki et al., 2003). The bi-orientation of homologous chromosomes in meiosis I is referred to as monopolar attachment. To bi-orient homologs instead of chromatids in metaphase I, the two sister kinetochores have to face the same spindle pole. In yeast, monopolar attachment requires the loading of the monopolin complex onto kinetochores (Petronczki et al., 2003; Tóth et al., 2000). Monopolar attachment will be described in greater details later in this introduction. For now, it is important to highlight that both meiotic recombination and monopolar attachment are indispensable for the bi-orientation of homologous chromosomes in metaphase I.
3. The physical linkage of homologous chromosomes (in meiosis I) and of sister chromatids (in mitosis and meiosis II) is crucial for accurate chromosome segregation (Petronczki et al., 2003). In meiosis, both homologous chromosomes and sister chromatids are held together by cohesin. Therefore, unlike mitosis where all cohesins are cleaved at anaphase onset, in meiosis, cohesins are cleaved in two steps (Petronczki et al., 2003). At anaphase I onset, the cohesin complexes along chromosome arms are cleaved, allowing the resolution of crossovers and homologous chromosome segregation, while cohesin complexes loaded around centromeres are protected from cleavage (Petronczki et al., 2003). At anaphase II, centromeric cohesin is cleaved, enabling sister chromatid segregation. The step-wise loss of cohesins will be described further.
4. While mitotic cells strictly alternates between DNA replication and division, quickly exiting M-phase after anaphase onset, meiotic cells successively carry out two nuclear divisions. This means that after undergoing the first wave of APC/C^{Cdc20} activity, instead of exiting from meiosis, cells quickly re-establish a high level of Cdk1-cyclin B activity to assemble meiosis II spindles (metaphase II) and, later, activate APC/C^{Cdc20} once again to trigger the second meiotic division (anaphase II, Figure 8) (Marston and Amon, 2004).

How meiotic cells perform these two waves of Cdk1 kinase activity that are timely opposed by two waves of APC/C^{Cdc20} activity remains unclear and will be discussed in details later.

1.4.1. Meiosis in budding yeast

In vertebrates, cells undergo meiosis only in a very small subset of germ line cells, making the study of meiosis challenging. The budding yeast, *Saccharomyces cerevisiae* can be found both in haploid and diploid form. Although, in its natural environment, budding yeast favours diploidy. Diploid yeast cells undergo mitosis in normal conditions but can, when deprived of carbon and nitrogen sources, switch to the meiotic program and produce sexual-bearing cells, called asci and containing 4 haploid cells (Roeder, 1995). These haploid cells are protected by a thick cell wall and are called spores. This simple model is ideal for the study of both mitosis and meiosis. Indeed, baker's yeast is extremely well characterized as it has been used as a classical model for studying cellular events and is particularly advantageous due to its ease of manipulation and the variety of genetic and biochemical tools that are available.

1.5. Bi-orientation of homologous chromosomes in meiosis I

In order to segregate homologous chromosomes at meiosis I, sister kinetochores need to attach to microtubules from the same pole (Figure 4). This is called mono-orientation and it allows kinetochores from maternal and paternal chromosomes to attach to microtubules from opposite poles (Östergren, 1951). The first evidence of a special configuration of kinetochores in meiosis I compared with meiosis II or mitosis was obtained through electron microscopy in *Drosophila melanogaster* spermatocytes (Goldstein, 1981). Goldstein observed structures that clamp sister kinetochores together in meiosis I and proposed that sister kinetochores might be fused into one (Goldstein, 1981). Recent work in maize meiocytes found that two outer kinetochore proteins, Mis12 and Ndc80, cross-link sister kinetochores together in meiosis I (Li and Dawe, 2009). To this day, molecular insights into the monopolar attachment machinery comes almost exclusively from budding yeast and fission yeast.

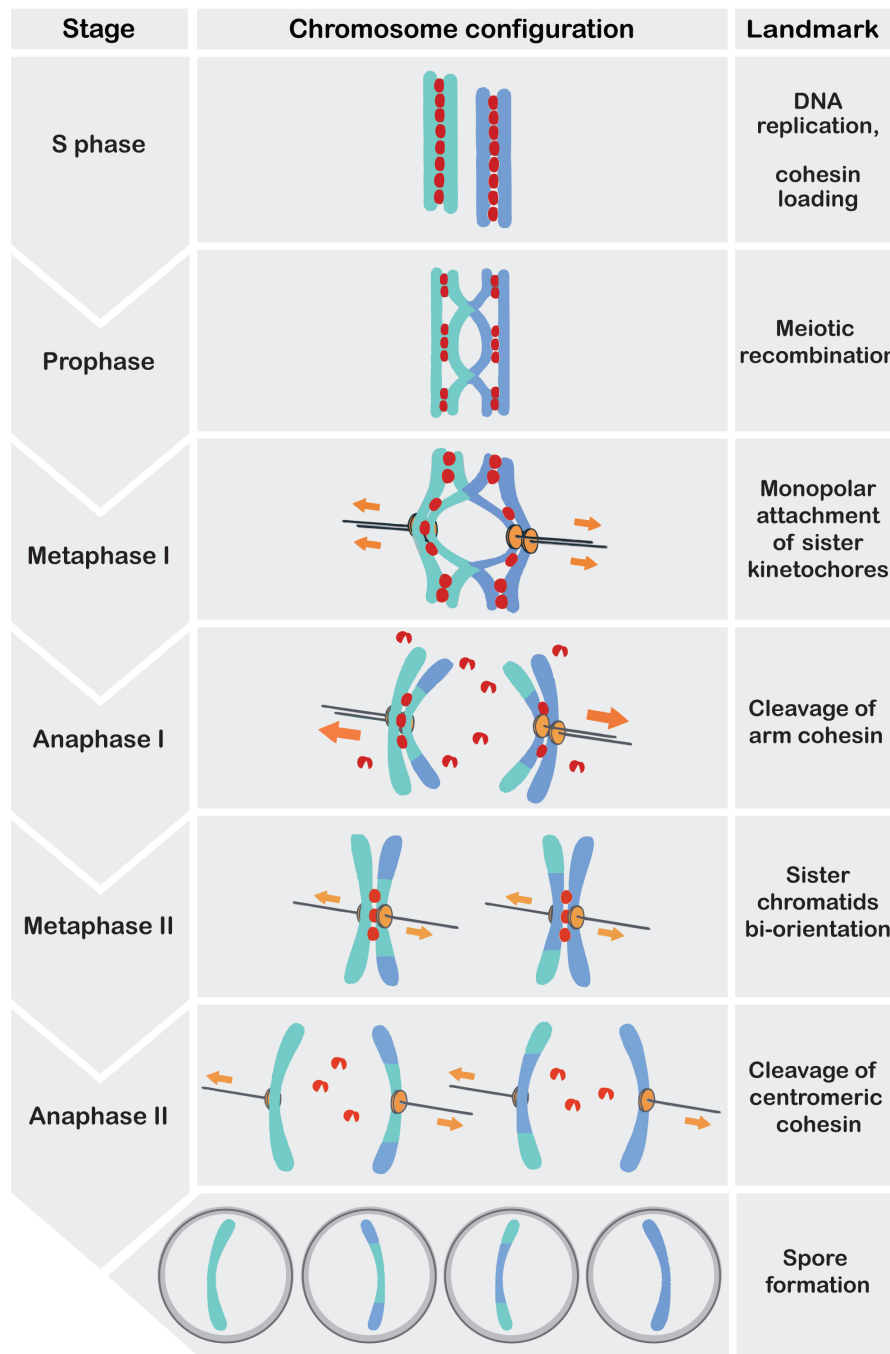


Figure 4: The meiotic program

DNA replication turns each chromosome into a pair sister chromatids held together by meiotic cohesins (red balls). Homologous chromosomes are linked together by the formation of crossovers during the long meiotic prophase. At metaphase I onset, homologous chromosomes are attached to opposite poles of the spindle. Once all chromosomes are properly connected to the spindle, cells enter anaphase I where cohesins present on chromosome arms are cleaved, allowing the resolution of crossovers and the segregation of homologous chromosomes. The cohesin present at centromeres is protected from cleavage in order to maintain sister chromatids cohesion until the second meiotic division. In metaphase II, sister kinetochores are attached to the opposite poles of the spindle and pulled apart at anaphase II after the cleavage of centromeric cohesins.

1.5.1. The budding yeast monopolin complex

In budding yeast, mono-orientation in meiosis I depends on the assembly of the monopolin complex onto kinetochores. This complex is formed by the meiosis I-specific protein Mam1, two nucleolar proteins Csm1 and Lrs4, and the conserved casein kinase 1 δ/ϵ , Hrr25 (Figure 5). Toth et al. identified Mam1 as the first protein required for monopolar attachment in budding yeast (Tóth et al., 2000). They found that Mam1 localizes to kinetochores solely in meiosis I and that its deletion triggers the premature bi-orientation of sister chromatids during metaphase I (Tóth et al., 2000). Importantly, *mam1* Δ mutant is not defective in the protection of centromeric cohesin, consequently *mam1* Δ cells fail to divide at anaphase I and undergo a single nuclear division in anaphase II. Unlike Mam1, Csm1 and Lrs4 are not meiosis-specific but are kept within the nucleolus for most of the cell cycle where they participate in rDNA silencing (Rabitsch et al., 2003). The monopolin complex is recruited to kinetochore's MIND complex through an interaction between Csm1 and Dsn1 (Sarkar et al., 2013; Ye et al., 2016). Lrs4 and Csm1 are released from the nucleolus upon accumulation of Cdc5 at metaphase I onset (Clyne et al., 2003; Lee and Amon, 2003). Mam1 fails to localize to kinetochore when Lrs4 and Csm1 are not released from the nucleolus indicating that the assembly of the monopolin complex on kinetochores depends on these two proteins (Clyne et al., 2003; Lee and Amon, 2003). Finally, Petronczki et al. found that Hrr25 is also part of the monopolin complex (Petronczki et al., 2006). Hrr25 kinase activity was shown to be required for monopolar attachment in meiosis I (Petronczki et al., 2006). However, the Hrr25 substrates whose phosphorylation is essential for mono-orientation are yet to be identified. The authors pointed out that Mam1 modifications depend on Hrr25 kinase activity and suggested that it might help to stabilize the monopolin complex (Petronczki et al., 2006).

1.6. The chromosomes pairing machinery

As stated earlier, the physical attachment of homologous chromosomes and sister chromatids is crucial for faithful chromosome segregation in meiosis I and meiosis II. In meiosis I, in order for each daughter cells to receive a single copy of each homologous chromosome, the maternal and paternal chromosomes of each pair need to be pulled to opposite pole of the spindle. The cell "figures out" who is paired with whom by attaching kinetochores to the spindle and pulling. If the homologues are attached to opposite poles of the spindle, the physical attachment, created by cross-overs, will result in physical tension that will stabilize the

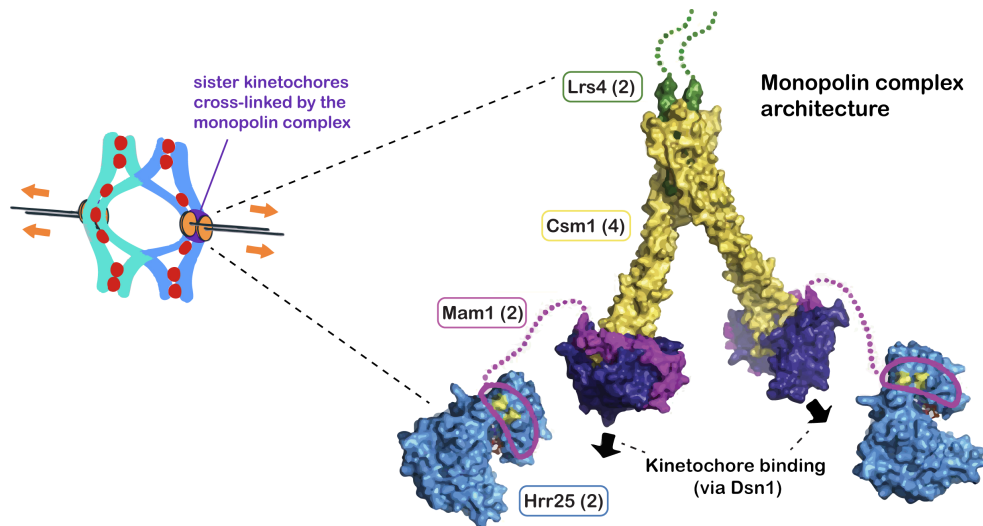


Figure 5: Reconstitution on the monopolin complex structure, adapted from Corbett et al. (Corbett and Harrison, 2012)

The model of Corbett et al. proposes that Lrs4 (green) and Csm1 (yellow) form a clamp that might cross-link sister-kinetochores, forcing them to face the same spindle pole (Corbett and Harrison, 2012). The two Csm1 globular domains interact with the kinetochore protein, Dsn1, and with the C-terminus region of Mam1 (Magenta). The Mam1 linker region (residues 192–220) is shown as a dotted magenta line and connects Hrr25 to the monopolin complex. Hrr25 is represented in blue and its N-terminal lobe interacts with the central domain of Mam1 (magenta outline) (Petronczki et al., 2006). The copy number of each protein in the complex is indicated in parentheses.

microtubule-kinetochore attachment (Petronczki et al., 2003). If the two homologous chromosomes are attached to the same spindle pole, no tension will be generated and the microtubule-kinetochore attachment is quickly dissolved so that it can "try again". The second meiotic division rely on the same principles. The two sister chromatids of each chromosome are bound together at centromere by cohesin and the binding of sister kinetochores to opposite pole of the spindle creates tension that stabilizes microtubule-kinetochores attachment. Cells that are deficient for chromosomes linkage are unable to generate tension and are therefore delayed in metaphase by the SAC (Petronczki et al., 2003). Both homologous chromosomes and sister chromatids are physically linked by cohesin rings. Therefore, the loading and removal of this complex is tightly regulated during meiosis.

1.6.1. Cohesin structure

Protein complexes containing structural maintenance of chromosomes (SMC) proteins are crucial for faithful chromosome segregation during cell division. The two main SMC complexes are condensin and cohesin. While condensin is required to organize mitotic chromosomes into compact structures, cohesin

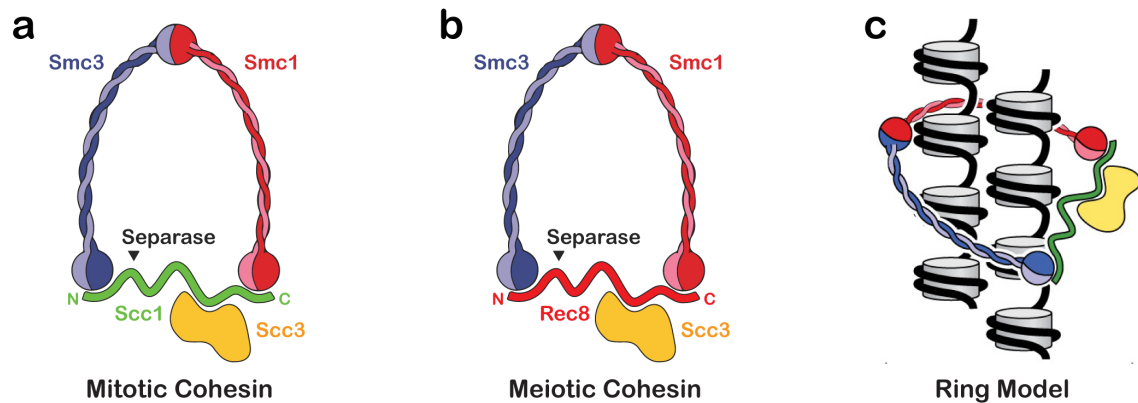


Figure 6: Structure of the cohesin complex and models of chromosomes binding, adapted from Nasmyth and Haering, 2009.

(a-b) The cohesin subunit Smc1, Smc3 and the α -kleisin form a tripartite ring that holds chromosomes together. Although the Scc3 protein is not part of the ring, its presence is also required for cohesion. (a) The mitotic cohesin complex contains the α -kleisin subunit Scc1. This subunit is cleaved by separase at anaphase onset (b) In meiosis, Scc1 is replaced by another α -kleisin, Rec8 (Buonomo et al., 2000; Kitajima et al., 2003; Klein et al., 1999). (c) The ring model proposes that sister chromatids (represented as 10 nm fibers) are trapped within a single cohesin ring. This system efficiently ensure the physical attachment of DNA strand until the cohesin rings cleavage by separase.

is required to hold sister chromatids together (Nasmyth and Haering, 2005). Cohesin is a complex of four subunits: Smc1, Smc3, Scc3 and the α -kleisin subunit Scc1 (Figure 6, a) (reviewed in Nasmyth and Haering, 2009). In meiosis, Scc1 is replaced by a meiosis-specific α -kleisin Rec8 (Figure 6, b) (Buonomo et al., 2000; Kitajima et al., 2003; Klein et al., 1999). Cohesin complexes form rings that capture DNA strands and physically link sister chromatids and, in meiosis, homologous chromosomes together (Gruber et al., 2003; Haering et al., 2008; Haering et al., 2002). How cohesin rings create those physical attachment is a very active topic of research and several models have been proposed. One popular model, called the ring model, proposes that the two strands of DNA are captured within a single cohesin ring (Figure 6, c) (Nasmyth and Haering, 2009; Haering et al., 2002; Haering et al., 2002).

1.6.2. Cohesin cleavage

The segregation of homologous chromosomes in meiosis I as well as the segregation of sister chromatids in meiosis II or mitosis requires the dissolution of the physical linkage between homologous chromosomes and sister chromatids, respectively. Before cohesin was even discovered, evidences were found that the APC/C^{Cdc20} up-regulation was required to disjoin sister chromatids in mitosis

(Irniger et al., 1995). We now know that the APC/C^{Cdc20} triggers cohesin cleavage indirectly. The Scc1 subunit is cleaved by the CD clan protease separase, called Esp1 in *S. cerevisiae* (Uhlmann et al., 2000; Uhlmann et al., 1999). For most of the cell cycle, separase is tightly inhibited by securin, called Pds1 in budding yeast (Uhlmann et al., 1999; Hauf et al., 2001). But when APC/C^{Cdc20} is activated at anaphase onset, it targets securin for degradation. The separase, now liberated from its inhibitor, cleaves the Scc1 subunit of cohesin, thereby allowing chromosome segregation (Cohen-Fix et al., 1996; Ciosk et al., 1998; Funabiki et al., 1996). Additionally, in budding yeast and human cells, the phosphorylation of Scc1 enhances its cleavability by separase (Alexandru et al., 2001; Hornig and Uhlmann, 2004; Hauf et al., 2005). Cohesin removal in meiosis I and meiosis II also depends on separase cleaving the Scc1 meiotic equivalent, Rec8 (Buonomo et al., 2000; Kitajima et al., 2003). At anaphase I, the cleavage of cohesin on chromosome arms leads to the resolution of chiasmata and to the segregation of homologous chromosomes (Nasmyth and Haering, 2009). However, the cohesin complexes located around centromeres and linking sister chromatids together are not cleaved until anaphase II since they are essential for the bi-orientation of sister chromatids in meiosis II (Klein et al., 1999). Therefore, meiotic cells need to specifically protect centromeric cohesin from separase during anaphase I.

1.6.3. The centromeric protection machinery

Studies in *D. melanogaster* first identified the Mei-S332 protein as an essential component for protecting centromeric cohesin from cleavage until meiosis II (Goldstein, 1980; Kerrebrock et al., 1995). It was shown that Mei-S332 localizes specifically at centromeres in meiosis and is removed shortly before anaphase II onset (Kerrebrock et al., 1995). In the absence of Mei-S332, sister chromatids are disjoined prematurely (Davis, 1971; Kerrebrock et al., 1992). Subsequent studies identified homologs of Mei-S332 in budding yeast, fission yeast, and vertebrates cells (Katis et al., 2004a; Kitajima et al., 2004; Marston et al., 2004; Rabitsch et al., 2004; McGuinness et al., 2005; Salic et al., 2004). These homologs were named Shugoshin (Sgo1 in *S. cerevisiae*), which means guardian spirit in Japanese (Kitajima et al., 2004; Watanabe, 2005). Shugoshin protects centromeric cohesin from separase by recruiting the PP2A phosphatase to the centromeres (Riedel et al., 2006; Tang et al., 2006; Kitajima et al., 2006). Katis et al. demonstrated that the phosphorylation of Rec8 by the Casein kinase 1 δ/ϵ , Hrr25, and by the Dbf4-dependent Cdc7 kinase (DDK) is essential for its cleavage by separase (Katis et al., 2010). Hence, PP2A-Shugoshin protects centromeric cohesion by opposing Hrr25- and Cdc7-dependent phosphorylation of Rec8 (Katis et al., 2010; Ishiguro

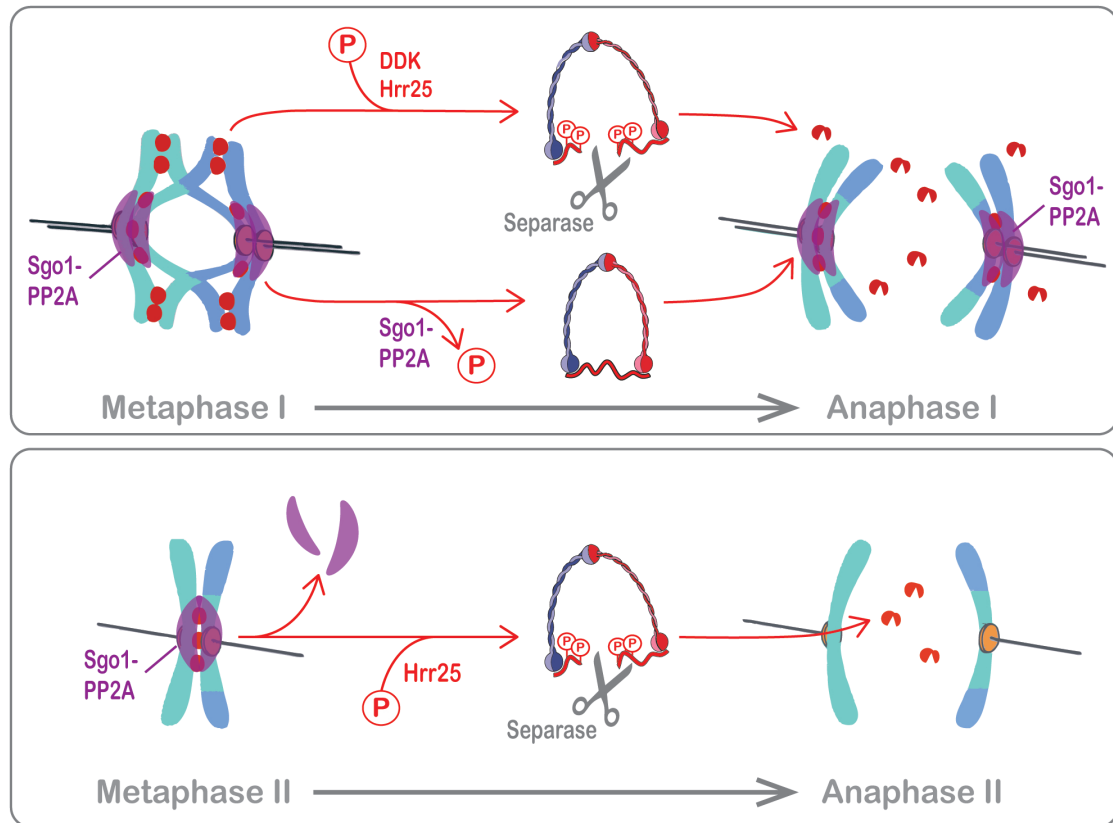


Figure 7: Model for a differential cohesin cleavage at anaphase I

The Rec8 subunit of cohesin complexes loaded on chromosome arms is phosphorylated by Cdc7-Dbf4 and by Hrr25. These phosphorylations are needed for the efficient cleavage of Rec8 by separase. The phosphorylations of cohesin complexes located on centromeres are actively removed by the PP2A phosphatase specifically recruited to centromeres by Shugoshin.

et al., 2010). A model for cohesin cleavage at anaphase I is depicted in Figure 7. Katis et al. identified 24 phosphorylated serine/threonine residues on Rec8 (Katis et al., 2010). Their mutation to alanine creates a non-phosphorylatable mutant of Rec8 that abolishes the cleavage of Rec8 and the resolution of chiasmata (Katis et al., 2010). Furthermore, the mutation of 14 of these sites to aspartate resulted into a phospho-mimetic version of Rec8 that causes precocious cleavage of centromeric Rec8. These results showed that Rec8 is cleaved by separase only upon phosphorylation by Hrr25 and Cdc7 and that Sgo1-PP2A protects centromeric Rec8 from cleavage at anaphase I by dephosphorylating Rec8 at centromeres. This protection mechanisms requires Rec8 to be part of the cohesin complex. Indeed, when Rec8 is replaced by Scc1 in meiosis, the cells lose the ability to retain centromeric cohesin after anaphase I (Tóth et al., 2000).

1.7. The M phase cyclins and APC/C regulation in meiosis

The regulation of cyclins in meiosis is complex and may be the key to understand how the two successive divisions are orchestrated (Carlile and Amon, 2008; Futcher, 2008; Dahmann and Futcher, 1995). In meiosis, M-phase cyclins seem to be partially redundant and the deletion of a single cyclin has moderate effects on meiotic progression. While Clb2 play a major role in mitosis, its expression is actively repressed during meiosis (Grandin and Reed, 1993; Okaz et al., 2012). The transcription of M-phase cyclins is positively regulated by the Ndt80 transcription factor (Chu and Herskowitz, 1998). Ndt80 expression is repressed during the long meiotic prophase by the recombination checkpoint (Hepworth et al., 1998; Tung et al., 2000). Once recombination is completed, Ndt80 accumulates and triggers the expression of M phase proteins, including B-type cyclins, Cdc5, and Cdc20 as well as many sporulation-specific proteins, such as Mam1 (Hepworth et al., 1998; Chu and Herskowitz, 1998). Although, most meiotic genes are regulated by Ndt80, the timing for Ndt80 transcribed genes accumulation varies greatly (Chu and Herskowitz, 1998; Cheng et al., 2018). For instance Clb1 and Clb4 accumulate at metaphase I onset, while Clb3 accumulation is restricted to meiosis II (Carlile and Amon, 2008). In meiosis, the major cyclin B seems to be Clb1 (Dahmann and Futcher, 1995). Indeed, cells that undergo meiosis with only Clb1 as M-phase cyclin still sporulate fairly well and produce a majority of tetrads (Dahmann and Futcher, 1995). Additionally, cells carrying a *CLB3* or *CLB4* deletion have no observable phenotype, while *clb1* null mutant forms a higher rate of dyads (14% of total asci) (Dahmann and Futcher, 1995).

1.7.1. Cdc20 and Ama1 regulate APC/C activity in meiosis

In yeast and higher organisms, APC/C^{Cdc20} activity is required for securin degradation and, hence, for chromosomes segregation in both meiotic divisions (Salah and Nasmyth, 2000; Buonomo et al., 2000; Kitajima et al., 2003; Furuta et al., 2000). In addition to Cdc20 and Cdh1, meiosis-specific APC/C co-activators play important roles for meiosis and gametogenesis. Studies in budding yeast, fission yeast and flies identified meiosis-specific APC/C activators that seem to target specific sets of substrates for degradation during meiosis (Cooper et al., 2000; Asakawa et al., 2001; Blanco et al., 2001). In *S. cerevisiae*, Ama1 was identified to be associated with the core APC/C throughout meiosis (Cooper et al., 2000). Ama1 is

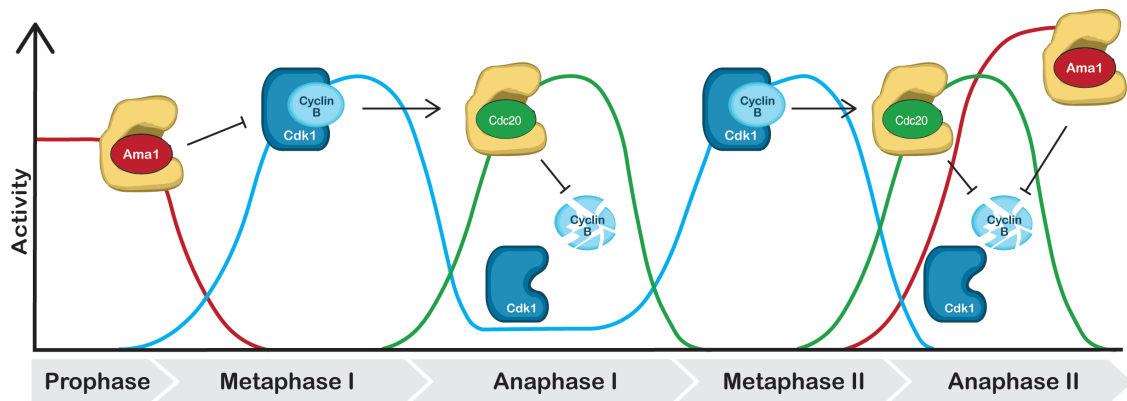


Figure 8: Cdk1-Cyclin B and APC/C activity in meiosis

The expression of M-phase proteins is actively repressed by APC/C^{Ama1} during the meiotic prophase. In metaphase I, M-phase cyclins accumulate and promote Cdk1 activity. Clb-Cdk1 phosphorylates the APC/C. These phosphorylations are required for the activation of the APC/C by Cdc20 at anaphase onset. APC/C^{Cdc20} triggers the (incomplete) degradation of cyclins B at anaphase I. Current knowledge suggests that Clb-Cdk1 activity is not fully suppressed at anaphase I in order to avoid re-replication of DNA. Cdk1-Cyclin B activity rises again in metaphase II and is counteracted by APC/C^{Cdc20} at anaphase II onset. While Ama1 is inactive during the two meiotic divisions, Ama1 protein level rises to high level toward the end of meiosis where it plays a role in the meiotic exit and sporulation.

essential for the yeast equivalent of gamete differentiation, sporulation, indicating that APC/C^{Ama1} is specifically adapted for germ cell development (Cooper et al., 2000). In addition to its function in meiotic exit, Okaz et al. found that APC/C^{Ama1} is active during the meiotic prophase where it represses the expression of mitotic M phase proteins (Okaz et al., 2012). In the absence of Ama1, cells enter M-phase before the completion of recombination (Okaz et al., 2012). In budding yeast, the Cdh1 cofactor is highly phosphorylated during the two meiotic divisions and its phosphorylations persist until after meiotic exit suggesting that Cdh1 is inactive for most of the meiotic program. Accordingly, Cdh1 depletion in meiosis does not seem to yield any phenotypes (Okaz et al., 2012; Oelschlaegel et al., 2005; Tan et al., 2011). A model of Clb-Cdk1 and APC/C activity in budding yeast meiosis is presented in Figure 8.

1.7.2. How to make two successive waves of Cdk1 activity?

The role for APC/C^{Cdc20} in both nuclear divisions imply that its activity must oscillates through meiosis (Cooper and Strich, 2011). Indeed, APC/C^{Cdc20} is first activated at anaphase I and is then inactivated to permit the re-accumulation of securin and Clb-Cdk1 activity at metaphase II, to be activated once again for the

second meiotic division (reviewed in Cooper and Strich, 2011; Salah and Nasmyth, 2000). How these two waves of Cdk1 activity and APC/C activity are created remains poorly understood. Although the meiotic program requires some serious changes from the mitotic program, these changes seem to be set by a relatively small number of meiotic specific proteins. This work attempts to understand the fundamental mechanisms that adapt the mitotic cell cycle machinery to perform two successive divisions. An attractive approach to this problem is to characterize meiotic mutants that perform only one division. The work presented here focuses on the meiosis I-specific protein Spo13 as its implication in the meiotic program and its molecular function remain poorly understood.

1.8. Spo13 is essential for the proper completion of meiosis

The *spo13* mutant was discovered and characterized in 1980 in a screen to identify genes involved in the regulation of the two meiotic divisions (Klapholz and Esposito, 1980a). Klapholz et al. isolated a *spo13* mutant from the *S. cerevisiae* strain, ATCC4117, that sporulates efficiently but only forms two-spored asci (Klapholz and Esposito, 1980a). Spo13 is a meiosis I-specific protein that is expressed during meiotic prophase and is degraded at anaphase I onset by APC/C^{Cdc20} (Buckingham et al., 1990; Sullivan and Morgan, 2007). The *SPO13* promoter contains a *URS1* site that is responsible for repressing *SPO13* transcription in mitotic cells and for stimulating its transcription during meiotic prophase. *URS1* site is found in most early meiotic genes such as *HOP1* or *IME2* (Buckingham et al., 1990; Mitchell, 1994). Sullivan et al. identified Spo13 as an APC/C target as Spo13 contains a D-box-related destruction-box motif, LxExxxN (Sullivan and Morgan, 2007). When the LxExxxN is mutated to AxLxxxN, Spo13 is stabilized and persists until the second meiotic division (Sullivan and Morgan, 2007). However, the non-degradable *SPO13* allele completes meiosis without noticeable defects. The authors concluded that Spo13 degradation in anaphase I is not essential for proper completion of the meiotic program.

Genetic analysis showed that *spo13*Δ cells segregate a mixture of homologous and sister chromatids, within the same cell, producing poorly viable spores (Lee et al., 2004; Klapholz and Esposito, 1980b; Hugerat and Simchen, 1993). However, the suppression of homologous recombination in *spo13* mutant increases the rate of sister chromatids segregation and improves the spore viability of *spo13*Δ asci (Klapholz and Esposito, 1980b; Lee et al., 2004). Hence, the suppression of

recombination and of Spo13 converts the meiotic divisions to a mitotic-like division. Therefore, Spo13 is believed to have a fundamental role in establishing the first meiotic division.

1.8.1. Spo13 is required for monopolar attachment

The mixture of homologous chromosomes bi- and mono-orientation occurring in *spo13Δ* strongly suggests that Spo13 is required for the bi-orientation of homologous chromosomes during meiosis I (Lee et al., 2004; Katis et al., 2004b). Indeed, it was reported that *spo13Δ* cells tend to pull apart sister centromeres in metaphase I significantly more frequently than the wild-type and similar to the monopolin mutant *mam1Δ* (Katis et al., 2004b; Lee et al., 2004). This observation indicates that *spo13Δ* mutants tend to bi-orient sister chromatids during metaphase I. In budding yeast, the monopolin complex localization at kinetochores is crucial for the establishment of homologous chromosomes bi-orientation. Hence, several studies inspected the potential interaction between Spo13 and the monopolin complex (Katis et al., 2004b; Lee et al., 2004). The monopolin subunit, Mam1, was not found at kinetochores in the absence of Spo13, although Mam1 protein level in the cells is comparable to the wild-type (Katis et al., 2004b; Lee et al., 2004). This result suggests that Spo13 is required for recruiting at least some components of the monopolin complex to kinetochores. Matos et al. then showed through a series of immuno-precipitation that, in absence of Spo13, all the subunits of the monopolin complex still interact with each other, indicating that the loading to kinetochores alone was impaired (Matos et al., 2008). Together, these evidences strongly show that Spo13 is directly required for the bi-orientation of homologous chromosomes by recruiting or stabilizing the monopolin complex onto kinetochores. How Spo13 recruits or maintains the monopolin complex at kinetochores is yet to be understood but seems to involve the Polo-like kinase (Cdc5 in yeast). Besides Cdc5's role in releasing Csm1 and Lrs4 from the nucleolus (Sarkar et al., 2013; Ye et al., 2016), Matos et al. show that its interaction with Spo13 is required for proper monopolar attachment (Matos et al., 2008). Indeed, impairing the interaction between Cdc5 and Spo13 by mutating Spo13's polo binding site (*spo13-m2* mutant) prevents monopolin localization to the kinetochore. This mutant display a monopolar attachment defect but, unlike the deletion, the majority of *spo13-m2* cells undergo two meiotic divisions and produce tetrads instead of dyads (Matos et al., 2008). These results strongly suggests that Cdc5 and Spo13 work together to promote monopolar attachment in meiosis I.

1.8.2. Spo13 has been linked to the maintenance of centromeric cohesin protection

Unlike monopolin mutants, *spo13* Δ cells are able to segregate sister chromatids at anaphase I, indicating a potential role of Spo13 in protecting sister chromatid cohesion at meiosis I (Hugerat and Simchen, 1993; Klapholz and Esposito, 1980b; Klapholz and Esposito, 1980a). Several studies reported that the retention of centromeric cohesin was at least partially affected by the deletion of *SPO13* (Klein et al., 1999; Katis et al., 2004b; Shonn et al., 2002; Lee et al., 2004). Klein et al. and Katis et al. observed on chromosome spreads that Rec8 centromeric signal at anaphase I was weaker in *spo13* Δ cells than in wild-type cells, although still perceptible (Klein et al., 1999; Katis et al., 2004b). The experiments of Katis et al. suggested that this residual centromeric cohesin confers some cohesion and that *SPO13* deletion does not completely abolish centromeric cohesion (Katis et al., 2004b). How Spo13 is involved in the two-step cleavage of cohesin is unknown. The loading of the centromeric cohesin protection machinery on kinetochores does not seem to be affected in *spo13* Δ cells. Indeed, Sgo1 accumulation and localization in metaphase I and anaphase I were compared in wild-type conditions and in the absence of Spo13 but no differences were detected (Lee et al., 2004). Lee et al. concluded that Spo13 must maintain centromeric cohesin until meiosis II independently of the Shugoshin-PP2A machinery (Lee et al., 2004). Katis et al. noticed that *spo13* Δ cells do not re-accumulate securin after anaphase I and proposed that a failure to inhibit separase in meiosis II could cause the precocious loss of centromeric cohesin (Katis et al., 2004b). Therefore, whether Spo13 is directly involved in centromeric cohesin protection and how it is required remains controversial.

1.8.3. How does Spo13 insure the completion of the two meiotic division?

The finding that Spo13 is required for the bi-orientation of homologous chromosomes and for the protection of centromeric cohesin from cleavage in meiosis could partially explain the *spo13* mutant phenotype: in the absence of the monopolin complex, sister chromatids bi-orient and, in the absence of centromeric protection, cohesin is cleaved during the first wave of separase activity (Lee et al., 2004; Shonn et al., 2000). However, the mechanisms underlying Spo13 function remain unknown. Although the defect in monopolar attachment of sister

chromatids and in the protection of centromeric cohesin could explain the behaviour of chromosomes in *spo13Δ* cells, it does not explain why *spo13Δ* cells fail to enter meiosis II. Two additional genetic interactions previously reported suggest that Spo13 might have additional role(s) in meiosis (Katis et al., 2004b; Shonn et al., 2000). First, the metaphase I arrest caused by Cdc20 depletion can be rescued by the deletion of *SPO13* (Katis et al., 2004b). This highly unusual phenotype shows that in the absence of Spo13, Cdc20 is not required for the onset of anaphase and suggests that Spo13 might regulate the APC/C in some way. Second, the second meiotic division can be restored in *spo13* mutant by inactivating the SAC. Indeed, Shonn et al. observed that the deletion of the SAC effector Mad2 rescues the second nuclear division and allows the formation of tetra-nucleated cells (Shonn et al., 2000). Their results suggest that the SAC might delay *spo13Δ* cells in metaphase I. In this work, we rely on live-cell imaging to re-assess the *spo13* mutant phenotype with high temporal resolution and focused on understanding how Spo13 controls the activity of the APC/C in meiosis and how this could affect our previous understanding of Spo13's role in centromeric cohesin protection.

1.8.4. Spo13 homologs: Moa1 and Meikin

Thus far, two proteins were proposed to be functional homologs of Spo13: Moa1 in fission yeast, and Meikin in mouse. Meikin (for meiosis-specific kinetochore protein) was identified in a two-hybrid assay looking for centromere protein C (CENP-C) interactors in mouse testis, as the authors sought to identify a meiosis-specific kinetochore protein that might be required for monopolar attachment and/or centromeric cohesin protection (Kim et al., 2015). Like Spo13, Meikin starts to accumulate during prophase, is degraded at anaphase I, and is not present during meiosis II (Kim et al., 2015). Similarly to the *spo13* mutant, *Meikin*^{-/-} oocytes are delayed by two hours in metaphase I, and this delay is fully suppressed by inactivating the SAC (Kim et al., 2015). The authors reported that *Meikin*^{-/-} oocytes are defective in the mono-orientation of sister kinetochores (Kim et al., 2015). This is an important discovery as there is so far no conserved machinery for monopolar attachment. Meikin is, so far, the only candidate for a factor promoting monopolar attachment in mammals. Spo13, Meikin and Moa1 seem to promote mono-orientation of sister-kinetochores with the assistance of Cdc5/Polo-like-kinase (Kim et al., 2015; Yokobayashi and Watanabe, 2005). All three proteins bind to the polo-like kinase via their PBD-binding domain, and Cdc5/Plk1 inhibition in both mouse and yeast creates monopolar attachment defects. More strikingly, reducing the interacting between Spo13/Moa1 and

Cdc5/Plp1 by mutating the polo-binding-domain also leads to sister-kinetochore bi-orientation in meiosis I (Kim et al., 2015; Matos et al., 2008). Finally, *meikin*^{-/-} mutants load cohesin on chromosome properly but, centromeric cohesin is not observed in metaphase II oocytes, strongly resembling the *spo13Δ* budding yeast mutant. The authors concluded that *meikin*^{-/-} is defective in protecting centromeric cohesin, although this defect is milder than in the *sgo2*^{-/-} oocytes (Kim et al., 2015). Therefore, though Meikin and Spo13 don't share sequence homology, they share many common functions during meiosis.

2 Results

2.1. Metaphase I is prolonged in absence of Spo13

Thus far, the *spo13* mutant has only been characterized by immuno-fluorescence microscopy (IF) and western blotting whereby samples are generally collected every 2 hours. These methods offer a very low temporal resolution of meiotic events but suggest that *Spo13* Δ cells might be delayed in meiosis (Shonn et al., 2002). Indeed, the *SPO13* deletion strain seems to accumulate more meiosis I spindles than the wild-type (Shonn et al., 2002). To confirm the potential delay of *spo13* mutant in metaphase I and observe how these cells progress through meiosis, we decided to use live-cell imaging. This microscopy technique allows to follow each cell individually through the whole meiotic program and to simultaneously monitor several hallmarks of meiosis, such as spindle formation, Cdc14 release/capture and nuclear divisions.

The characterization of *spo13* Δ by time-lapse microscopy shows that this mutant experiences a significant delay in metaphase I (Figure 9A). The metaphase I spindle is formed with wild-type kinetics, but spindle elongation, Cdc14 release and nuclear division are all delayed by 40 minutes compared to the wild-type strain. Indeed, the average duration of metaphase I in the wild-type is 25 minutes, while metaphase I lasts for 67 minutes in *spo13* Δ cells (Figure 9B). *spo13* Δ cells finally release Cdc14 from the nucleolus, extend their spindle and undergo a nuclear division. The spindle is then disassembled and Cdc14 is recapture. We do not see any attempt of this mutant to form a meiosis II spindle or to release Cdc14 for a second time. As a matter of fact, cells start forming spores quickly after their single division, as wild-type cells do after their second round of chromosome segregation. These results strongly suggest that *spo13* Δ cells exit meiosis after only one division. Furthermore, they suggest that the APC/C is activated only once in the absence of Spo13.

IF and western blotting show that APC/C^{Cdc20} substrates, such as Pds1 or Dbf4, are not degraded during this extended metaphase I until shortly before *spo13* Δ cells undergo nuclear division (Figure 10). Therefore, the nuclear division delay is most likely due to a delay in the activation of APC/C^{Cdc20}. Western blots of a *spo13* Δ time course show that Cdc20 accumulates to levels comparable to

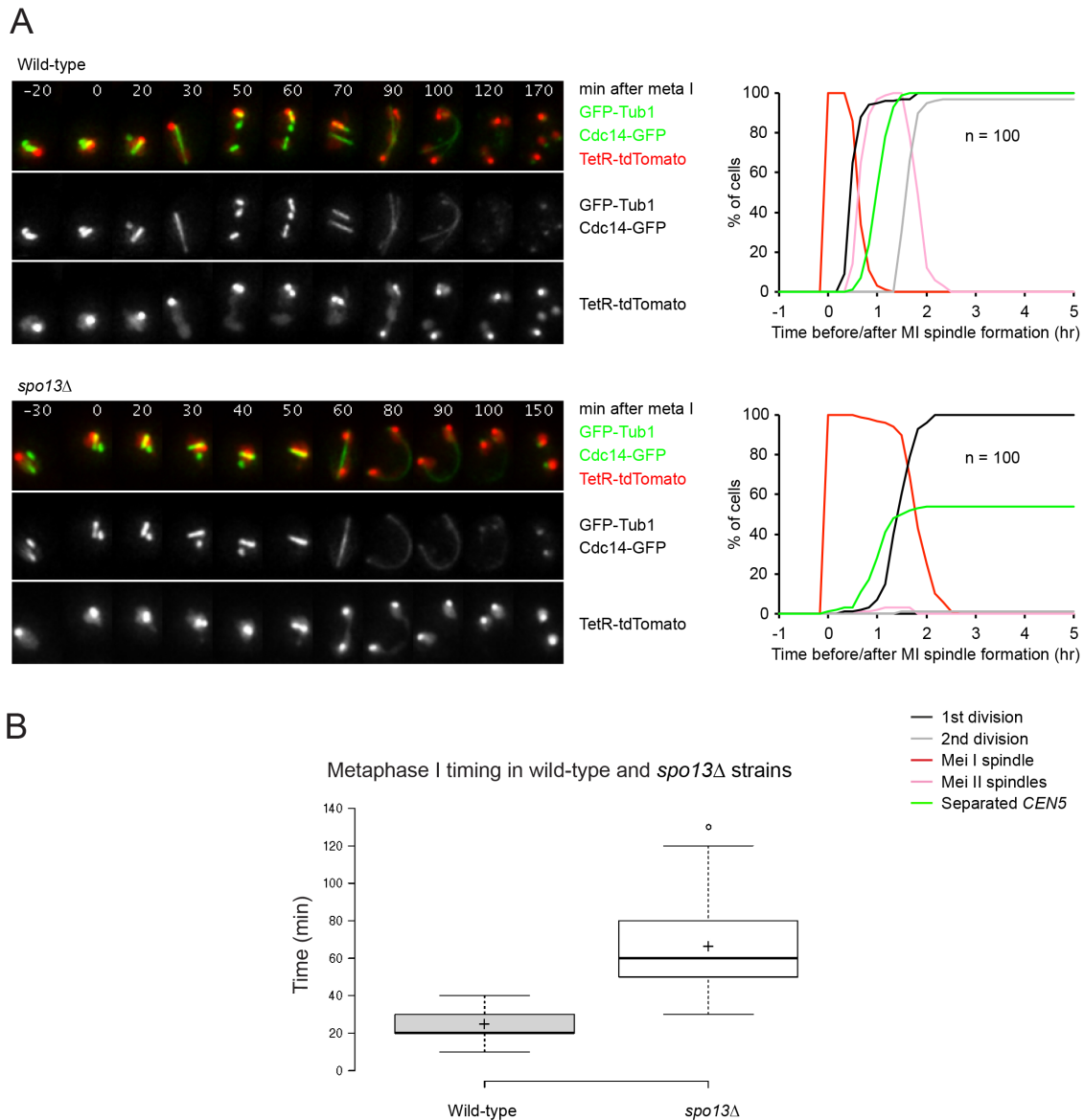


Figure 9: *spo13Δ* cells are delayed in metaphase I.

Wild-type (Z24864) and *spo13Δ* (Z24862) strains containing the heterozygous markers Tub1-GFP, Cdc14-GFP, TetR-tdTomato, and *CEN5*-tetO were filmed. (A) From the green channel, we quantified the formation of one and two spindles. From the red channel, we quantified nuclear divisions (1st division and 2nd division) marked by the diffuse TetR-tdTomato signal while the dot splitting indicates bi-polar attachment of chromosome 5 sister chromatids (separated *CEN5*). 54% of *spo13Δ* cells split centromeric dots during their single nuclear division. By contrast, 100% in wild-type cells split centromeric dots during the second meiotic division. Countings are synchronized in silico to the formation of meiosis I spindle (Mei I spindle) and displayed on the right. On the left are representative time-lapse series for each strain. (B) Box plots displaying the timing of metaphase I for wild-type cells and *spo13Δ* cells. Metaphase I is defined as the time between the formation of the metaphase I-spindle and Cdc14 first release (marker for anaphase onset) from the nucleolus. The center lines show the medians (20 minutes for the wild-type and 60 minutes for *spo3* mutant), the box limits indicate the 25th and 75th percentiles. Whiskers extend 1.5 times the interquartile range from the 25th to 75th percentiles and outliers are represented by circles. Crosses represent the sample means. On average, metaphase I lasts for 25 ± 7 minutes in the wild-type and 67 ± 19 minutes in the *spo13Δ* mutant.

that of a wild-type. Thus, the inactivation of known Cdc20 inhibitors might cause Cdc20 activation and restore a normal meiotic timing in the *spo13Δ* mutant.

2.2. SAC activity delays anaphase onset in *spo13Δ*

Shonn et al. observed that the deletion of *MAD2* restores the second nuclear division in the *spo13Δ* mutant (Shonn et al., 2002). We confirmed that the inactivation of the SAC suppresses the metaphase I delay of *spo13Δ* and fully rescues the entry of *spo13Δ* cells into meiosis II (Figures 11). This rescue suggests that the SAC is either hyper-activated or fails to be inactivated in *spo13Δ* cells. To assess whether the SAC is 'hyper-activated' in the absence of Spo13, we developed an assay to monitor SAC activity by live-cell imaging.

2.2.1. A SAC activity assay for time-lapse microscopy

We used the fact that the Mad2 and Mad1 proteins were found to be recruited solely to unattached kinetochores to create a live-cell imaging assay for SAC activity (Chen et al., 1996; Musacchio and Hardwick, 2002; Gorbsky et al., 1999). We tagged Mad2 with the green fluorescent protein neonGreen and followed its localization through meiosis. To determine at which stage of the meiotic program each cell is at a specific time point, we simultaneously followed the equivalent of centrosomes in budding yeast, the spindle pole bodies (SPBs), whose behaviour through meiosis is well characterized (Jaspersen and Winey, 2004) by tagging the SPBs protein Cnm67 with the red fluorescent protein td-Tomato. Cells start meiosis with a single SPB that is duplicated during S-phase. However, the two SPBs remain closely associated and appear as one dot until entry into metaphase I (Jaspersen and Winey, 2004). When the meiosis I spindle is formed, the two SPBs are located at the two ends of the short metaphase I spindle, and as cells enter anaphase I, the spindle extend and the two SPBs get further apart. As cells enter metaphase II, SPBs are re-duplicated and appear as four dots when the meiosis II spindles are formed (Jaspersen and Winey, 2004). Hence, following SPB numbers through meiosis indicates entry into metaphase I and, later, entry into metaphase II. Furthermore, in budding yeast, kinetochores localize very close to the SPBs (Sobel, 1997). Therefore, we expect Mad2 to cluster near the SPBs when the SAC is active. In wild-type cells, Mad2-neonGreen forms a diffuse nuclear signal until metaphase I onset when it forms bright cluster(s) in the vicinity of the SPBs (Figure 12). On average, these foci persist for 16 minutes before they disappear. Mad2-neonGreen clusters form again at metaphase II for 10 minutes on average.

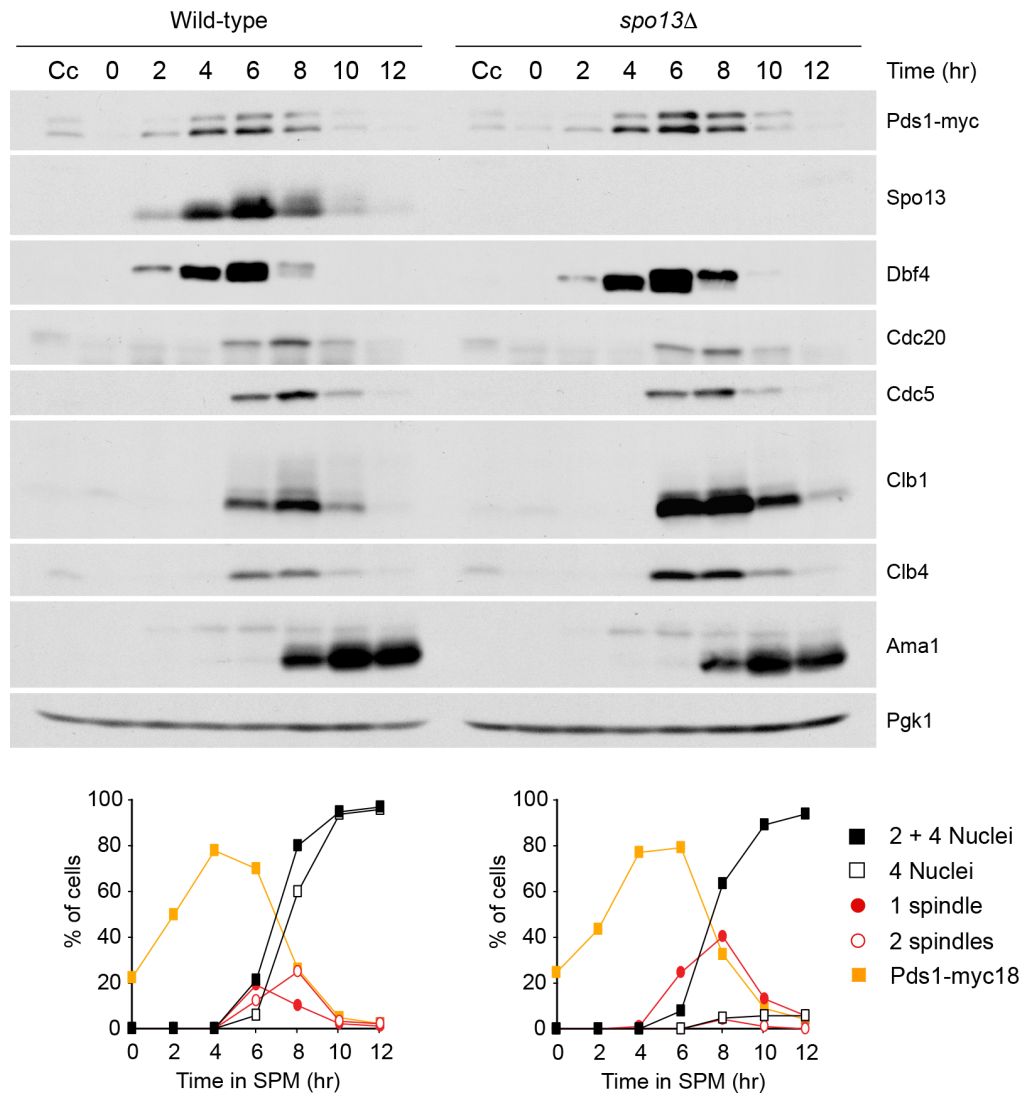


Figure 10: *spo13Δ* cells accumulates M-phase proteins normally but undergo a single nuclear division.

Meiosis was induced in synchronized cultures of wild-type (Z23604) and *spo13Δ* (Z23605) strains cells. After transfer to sporulation medium (SPM), samples for immunofluorescence and TCA protein extraction were collected every 2 hours. On the upper part, immunoblot analysis of protein levels is shown. Cc stands for "cycling cells", these samples were collected from proliferating cells. On the lower part, immuno-fluorescence detection of securin (Pds1-myc), bipolar spindles (α -tubulin) and of the number of nuclei (DAPI) were quantifies. M-phase proteins accumulate with a normal timing compared to the wild-type strain. The proteins levels of meiosis I proteins such as Dbf4, Clb1 and Clb4 are higher in *spo13Δ* strain compared to the wild-type strain. This is most likely due to *spo13Δ* cells delay is metaphase I. Furthermore, IF countings show that the *spo13Δ* strain accumulates more meiosis I spindle (1 spindle) than the wild-type. Pds1-myc signal is lost shortly before *spo13Δ* single division, suggesting that APC/C^{Cdc20} activation is delayed. *spo13Δ* cells do not forms meiosis II spindle (2 spindles).

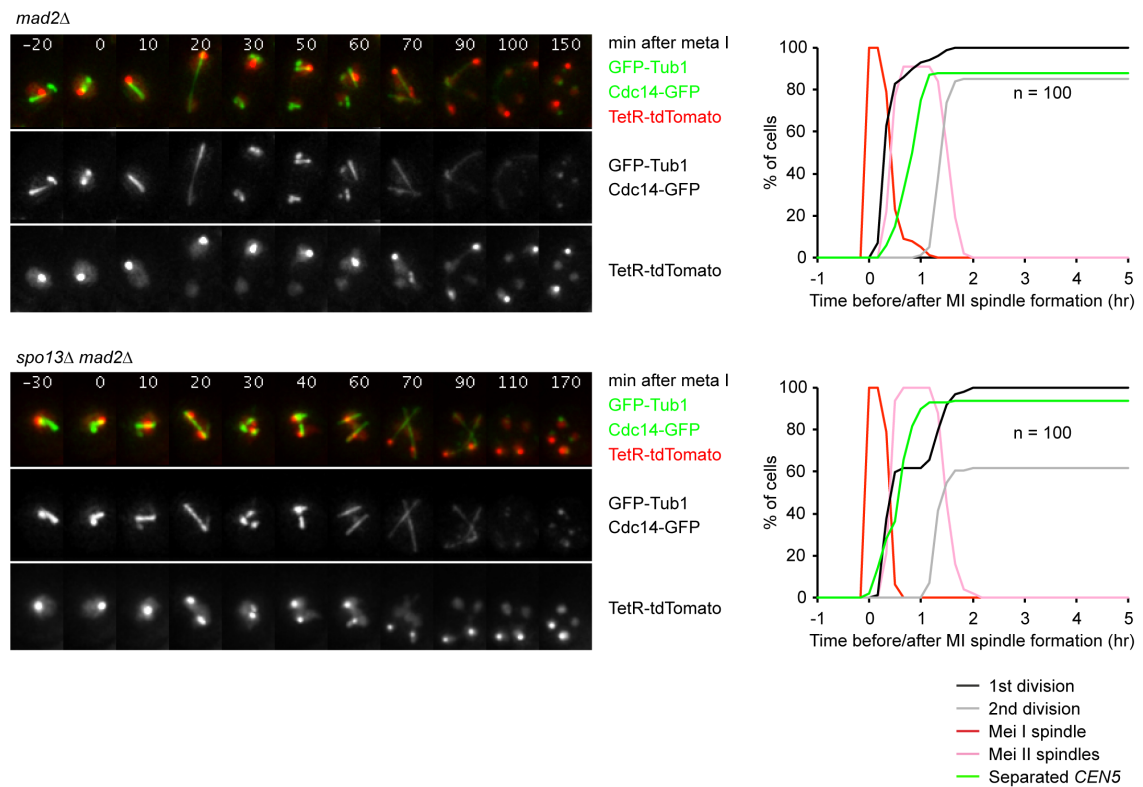


Figure 11: The *MAD2* deletion restores the entry into meiosis II in *spo13 Δ* cells.

mad2 Δ (Z24863) and *spo13 Δ mad2 Δ* (Z24861) strains containing the heterozygous markers Tub1-GFP, Cdc14-GFP, TetR-tdTomato, and CEN5-tetO were filmed. From the green channel, we quantified the formation of one and two spindles. From the red channel, we quantified nuclear divisions (1st division and 2nd division) marked by the diffuse TetR-tdTomato signal while the dot splitting indicates the bipolar attachment of the fifth chromosome sister chromatids (separated CEN5). Countings are synchronized to the formation of the meiosis I spindle and representative time-lapse pictures are displayed on the left. The average time for metaphase I in *mad2 Δ* and *spo13 Δ mad2 Δ* cells is 13 ± 6 and 10 ± 4 minutes, respectively.

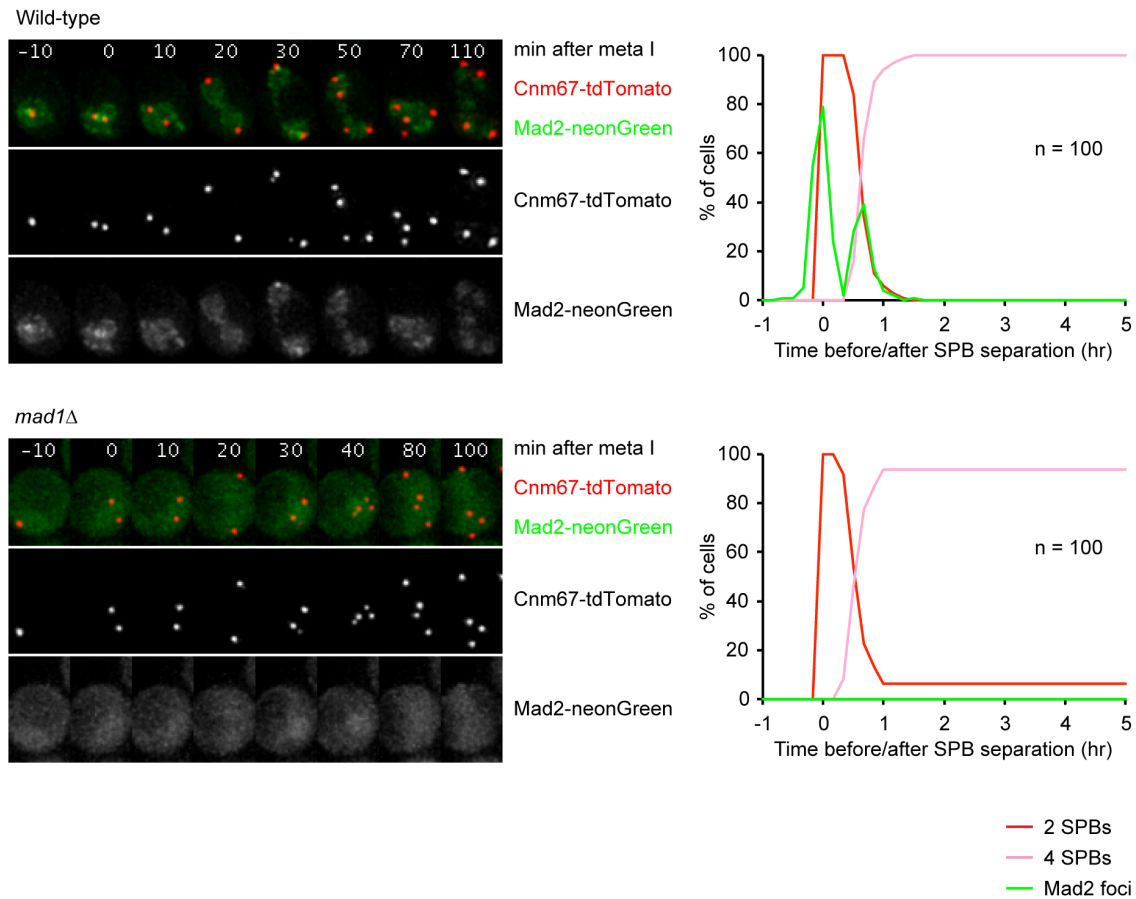


Figure 12: Formation of Mad2 foci depends on Mad1.

*mad1*Δ strain (Z23072) is compared to wild-type cells (Z23073) to ensure that the Mad2 clusters observed correspond to its recruitment by Mad1 to kinetochores. Representative time-lapse series are displayed on the left while the countings displayed on the right are synchronized in-silico to the formation of two SPBs. We observe Mad2-neonGreen clusters transiently forming near SPBs as cells enter metaphase I (appearance of two SPBs) and at entry in metaphase II (formation of four SPBs). In the wild-type strain, clusters persist for a mean time of 16 ± 7 minutes and 9 ± 5 minutes in metaphase I and II, respectively, while no clusters were detected in *mad1*Δ cells.

These clusters fit our current knowledge about the timing of SAC activity. Previous studies in budding yeast followed Mad2 tagged with GFP during mitosis (Gillett et al., 2004; Iouk et al., 2002). However, they found that Mad2-GFP was not visible at kinetochore during an undisturbed metaphase, but only in mitotic cells treated with nocodazole to activate the SAC, causing an arrest in metaphase (Gillett et al., 2004; Iouk et al., 2002). The accumulation of SAC proteins at kinetochores during the meiotic metaphase I and II might be higher than in mitosis, rendering the detection of Mad2 at kinetochores easier.

To confirm the validity of our assay, we first deleted *MAD1*, as it is known that Mad1 is required for the proper localization of Mad2 to kinetochores (Chen et al., 1996; Chen et al., 1998; Chen et al., 1999). In the absence of Mad1, Mad2

forms a diffuse cellular signal and is unable to form any foci (Figure 12). Importantly, Mad2 clusters should persist longer in mutants, which are unable to establish microtubule-kinetochore attachments that generate tension. In the absence of Spo11, meiotic cells cannot initiate recombination (Klapholz et al., 1985; Keeney et al., 1997). Homologous chromosomes are therefore unlinked and the monopolar attachment of chromosomes cannot create tension in meiosis I. Furthermore, Shonn et al. suggested that *spo11Δ* cells were delayed in metaphase I by the SAC (Shonn et al., 2000). As expected, Mad2-neonGreen clusters persist for 57 minutes on average in *spo11Δ* cells at metaphase I (Figure 13). The timing of Mad2 clusters is not affected in metaphase II in *spo11Δ*. To check whether defects in chromosome bi-orientation in metaphase II could trigger a SAC response and delay anaphase II onset, we used the phospho-mimetic mutant *rec8-18D*. In this mutant, cohesin is fully removed at anaphase I onset, letting sister chromatids unattached in metaphase II (Argüello-Miranda et al., 2017; Argüello-Miranda, 2015). We observed a prolongation of Mad2-neonGreen foci for 59 minutes during metaphase II in cells containing the phospho-mimetic mutant *rec8-18D* (Figure 14). These results confirm that lack of tension activates the SAC in both metaphase I and metaphase II.

2.2.2. SAC activity in metaphase I is prolonged in the *spo13* mutant

Next, we followed Mad2-neonGreen foci formation in *spo13Δ* cells. On average, Mad2 clusters persist for 47 minutes in metaphase I, that is, 2.8 times longer than in wild-type cells. This result is consistent with our hypothesis that anaphase I onset is delayed in *spo13Δ* due to prolonged activation of the SAC. Interestingly, we noticed that, although Mad2 foci persist longer in *spo11Δ* than in *spo13Δ* cells, *spo11Δ* mutants nevertheless undergo a second meiotic division during which Mad2 foci re-appear for 13 minutes on average (Figure 13). By contrast, the second division is absent in *spo13Δ* cells (Figure 15). It therefore appears that an extensive delay of Cdc20 activation due to SAC activity cannot be the only cause of the absence of the second meiotic division in the *spo13Δ* mutant. We speculated that Spo13 is required for delaying the meiotic exit until the two meiotic divisions are completed thereby avoiding the second division to be "cut off" in case of a delay in metaphase I.

Katis et al. and Lee et al. found that Spo13 is involved in monopolar attachment (Katis et al., 2004b; Lee et al., 2004). SAC activation and the subsequent

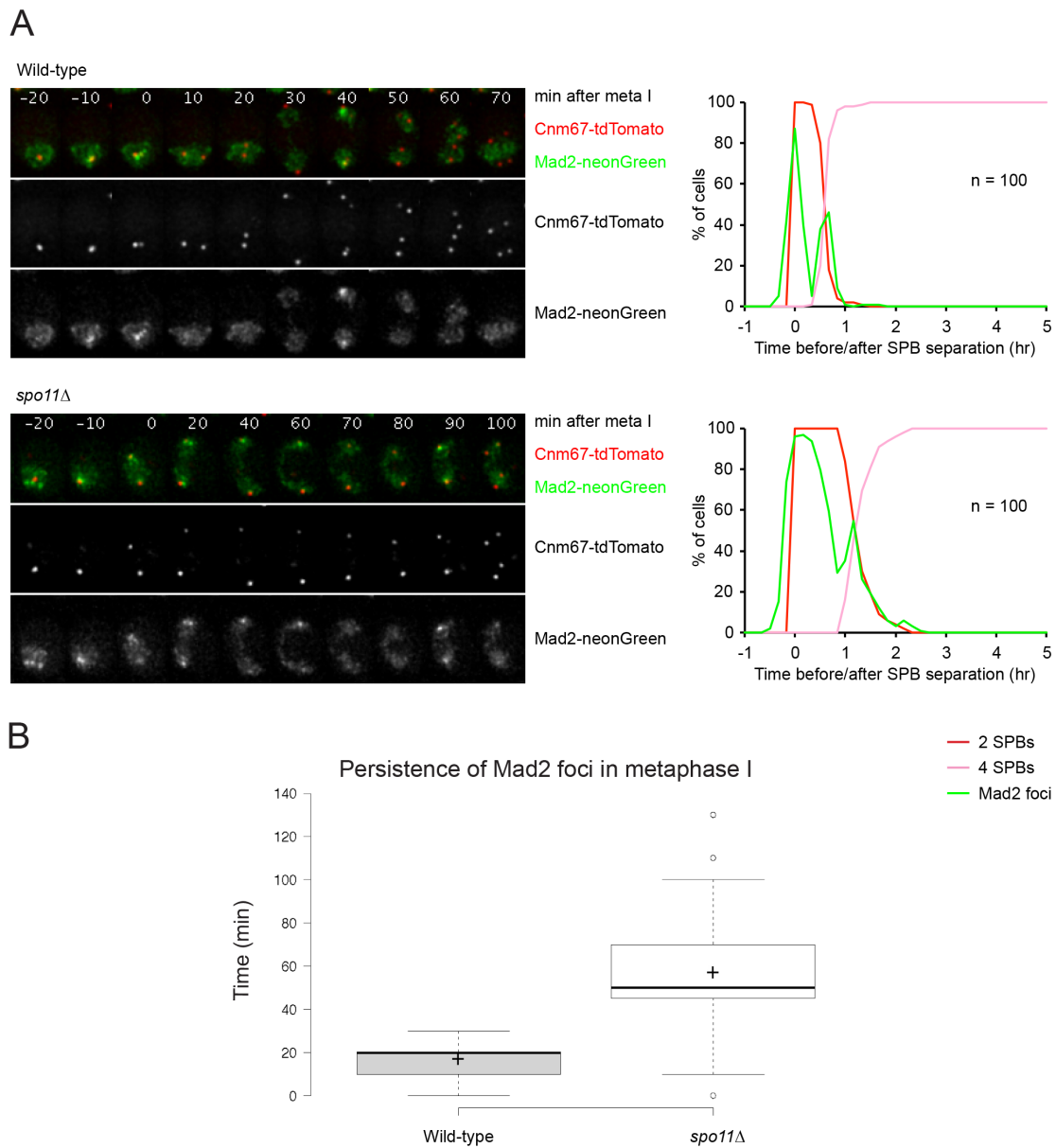


Figure 13: Mad2 foci persist longer in metaphase I in the absence of Spo11.

Mad2-neonGreen foci timing in the *spo11Δ* strain (Z23549) and in wild-type cells (Z23073) is compared. (A) On the left are representative time-lapse images of each strain. On the right are countings of Mad2-neonGreen clusters and SPBs numbers synchronized in silico to the appearance of two SPBs. (B) Box plots comparing the persistence of Mad2 cluster during metaphase I between wild-type cells and *spo11Δ* cells. The center line shows the median (20 minutes for the wild-type and 50 minutes for *spo11* mutant), the box limits indicate the 25th and 75th percentiles. Whiskers extend 1.5 times the interquartile range from the 25th to 75th percentiles and outliers are represented by circles. Crosses represent the samples means. In wild-type cells, clusters persist for a mean time of 17 ± 6 minutes and 10 ± 5 minutes in metaphase I and II respectively while in *spo11Δ*, Mad2-neonGreen clusters persist for 57 ± 21 minutes in metaphase I and 13 ± 8 minutes in metaphase II.

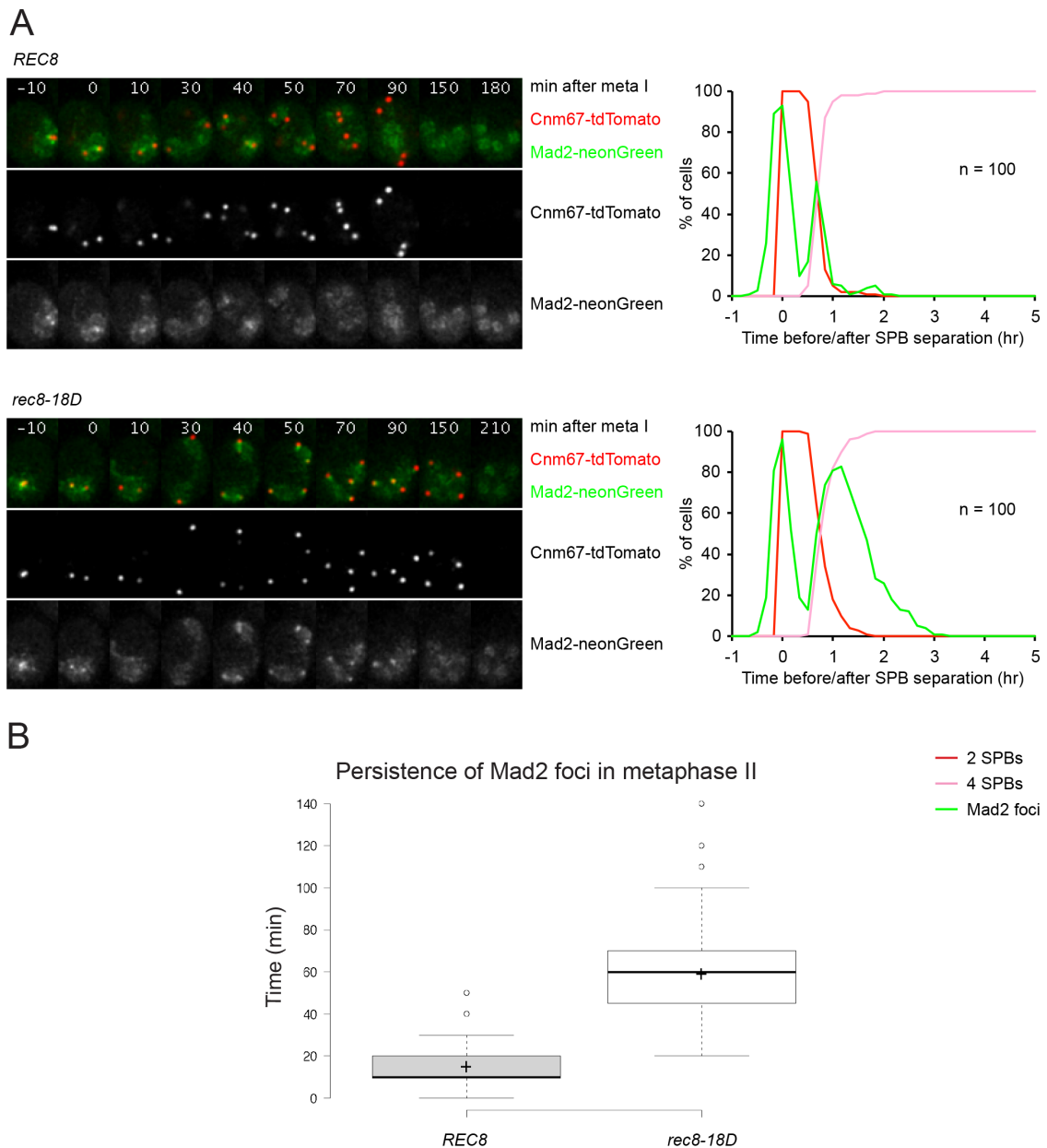


Figure 14: The phospho-mimic Rec8 mutant *rec8-18D* causes prolonged persistence of Mad2 at kinetochores in meiosis II.

Mad2-neonGreen foci timing in wild-type *REC8* (Z27295) cells and *rec8-18D* (Z27294) cells were compared. (A) The countings on the right are synchronized in silico to the appearance of two SPBs. On the left are pictures of a representative cell for each strain. As expected, in metaphase I (2 SPBs), the SAC activation in wild-type cells and in *rec8-18D* cells is comparable: Mad2-neonGreen dots persist on average for 25 ± 9 minutes in wild-type cells and 26 ± 10 minutes in *rec8-18D* cells (B) Box plots comparing the persistence of Mad2 clusters during metaphase II in *REC8* and *rec8-18D* cells. The center lines show the medians (10 minutes for *REC8* cells and 60 minutes for *rec8-18D* mutant), the box limits indicate the 25th and 75th percentiles. Whiskers extend 1.5 times the interquartile range from the 25th to 75th percentiles and outliers are represented by circles. Crosses represent the sample means. Mad2-neonGreen clusters persist for 15 ± 9 minutes in the wild-type and for 59 ± 21 minutes in *rec8-18D* cells.

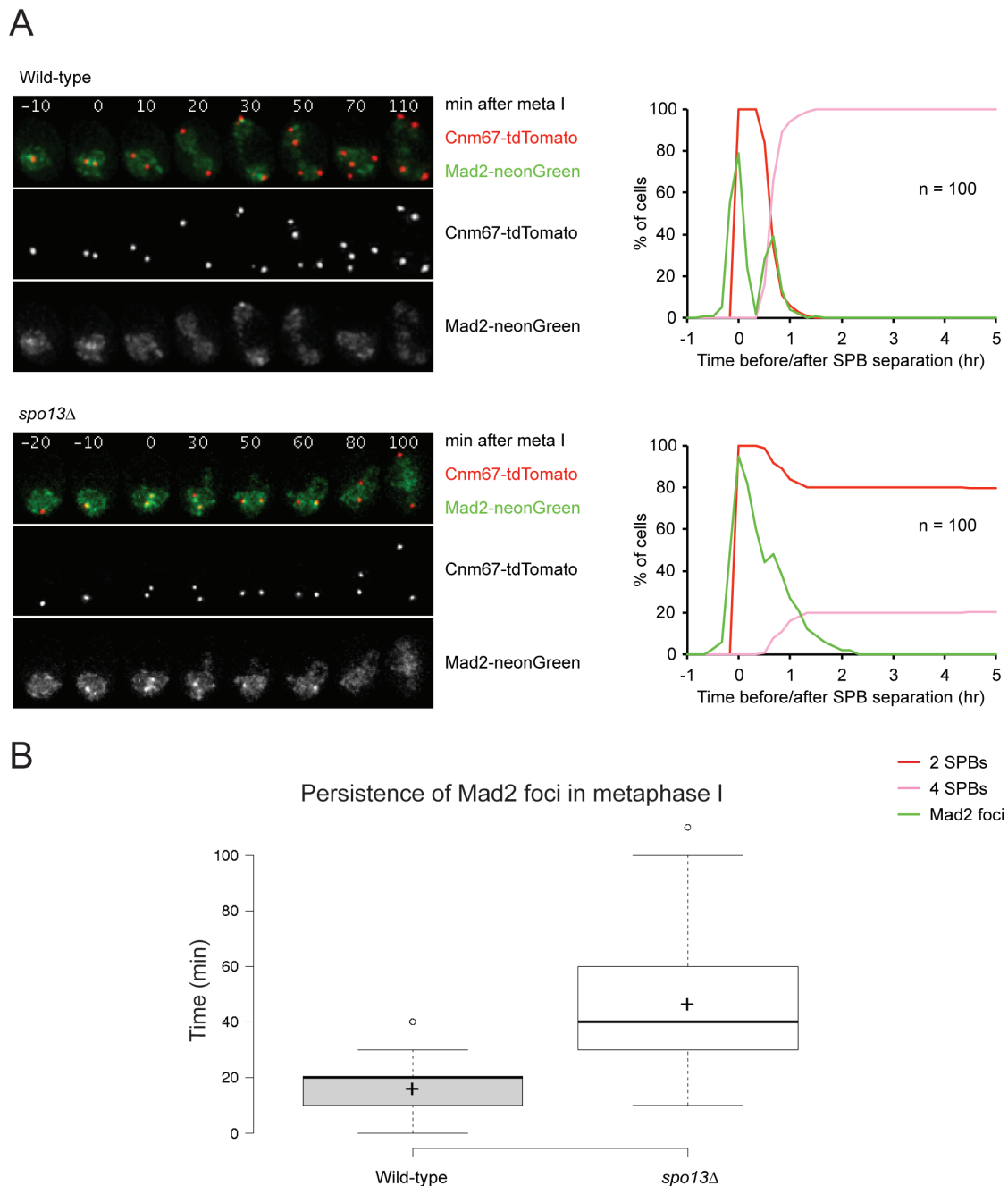


Figure 15: Mad2 foci persist longer in *spo13Δ* than in wild-type cells.

spo13Δ (Z23074) and wild-type (Z23073) strains containing Mad2-neonGreen and Cnm67-tdTomato were filmed and the persistence of Mad2-neonGreen foci was compared between the two strains. (A) The countings are synchronized in-silico to the appearance of two SPBs (entry into metaphase I) and are displayed on the right. On the left are montages for a representative cell of the corresponding strain. The strains showed here are part of the same experiment presented in Figure 12, the wild-type cell is therefore the same. (B) Box plots comparing the persistence of Mad2 clusters between wild-type cells and *spo13Δ* cells during metaphase I. The center lines show the medians (20 minutes for wild-type cells and 40 minutes for *spo13* mutant), the box limits indicate the 25th and 75th percentiles. Whiskers extend 1.5 times the interquartile range from the 25th to 75th percentiles and outliers are represented by circles. Crosses represent the sample means. Mad2-neonGreen foci are observed for 16 ± 7 minutes on average, while in *spo13Δ* cells foci persist for 46 ± 23 minutes.

metaphase I delay in *spo13Δ* cells could be a consequence of a monopolar attachment defect. We therefore assessed the formation and persistence of Mad2 foci in the monopolin mutants *mam1Δ* and *hrr25-zo* (Figure 16). The *hrr25-zo* mutant contains two mutated residues H25R and E34K that are important for Hrr25 function in monopolar attachment (Petronczki et al., 2006). *hrr25-zo* displays a strong defect in sister kinetochores mono-orientation during meiosis I, while the other functions of Hrr25 seem unaffected (Petronczki et al., 2006). In *mam1Δ* cells, Mad2 foci persist for 33 minutes in metaphase I and 23 minutes in metaphase II. In *hrr25-zo*, Mad2 foci are observed for 31 minutes in metaphase I and 25 minutes in metaphase II. Therefore, monopolar attachment defects do trigger a SAC response, as the Mad2 foci persist longer than in the wild-type and anaphase I onset is delayed accordingly. However, the SAC remains active significantly longer in *spo13Δ* cells than in *mam1Δ* or *hrr25-zo* mutants. In *SPO13* deletion, monopolin subunits bind to each other but are unable to form a stable attachment to kinetochores (Katis et al., 2004b; Matos et al., 2008). The reason why the *SPO13* deletion triggers a stronger SAC response than classic monopolin mutants is unclear.

2.2.3. Improving bi-orientation in *spo13Δ* cells partially rescues meiosis II

The lower ratio of bi-oriented versus mono-oriented chromosomes in *spo13Δ* as compared to classic monopolin mutant might increase the number of bivalents with one bi-oriented and one mono-oriented pair of sister kinetochores. This mixture of bi- and mono-orientation could explain why kinetochore-microtubule attachments in *spo13Δ* cells are unable to satisfy the SAC. Another explanation could be that Spo13 is required for inactivating the SAC or to help activating APC/C^{Cdc20}. Katis et al. found that deleting *MAM1* in *spo13Δ* cells increases the rate of sister kinetochores bi-orientation, suggesting that Mam1 retains some residual activity in the absence of Spo13 (Katis et al., 2004b). We used this result to check our first hypothesis and observed that "improving" bi-orientation partially restores the entry into meiosis II in *spo13Δ* cells. Indeed, the deletion of *MAM1* in *spo13Δ* cells partially rescues SPB re-duplication and the second Cdc14 release/capture (Figures 17, data not shown). 64% of *spo13Δ mam1Δ* cells re-duplicates SPBs while only 7% of *spo13Δ* cells do so. However, *spo13Δ mam1Δ* cells still undergo only one nuclear division in what appears to be meiosis II (4 SPBs, Figure 17). The best bi-orientation is obtained in the *spo13Δ spo11Δ mam1Δ* background where almost all the cells enter meiosis II (Figure 18). This rescue is significantly higher than in the *spo13Δ mam1Δ* background.

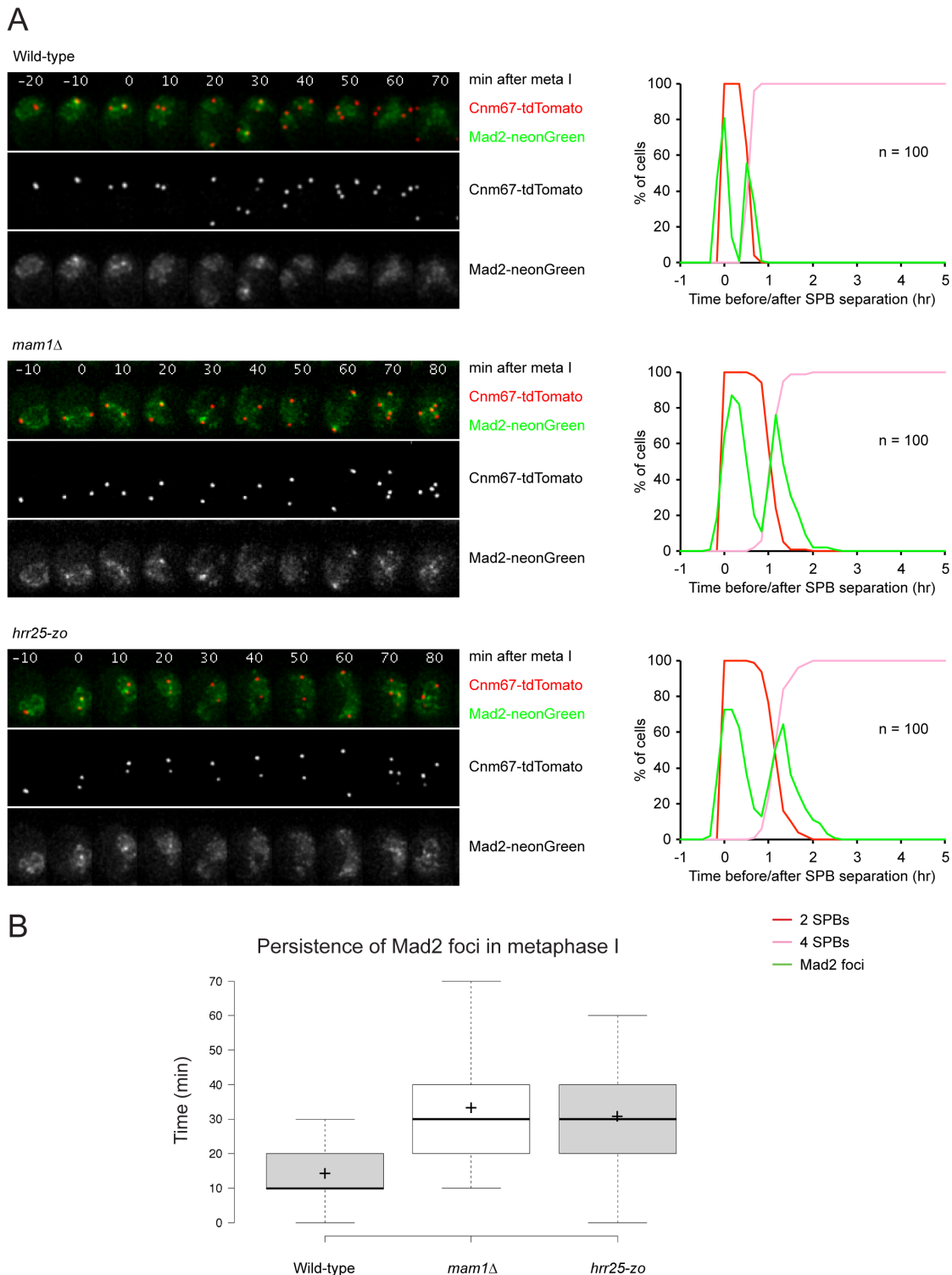


Figure 16: Mad2 foci persist longer in monopolin mutants than in the wild-type.

Filming of wild-type (Z23073), *mam1* Δ (Z23477), and *hrr25-zo* (Z23586) strains containing Mad2-neonGreen and Cnm67-tdTomato. (A) The countings are synchronized in-silico to the appearance of two SPBs and are displayed on the right. On the left are representative time-lapse series of each strain. (B) Box plots comparing the persistence of Mad2 foci during metaphase I between wild-type cells and monopolin mutants. The median times (line) are 10 min for wild-type cells, 30 min for *mam1* Δ cells, and 30 min in *hrr25-zo*. In the wild-type, Mad2-neonGreen foci persist for 14 ± 6 minutes on average (cross) while remaining for 33 ± 12 and 31 ± 15 minutes in *mam1* Δ and *hrr25-zo* cells, respectively.

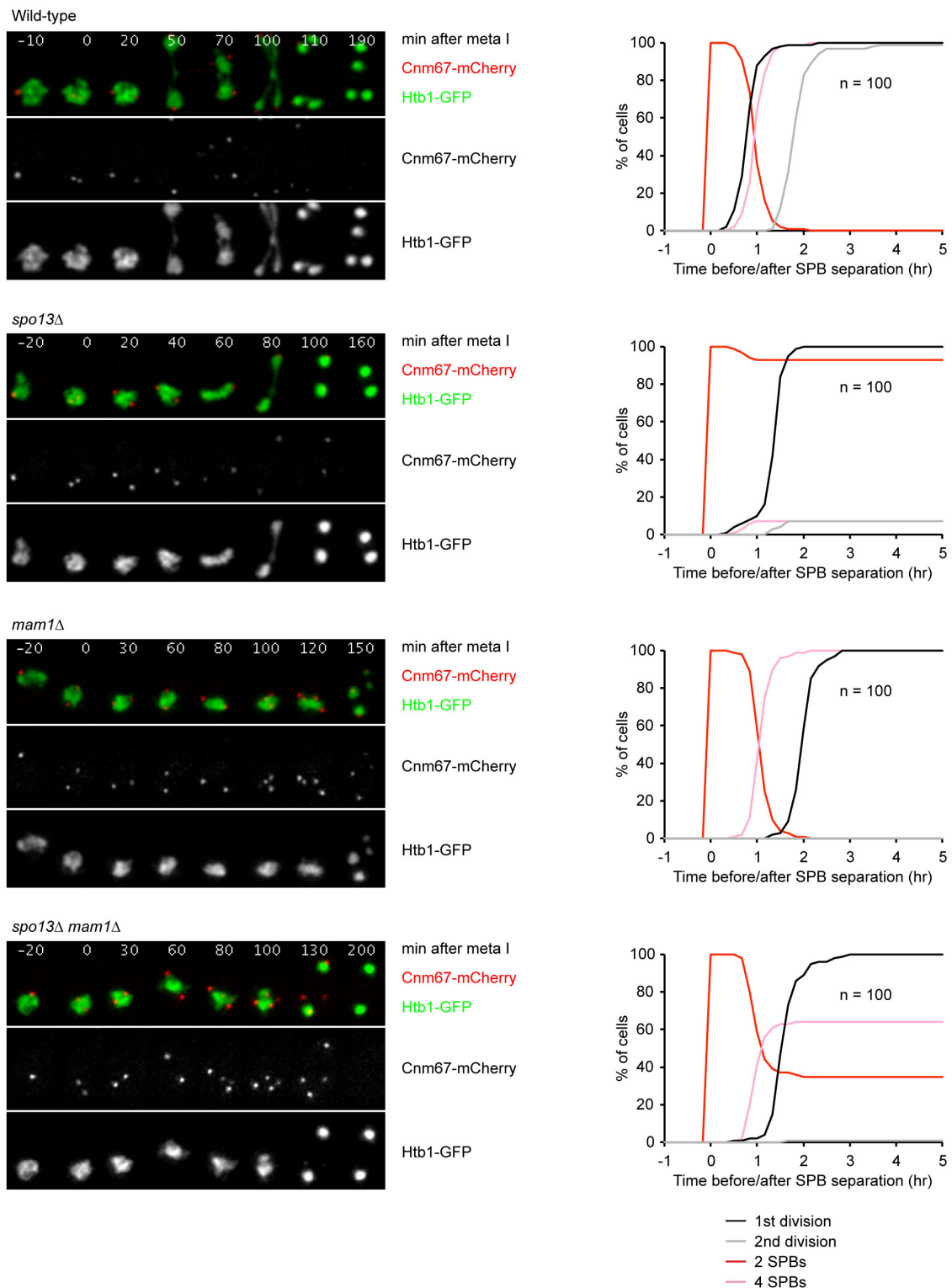


Figure 17: The *MAM1* deletion partially rescues entry into meiosis II in *spo13Δ* cells. Live-cell imaging of wild-type (Z24690), *spo13Δ* (Z24689), *mam1Δ* (Z24688) and *spo13Δ mam1Δ* (Z24687) strains containing Htb1-GFP and Cnm67-tdTomato. On the left are representative time-lapse series for each strain and on the right are the corresponding countings synchronized in-silico to the appearance of two SPBs. While only 7% of *spo13Δ* cells re-duplicate SPBs, we quantified 64% of *spo13Δ mam1Δ* cells with 4 SPBs.

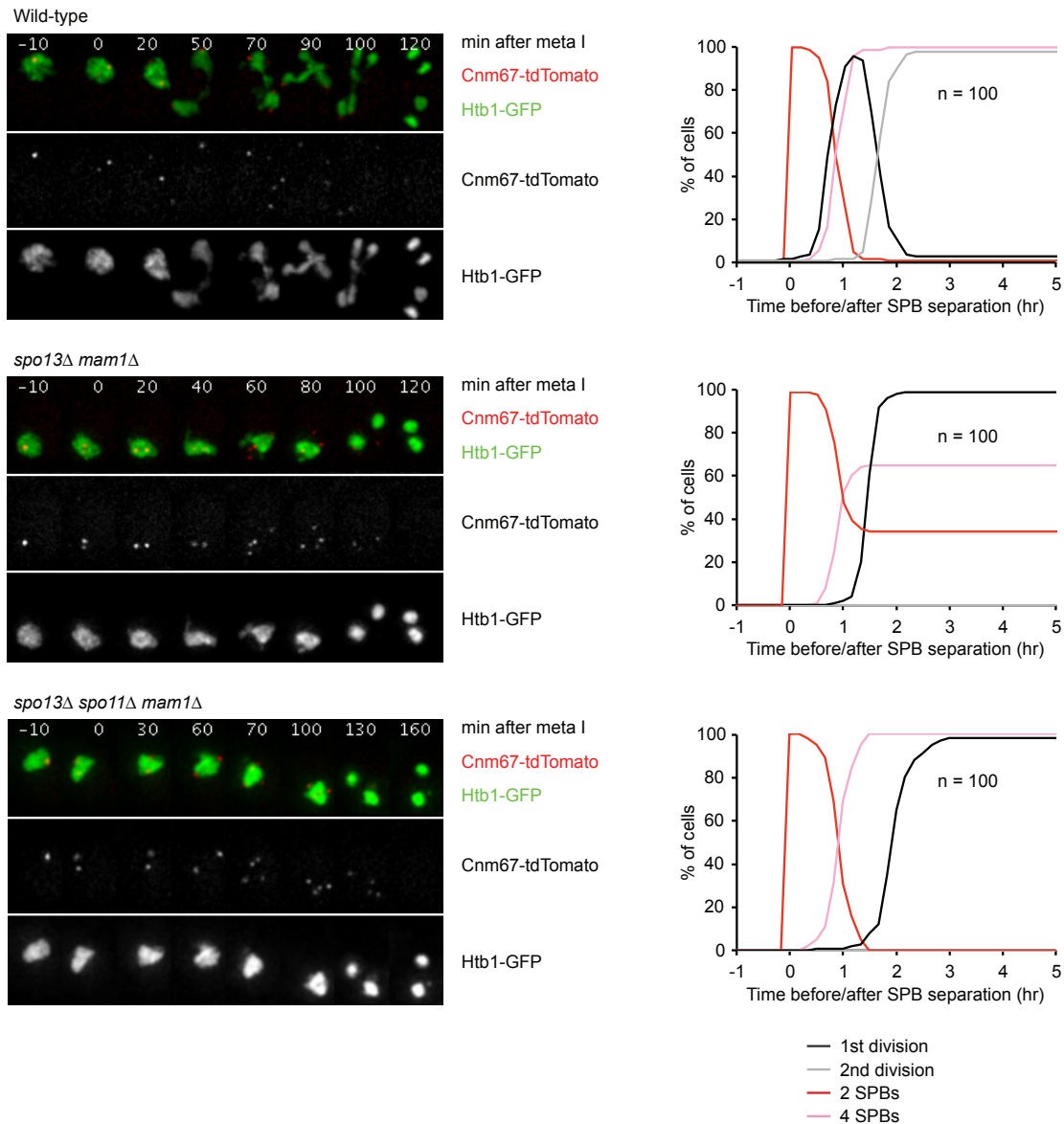


Figure 18: *spo13Δ spo11Δ mam1Δ* cells fully rescue SPBs re-duplication.

Live-cell imaging of wild-type (Z24690), *spo13Δ mam1Δ* (Z33587), and *spo13Δ spo11Δ mam1Δ* (Z33585) strains containing Htb1-GFP and Cnm67-tdTomato. On the left are representative time-lapse series for each strain and on the right, the corresponding countings synchronized in-silico to the appearance of two SPBs. We observe 4 SPBs in 65% of *spo13Δ mam1Δ* cells and in 100% of *spo13Δ spo11Δ mam1Δ* cells. In cells re-duplicating SPBs, nuclear division only occurs when cells have 4 SPBs, indicating that cohesion between sister chromatids is maintained until anaphase II.

2.2.4. Bi-orientation of sister kinetochores in meiosis I does not trigger a strong SAC response

In order to understand why *SPO13* deletion elicits such a strong SAC response, we sought to understand what kind of attachment is sensed by the SAC in metaphase I. Indeed, the bi-orientation of sister chromatids or homologous chromosomes both create tension and are both able to satisfy the SAC. Whether the SAC is able to discriminate between monopolar attachment or bipolar attachment during metaphase I remains unclear. To understand this, we follow Mad2 localization at kinetochores together with the sister chromatids mono- or bi-orientation. For that purpose, we assessed the persistence time of Mad2 clusters for our mutants in metaphase I-arrested cells. To do so, we depleted the two APC/C co-activators involved in meiosis: Cdc20 and Ama1. On average, our control strain *SCC1p-CDC20 ama1Δ* displays Mad2 clusters for 37 minutes and centromeric dots are rarely seen apart since sister kinetochores do not bi-orient in an undisturbed metaphase I (we observed splitting in 23% of cells and only after 147 minutes in metaphase I, Figure 19). The time of Mad2 clusters persistence in *SCC1p-CDC20 ama1Δ* is longer than in the wild-type (16 minutes). This is easily explained by the fact that the SAC and APC/C^{Cdc20} are forming a double-negative feedback loop and shows that APC/C^{Cdc20} plays a part in silencing the SAC (Rattani et al., 2014). Indeed, the SAC and the APC/C^{Cdc20} are inhibiting each other. The MCC inhibits directly the APC/C^{Cdc20} and APC/C^{Cdc20} inhibits the SAC by degrading B-types cyclins (Rattani et al., 2014). *spo13Δ SCC1p-CDC20 ama1Δ* strain splits CEN5 dots in 80% of the cells and 97 minutes after metaphase I entry, on average. This result is consistent with the *spo13Δ* cells monopolar attachment defect. Mad2 foci are observed for 86 minutes on average. We then analysed *spo13Δ mam1Δ* cells that should bi-orient sister chromatids better. 80% of the cells split sister dots 72 minutes after entry into metaphase I on average, which is a rather small improvement compare to *spo13Δ*. Accordingly, Mad2 foci persist for 74 minutes in *spo13Δ mam1Δ*. Finally, 98% of *spo13Δ mam1Δ spo11Δ* cells split CEN5 dots 52 minutes after entry into metaphase I, and Mad2 foci persist for 48 minutes on average (Figure 19). These results suggest that the persistence of SAC activity is inversely correlated to the proportion of sister chromatids bi-orientation. Therefore, bi-orienting sister chromatids faster in *spo13Δ* cells turns off the SAC faster. This explains why deleting *MAM1* or both *MAM1* and *SPO11* can partially rescue the second meiotic division in *spo13* mutant. It also makes unlikely the idea that Spo13 might play a role in silencing the SAC. These results re-enforce the idea that

a mixture of bi- and mono-orientation elicits the strong SAC response and subsequent metaphase I delay observed in *spo13Δ* cells.

Our data shows that *spo13Δ* cells are delayed in metaphase I by the SAC-inhibitory effect on the APC/C. Since reducing the SAC mediated delay either by impairing the SAC or by improving bipolar attachment rescues meiosis II, we can conclude that the metaphase I delay prevents meiosis II from occurring in *spo13Δ* cells. However, the metaphase I delay caused by the SAC is not sufficient to recapitulate the *spo13Δ* phenotype. Indeed, *spo11Δ* mutants experience a very similar delay in metaphase I than *spo13Δ* cells but still undergoes a second meiotic division. Unlike *spo11Δ* cells, where all aspects of meiosis seem to be delayed according to the metaphase I delay, meiosis II seems to be "cut off" in *spo13Δ* cells. The *SPO13* deletion must have additional phenotypes beside this metaphase I delay. Previous works on Spo13 function suggested that the *spo13Δ* phenotype was a combination of monopolar attachment defect and of centromeric attachment defect (Katis et al., 2004b; Lee et al., 2004). However, these studies did not take into account the delay of *spo13Δ* cells in metaphase I. This delay might be responsible for the phenotypes previously observed. We sought to characterize the *spo13Δ mad2Δ* mutant as it represents a good opportunity to characterize Spo13's direct role in certain meiosis-specific functions without them being a consequence of the metaphase I delay we observed.

2.3. Characterization of the *spo13Δ mad2Δ* mutant

The progression of *spo13Δ* cells through meiosis is very different from a wild-type strain, as the mutant cells are delayed for a long time in meiosis I and perform a single division. The published implication of Spo13 in monopolar attachment or cohesin centromeric protection might reflect a direct involvement of Spo13 in these two processes or might be mere effects of the delay that *spo13Δ* cells experience in metaphase I (Shonn et al., 2002; Katis et al., 2004b; Lee et al., 2004). Studying *spo13Δ mad2Δ* mutant gives us the opportunity to scrutinize Spo13's potential roles in these two meiosis-specific processes while leaving aside its abnormal progression through meiosis. We carefully analysed the progression of *spo13Δ mad2Δ* cells through meiosis by live-cell imaging to determine whether Spo13 is directly involved in monopolar attachment and centromeric protection.

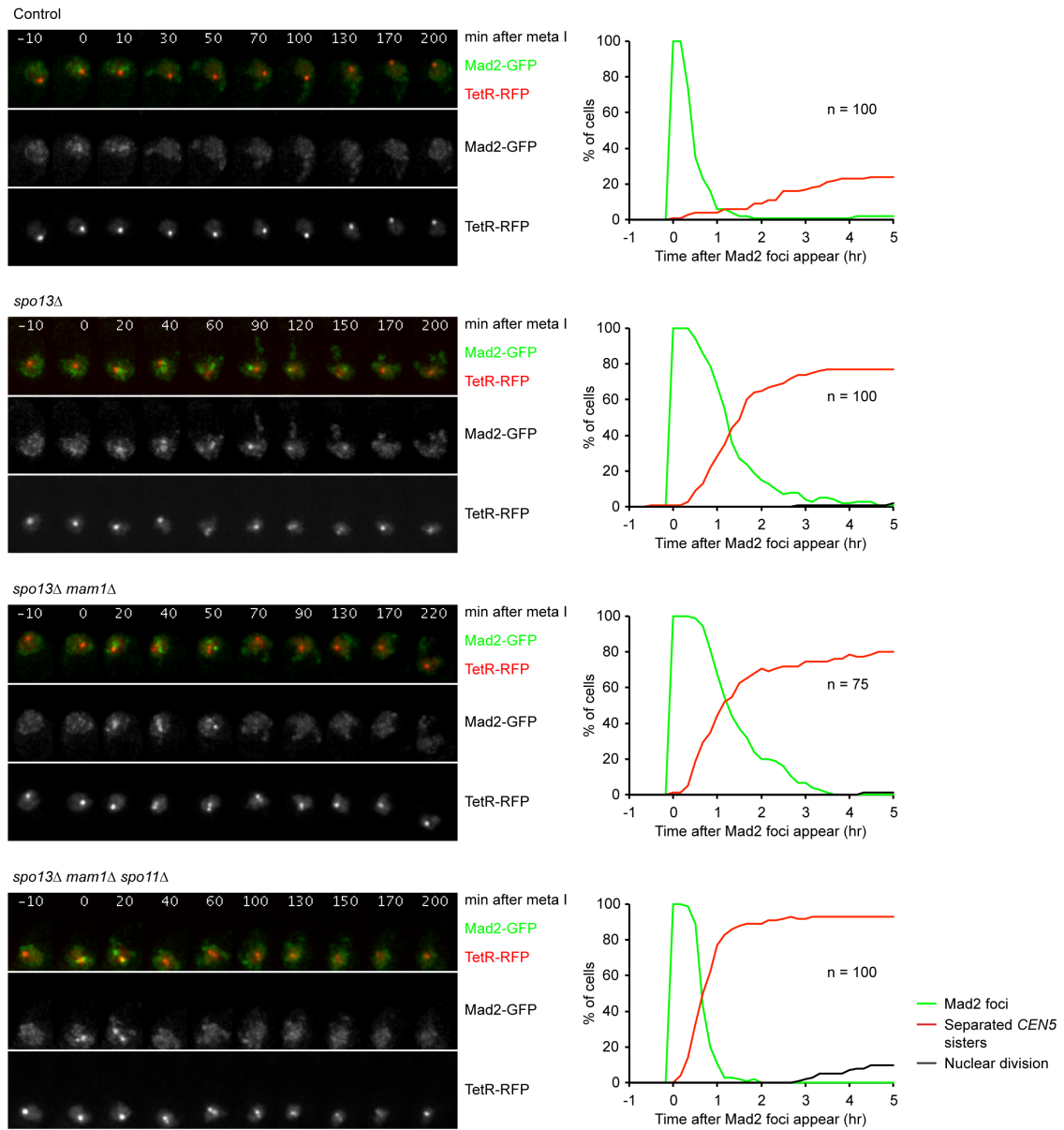


Figure 19: Improving sister chromatids bi-orientation in *spo13Δ* cells reduces the timing of Mad2 clusters.

Live-cell imaging of wild-type (Z29310), *spo13Δ* (Z26965), *spo13Δ mam1Δ* (Z26963), and *spo13Δ mam1Δ spo11Δ* (Z29307) strains arrested in metaphase I by depleting the APC/C co-activators Cdc20 and Ama1 (*SCC1p-CDC20 ama1Δ*) and containing Mad2-neonGreen and heterozygous CEN5 dots. On the left are representative time-lapse series for each strain and on the right are the corresponding countings synchronized in-silico to the appearance of Mad2-neonGreen clusters. The control, in which homologous chromosomes are bi-oriented, keep Mad2 clusters for an average time of 37 ± 23 minutes, while Mad2 clusters persist for 86 ± 35 minutes in *spo13Δ* cells, 72 ± 33 minutes in *spo13Δ mam1Δ* cells and 48 ± 19 minutes in *spo13Δ mam1Δ spo11Δ* cells.

2.3.1. Spo13 is directly involved in monopolar attachment

We first quantified the timing of centromeric dot splitting in the *spo13Δ mad2Δ* mutant. If Spo13 is directly required for monopolar attachment, we should see an elevated proportion of centromeric dot splitting during the first meiotic division compared to the wild-type. If not, centromeric dots should separate exclusively during the second meiotic division, as wild-type cells do (Figures 9 and 21 A). We can see that 14% of *spo13Δ mad2Δ* cells pull centromeric dots apart in meiosis I (segregate on one spindle) while only 7% of *mad2Δ* cells do (Figures 20 and 21 A). Intriguingly, this percentage of dot segregation on one spindle is much lower than one might have expected, as the *spo13Δ* single mutant segregates centromeric dots in 54% of cells (Figures 9). In an attempt to understand the difference in monopolar attachment defect severity between *spo13Δ* and *spo13Δ mad2Δ*, we compared dot splitting in a classical monopolar mutant, *mam1Δ* and *mam1Δ mad2Δ* mutant. We consider that cells split centromeric dots in meiosis I, if we observe two dots for at least two frames, between meiosis I spindle formation and the release of Cdc14. In absence of Mam1, 68% of cells split centromeric dots in meiosis I (Figure 22). However, only 20% of *mam1Δ mad2Δ* cells split centromeric dots in meiosis I (Figures 20 and 21). We conclude that the milder monopolar defect observed in *mam1Δ mad2Δ* or *spo13Δ mad2Δ* mutants is due to the absence of microtubule-kinetochore attachment correction. Finally, we observed that the monopolar attachment defect is increased when *MAM1* and *SPO13* are both deleted as 44% of *spo13Δ mam1Δ mad2Δ* cells split centromeric dots in meiosis I (Figure 21, A). This additive effect of *SPO13* deletion and *MAM1* deletion on monopolar attachment might imply that Spo13 has an additional role in establishing monopolar attachment besides recruiting Mam1 to the kinetochores. Additionally, Mam1-GFP localization to kinetochores is highly reduced in *spo13Δ mad2Δ* cells compared to *mad2Δ* cells but not completely absent (Figure 23). These results, together with the data presented in the previous chapter, re-enforce the idea that monopolin activity is not fully abolished in the absence of Spo13.

2.3.2. *spo13Δ mad2Δ* strain does not display centromeric protection defect

We then looked for evidences of a centromeric protection defect in *spo13Δ mad2Δ* mutant. We noticed that although 98% of *spo13Δ mad2Δ* cells undergoes two rounds of spindle formation and of Cdc14 release/capture, 40% of them fail to divide nuclei in anaphase I and segregates DNA only once in anaphase II while the

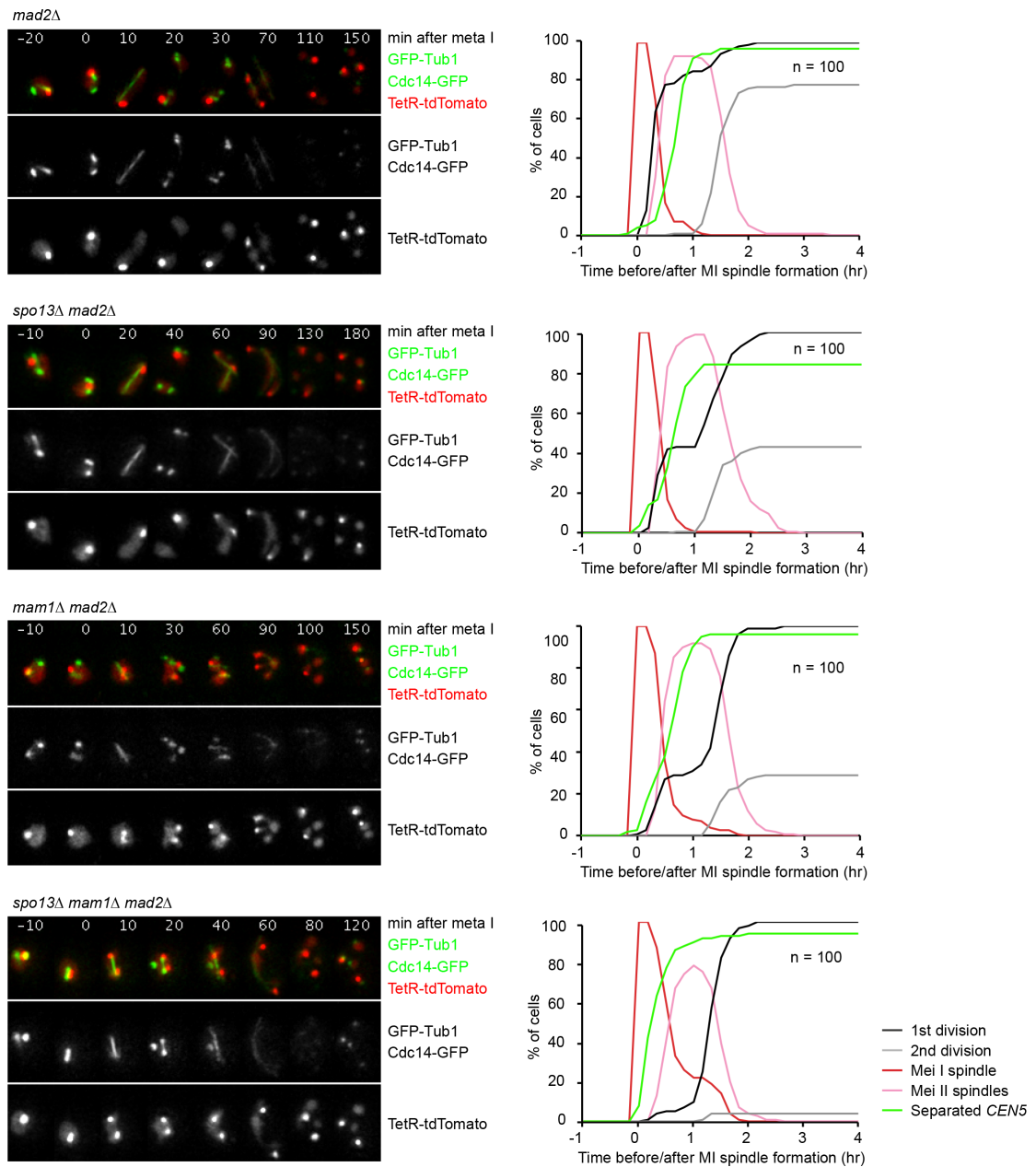


Figure 20: *spo13Δ mad2Δ* cells have a monopolar attachment defect.

mad2Δ (Z24863), *spo13Δ mad2Δ* (Z24861), *mam1Δ mad2Δ* (Z33012) and *spo13Δ mam1Δ mad2Δ* (Z24862) strains containing the heterozygous markers Tub1-GFP, Cdc14-GFP, TetR-tdTomato and CEN5-tetO dots were filmed. On the left are time-lapse series of a representative cell of each strain. On the right are countings synchronized in-silico to the formation of meiosis I spindles. Quantifications of centromeric dots splitting in meiosis I are displayed in Figure 21.

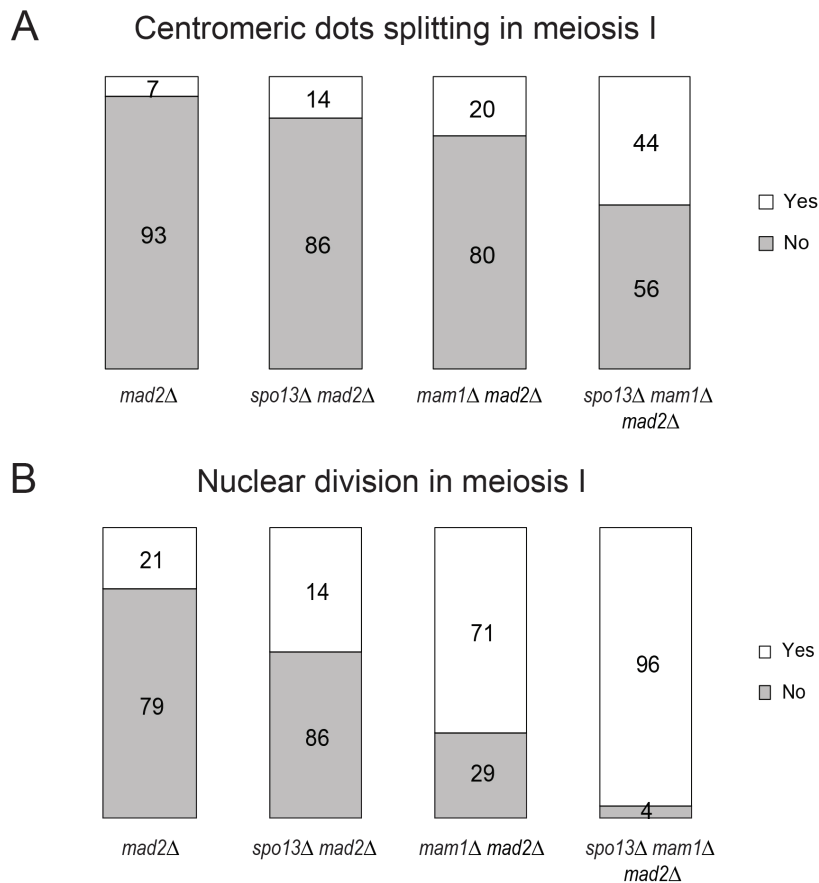


Figure 21: Comparison of monopolar attachment defect in *spo13Δ mad2Δ* and *mam1Δ mad2Δ* cells.

Quantification of centromeric dot splitting and nuclear division in meiosis I for the experiment presented in Figure 20. (A) We quantified the number of cells that split tetO dot on a single spindle against the ones that do not. 14% of *spo13Δ mad2Δ* cells split CEN5 dots in meiosis I while this percentage reached 20% in *mam1Δ mad2Δ*. In *spo13Δ mam1Δ mad2Δ*, 44% of cells split CEN5 centromeric dot in meiosis I. (B) Quantification of cells failing to undergo nuclear division in meiosis I. As expected, the defect in the first nuclear division correlates with the monopolar attachment defect quantified in the panel A.

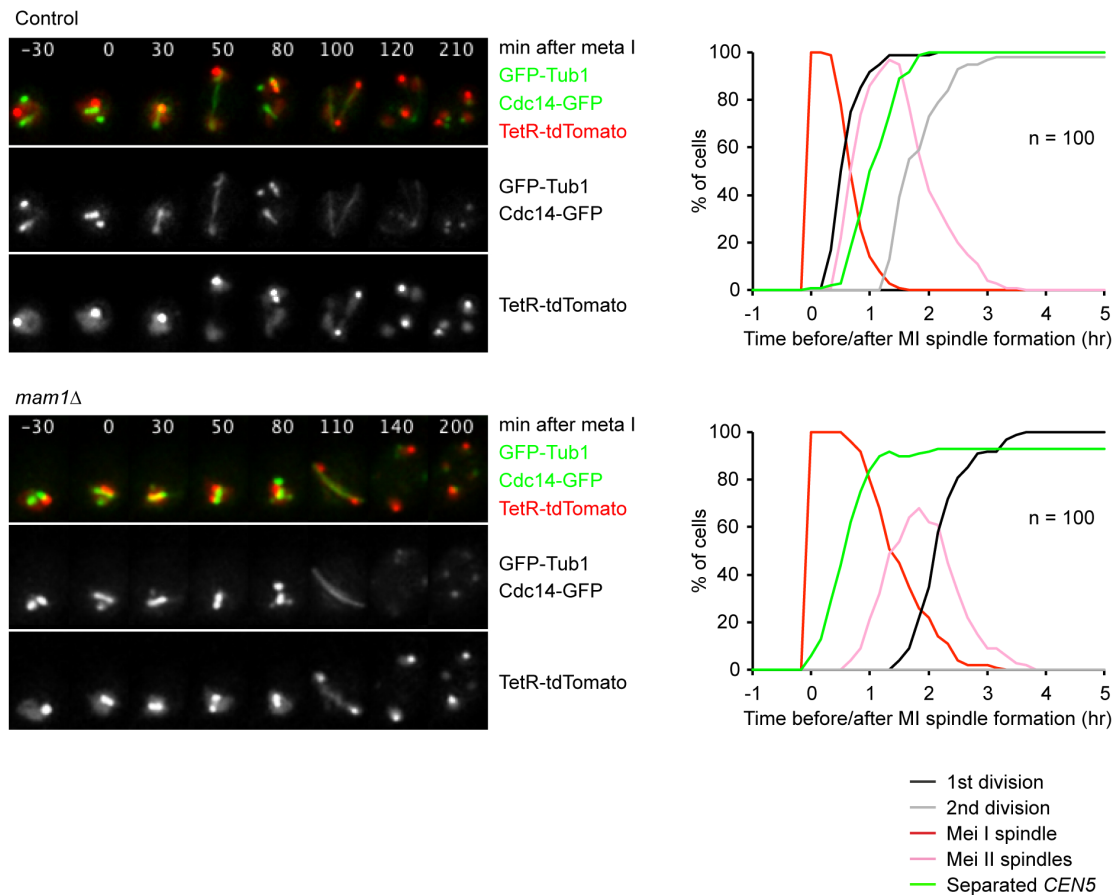


Figure 22: *mam1* Δ cells bi-orient sister kinetochores in meiosis I.

Wild-type (Z24864) and *mam1* Δ (Z31843) strains containing the heterozygous markers Tub1-GFP, Cdc14-GFP, TetR-tdTomato, and centromeric dots CEN5-tetO were filmed. On the right are countings of each strain synchronized to the formation of meiosis I spindle, and on the left are corresponding time-lapse series of representative cells. In the wild-type strain, 100% of cells segregate CEN5 dots in meiosis II, while 68% of *mam1* Δ cells split CEN5 dots in meiosis I. More specifically, we consider that CEN5 dots split in meiosis I if we observe two dots after the formation of meiosis I spindle and until the first release of Cdc14. Because centromeric cohesin protection is not affected, *mam1* Δ cells fail to divide nuclei at anaphase I onset and undergoes a single nuclear division in anaphase II, once centromeric cohesin has been destroyed.

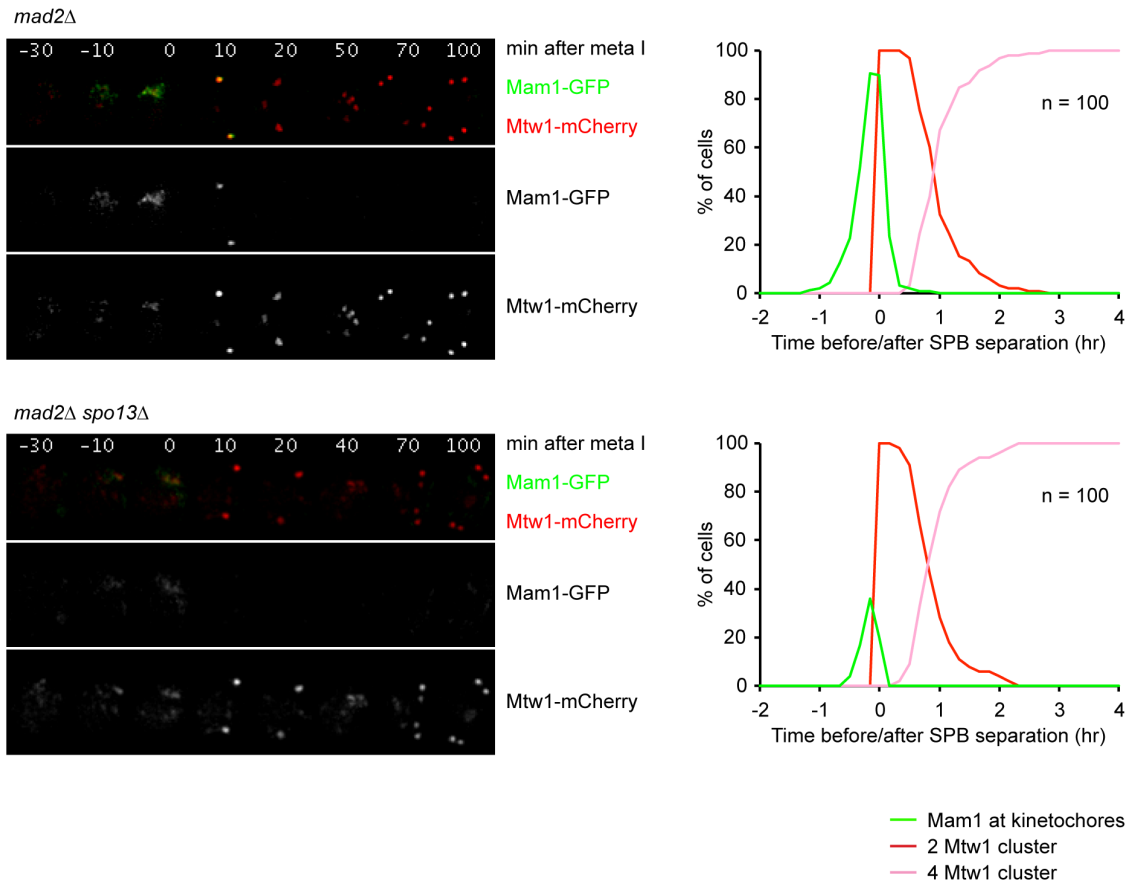


Figure 23: Mam1-GFP does not localize to kinetochores in *spo13Δ mad2Δ* cells.

Filming of *mad2Δ* (Z24519) and *spo13Δ mad2Δ* (Z25101) strains containing Mam1-GFP and the kinetochore protein Mtw1-mCherry. On the right are countings of each strain synchronized to the clustering of kinetochores into one cluster and on the left are the corresponding time-lapse series of a representative cell. Mam1-GFP localizes at kinetochores in metaphase I and disappears around anaphase I in wild-type cells. In *spo13Δ* however, Mam1-GFP localizes poorly to kinetochores and its intensity is strongly reduced.

remaining 60% undergo two meiotic divisions. This first 40% of cells strongly resemble a classic monopolin mutant such as a *mam1* Δ or a *hrr25-zo* strains. Consistent with previous work, in these two mutants, sister kinetochores are bi-oriented in metaphase I but failed to divide in anaphase I since centromeric cohesin complexes prevent it by maintaining sister kinetochores bound together (Figure 22 and 20) (Tóth et al., 2000). Sister chromatids are then segregated in anaphase II, once centromeric protection is lost. The fraction of cells unable to divide in meiosis I should increase if the fraction of sister chromatids bi-orientation in metaphase I is increased. Indeed, deleting *SPO11* in a *spo13* Δ *mad2* Δ cells increases the fraction of cells unable to divide in meiosis I to 65%. This result strongly suggests that centromeric cohesin protection is not impaired in *spo13* Δ *mad2* Δ cells.

If true, abrogating centromeric protection in meiosis I should restore the first nuclear division in *spo13* Δ *spo11* Δ *mad2* Δ cells. Indeed, the depletion of Sgo1 protein in *spo13* Δ *spo11* Δ *mad2* Δ cells restores the first meiotic division in more than 90% of these cells (Figure 24). We also checked nuclear division in the phosphomimic mutant of Rec8, *rec8-18D*, which cannot be protected from separase in anaphase I. We observed an almost complete rescue of the first nuclear division in *rec8-18D* *spo13* Δ *spo11* Δ *mad2* Δ cells with 94% of cells undergoing two nuclear divisions, while only 27% of *spo13* Δ *spo11* Δ *mad2* Δ cells manage to do so (Figure 25). This set of experiments suggests that, unlike the *spo13* single mutant, *spo13* Δ *mad2* Δ *spo11* Δ cells are able to maintain the cohesion between sister chromatids until anaphase II.

Rec8 localization and removal is undisturbed in *spo13* Δ *mad2* Δ cells

To further confirm these results, we directly examined the players of sister-chromatids protection by time-lapse imaging. First, we imaged the cohesin subunit Rec8 tagged with the green fluorescent protein, neonGreen (Argüello-Miranda et al., 2017). In wild-type cells, which protect centromeric Rec8, the Rec8-neonGreen signal is lost in two steps: the strong nuclear-like signal, corresponding to Rec8 loaded on chromosome arms, is removed at the onset of anaphase I, while two weak Rec8 clusters, localized close to the SPBs and corresponding to centromeric cohesin, persist until the onset of anaphase I (Figure 26) (Argüello-Miranda et al., 2017). When the centromeric protection machinery is disturbed, for instance by depleting shugoshin, all Rec8 signals are lost as cells undergo anaphase I (Argüello-Miranda et al., 2017).

Most *spo13* Δ cells remove Rec8 completely as they undergo their single division (Figure 26). This result is consistent with articles reporting a defect in

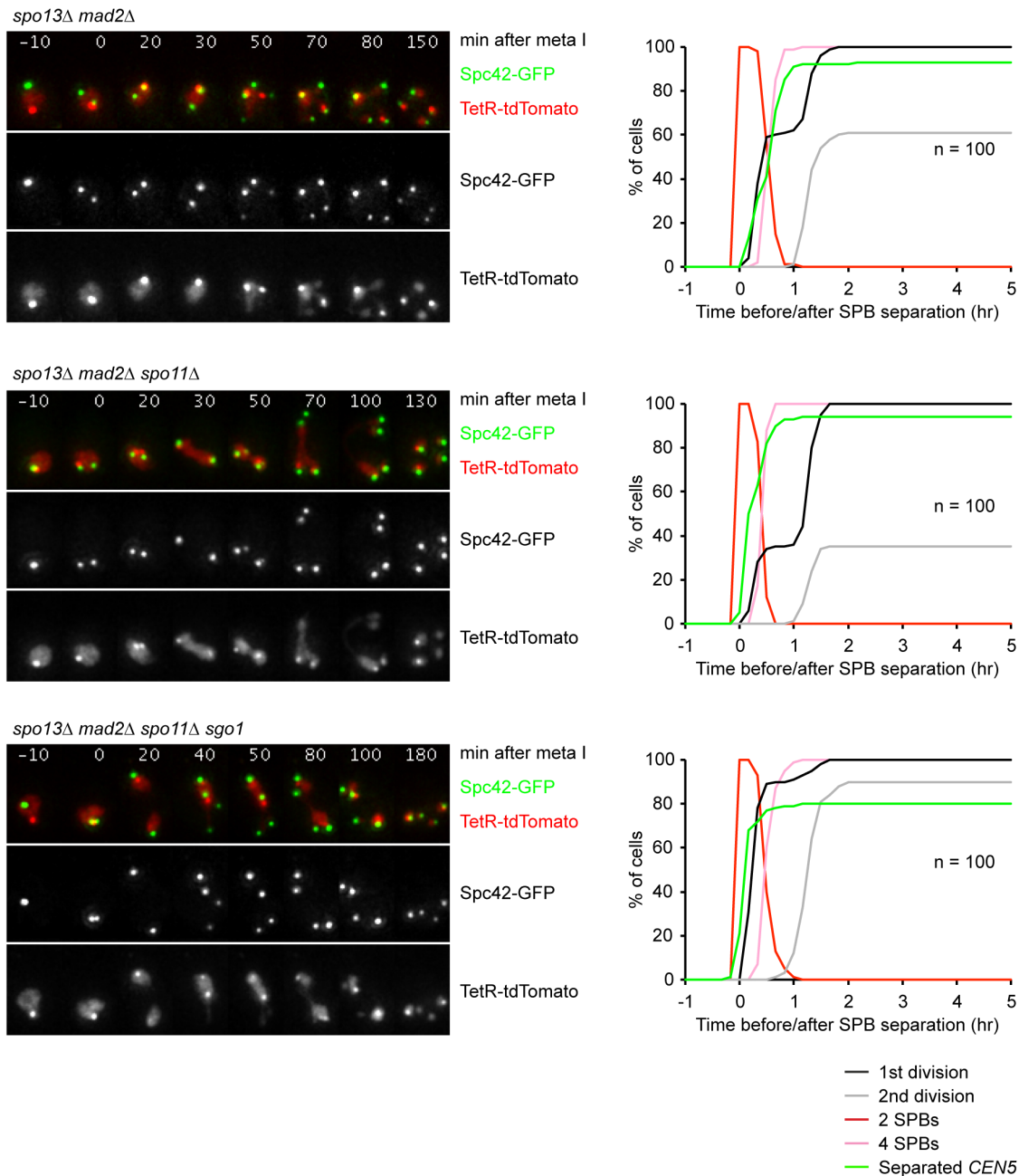


Figure 24: Shugoshin depletion rescues the first nuclear division in *spo13Δ spo11Δ mad2Δ* cells.

spo13Δ mad2Δ (Z25958), *spo13Δ spo11Δ mad2Δ* (Z25957) and *spo13Δ spo11Δ mad2Δ CLB2p-SGO1* (Z25956) strains containing the SPB marker SPC42-GFP, TetR-tdTomato, and centromeric CEN5-tetO dots were filmed. On the left side are montages of a representative cell of each strain. On the right side are countings of the corresponding strains synchronized in-silico to the appearance of two SPBs. 39% of *spo13Δ mad2Δ* cells fail to undergo a nuclear division in meiosis I while 65% of *spo13Δ spo11Δ mad2Δ* strains fail to divide in meiosis I. The depletion of Sgo1 restores the first nuclear division, as 90% of *spo13Δ spo11Δ mad2Δ CLB2p-SGO1* cells undergo two nuclear divisions.

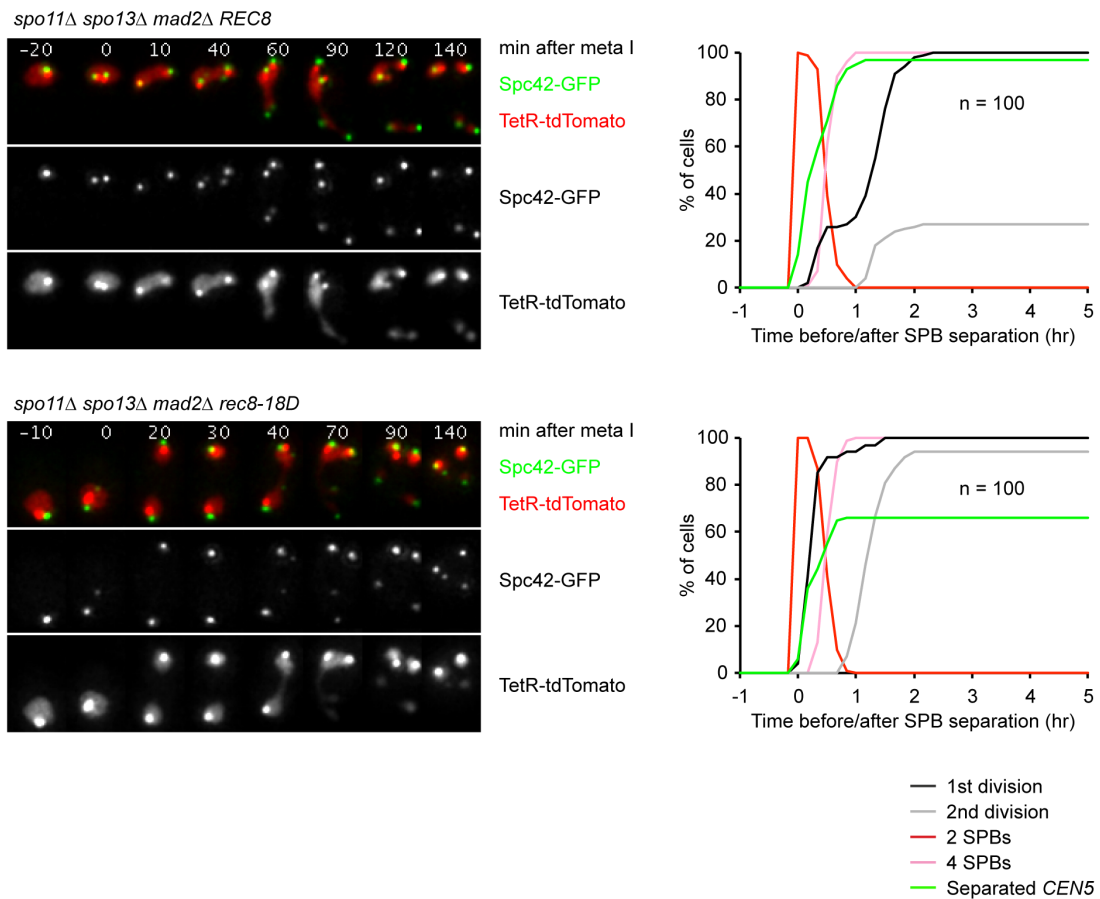


Figure 25: The *rec8-18D* mutation restores the first nuclear division in *spo13Δ spo11Δ mad2Δ* cells.

spo13Δ spo11Δ mad2Δ (Z32951), and *spo13Δ spo11Δ mad2Δ rec8-18D* (Z32950) strains containing the SPB marker *SPC42-GFP*, TetR-tdTomato, and centromeric dots *CEN5-tetO* were filmed. On the left are representative time-lapse series for each strain. On the right are countings of each strain synchronized in-silico to the appearance of two SPBs. 73% of *spo13Δ spo11Δ mad2Δ* cells undergo a single nuclear division while only 6% of *spo13Δ spo11Δ mad2Δ rec8-18D* cells fail to undergo two nuclear divisions.

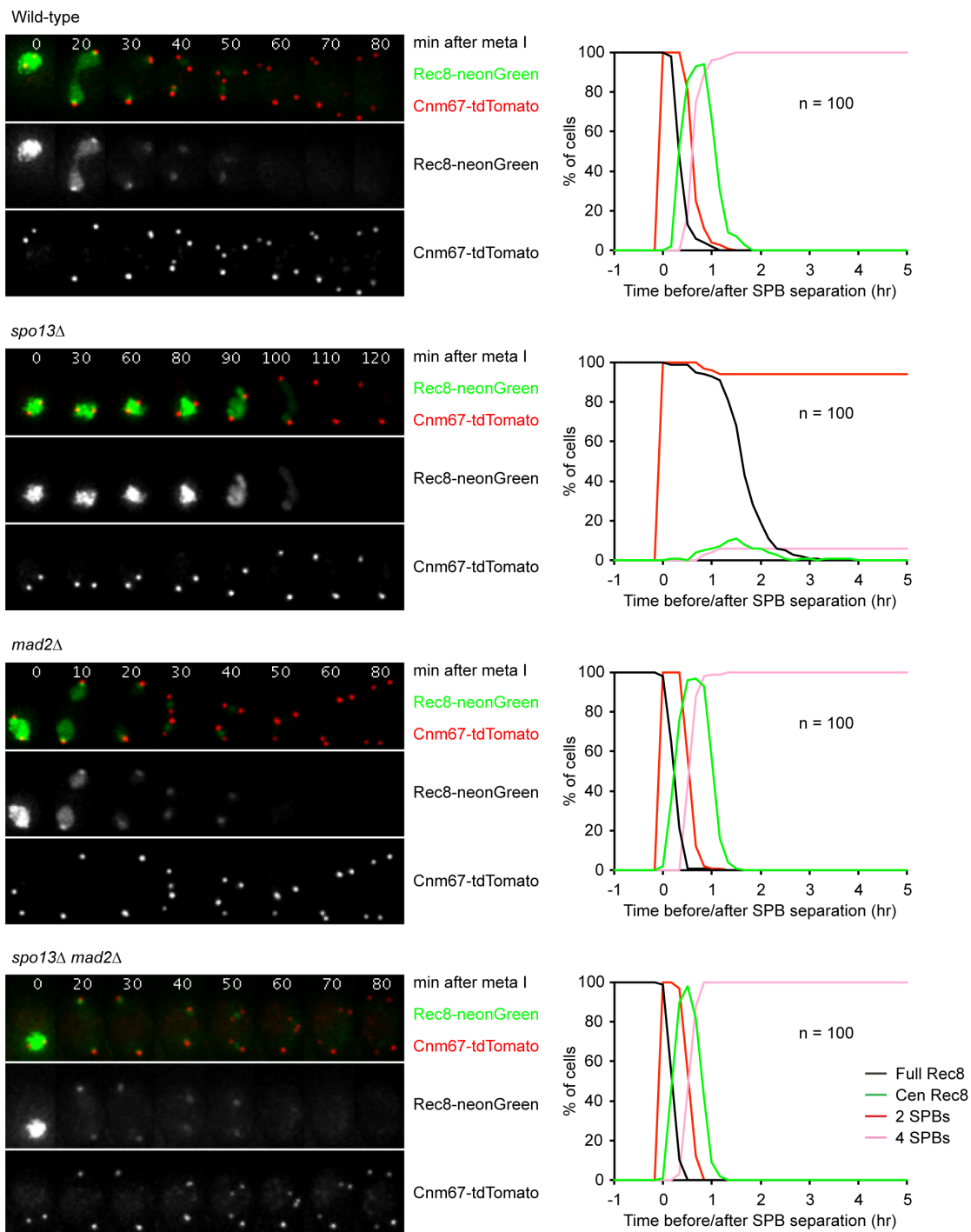


Figure 26: Rec8 is degraded in two steps in wild-type cells, *mad2Δ* and *spo13Δ mad2Δ* cells, while being degraded in a single step in the *spo13Δ* single mutant.

Filming of wild-type (Z25869), *spo13Δ* (Z25867), *mad2Δ* (Z25868), and *spo13Δ mad2Δ* (Z25866) strains containing Rec8-neonGreen and Cnm67-tdTomato were compared. On the left are representative time-lapse series for each strain, and on the right are the corresponding counting synchronized in silico to the formation of 2 SPBs. In the wild-type, *mad2Δ* and *spo13Δ mad2Δ* cells, Rec8 is cleaved in two steps: the bulk of the Rec8-neonGreen signal disappears at anaphase I, while centromeric Rec8 persists until after the appearance of four SPBs. In *spo13Δ* mutant, however, almost all cells lose the Rec8-neonGreen signal at anaphase I onset.

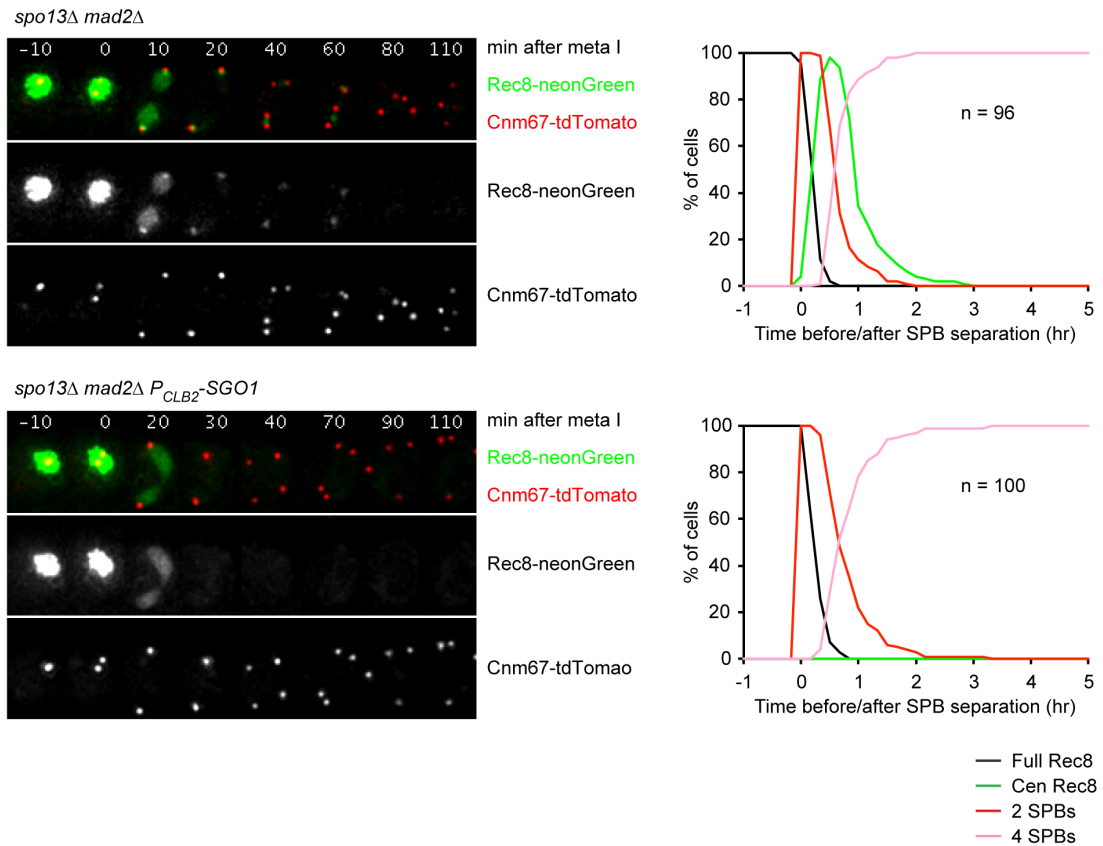


Figure 27: Rec8 is degraded in two steps in *spo13Δ mad2Δ* cells, whereas it is degraded in a single step in *CLB2p-SGO1 spo13Δ mad2Δ* cells.

Filming of *spo13Δ mad2Δ* (Z32304), and *CLB2p-SGO1 spo13Δ mad2Δ* (Z32302) strains containing Rec8-neonGreen and Cnm67-tdTomato. On the left are representative time-series for each strain, and on the right are the corresponding countings synchronized in silico to the formation of two SPBs. In *spo13Δ mad2Δ* cells, Rec8 is cleaved in two steps: the bulk of the Rec8-neonGreen signal disappears at anaphase I, while centromeric Rec8 persists until after the appearance of four SPBs. Upon depletion of Sgo1, all Rec8-neonGreen signals are lost at once at anaphase I onset (*spo13Δ mad2Δ CLB2p-SGO1*).

centromeric protection in *spo13Δ* (Lee et al., 2004; Katis et al., 2004b; Shonn et al., 2002). However, *spo13Δ mad2Δ* cells remove Rec8 in two steps as does the wild-type strain and the *mad2Δ* strains (Figure 26). In these 3 strains, the bulk of chromosomal arm cohesin signal is lost at anaphase I onset, whereas the two Rec8 foci corresponding to centromeric cohesin persist until anaphase II onset. We did not detect any significant difference in cohesin removal between *spo13Δ mad2Δ* and the *mad2Δ* single mutants used as a control (Figure 26). When shugoshin is depleted from *spo13Δ mad2Δ* cells, the entire Rec8 signal is lost in a single step at anaphase I onset and centromeric Rec8 foci are never observed (Figure 27). These results confirm that centromeric cohesin is cleaved normally at the onset of anaphase II in *spo13Δ mad2Δ* cells.

The centromeric protection machinery localizes normally at kinetochores in *spo13Δ mad2Δ* cells

Additionally, we looked directly at the protection machinery by imaging the regulatory subunit of the PP2A phosphatase Rts1 tagged with neonGreen in *spo13Δ mad2Δ* and in *mad2Δ* cells (Figure 28). We did not detect any differences in either loading or removal of Rts1 from kinetochores between these two strains: in both, Rts1 remains clustered at kinetochores for 49 minutes on average. Rts1 localizes at kinetochores at metaphase I entry and is removed in meiosis II, that is, after SPB re-duplication. Hence, the loading of the centromeric protection machinery is not affected by Spo13, at least in SAC-defective cells.

The centromeric protection machinery localizes normally at kinetochores in metaphase I in the *spo13* single mutant

Several studies suggest that centromeric protection is defective in the *spo13Δ* single mutant (Shonn et al., 2002; Lee et al., 2004; Katis et al., 2004b). This defect might be easily explained if Sgo1-Rts1 was unable to persist at kinetochores during the long metaphase I arrest caused by the deletion of Spo13. Therefore, we sought to assess the localization of Rts1 in the absence of Spo13 only. We compared Rts1-neonGreen loading and removal in a wild-type strain and in the *spo13Δ* mutant (Figure 28). It appears that Rts1 localizes normally to kinetochores in the absence of Spo13. The signal becomes even stronger than in wild-type cells due to the metaphase I delay. On average, Rts1 signal localizes to kinetochores for a total time of 58 minutes in the wild-type and 90 minutes in *spo13Δ* cells. Although this combination of tagged proteins does not allow us to assess the timing of nuclear division, we can see that Rts1 remains loaded onto kinetochores for the whole *spo13Δ* mutant's metaphase I delay and is fully removed as SPBs segregate away from each other. Additionally, this timing fits with the timing of Rec8 removal we assessed earlier (Figure 26). It seems that, although the centromeric cohesin protection machinery is present at metaphase I in *spo13Δ* cells, it is removed at anaphase I onset and that, consequently centromeric cohesin is cleaved during the first and only division of the *spo13* mutant.

2.3.3. Conclusion

A careful analysis of the *spo13Δ mad2Δ* mutant, in which the metaphase I delay caused by SAC inhibition of APC/ C^{dc20} is abolished, shows that the *spo13Δ* mutant is defective in chromosomes mono-orientation. Similarly to the *spo13* single

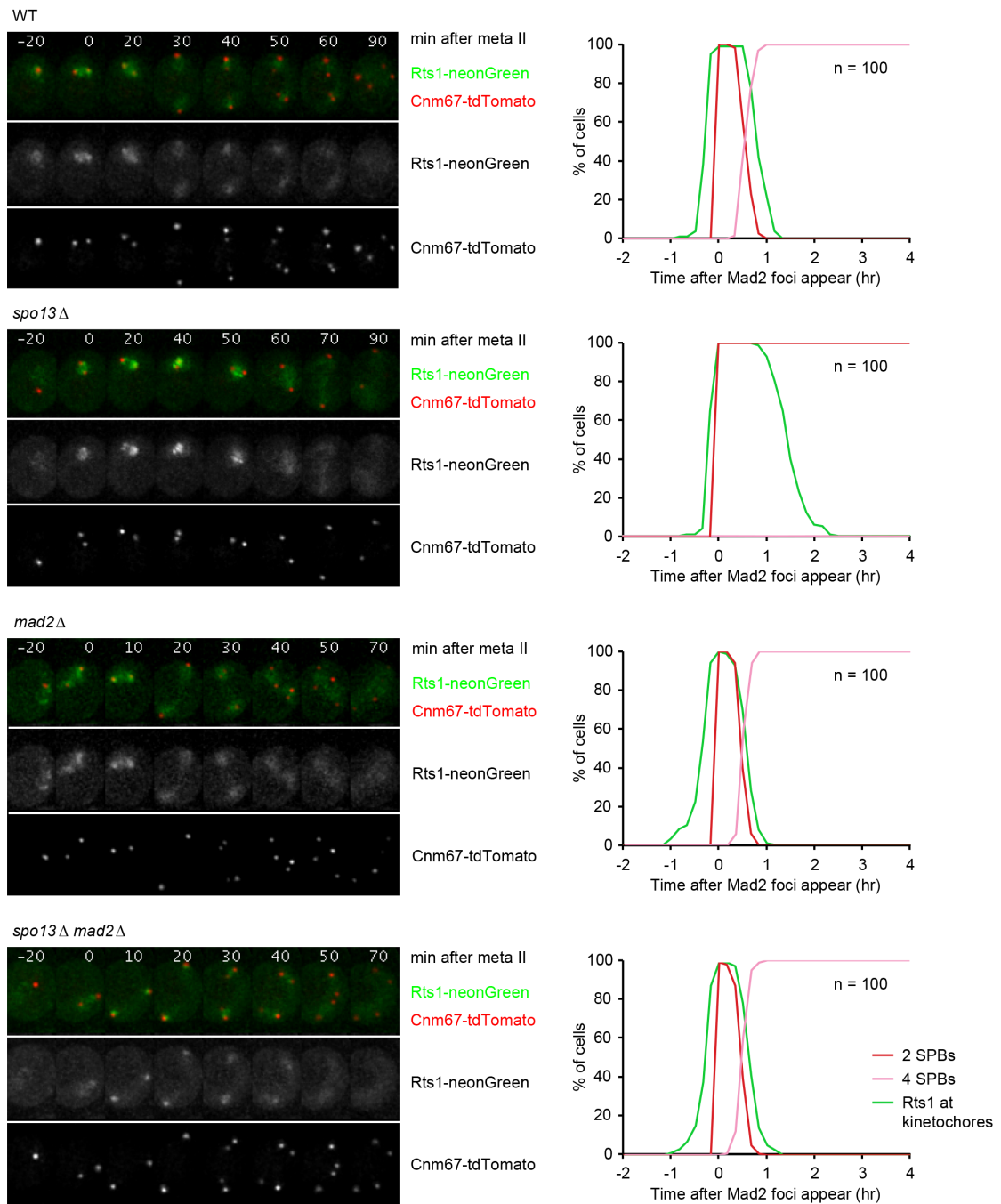


Figure 28: Rts1 localization in *spo13Δ* and *spo13Δ mad2Δ* cells.

Wild-type (Z33198), *spo13Δ* (Z33197), *mad2Δ* (Z33196) and *spo13Δ mad2Δ* (Z33195) strains containing Rts1-neonGreen and Cnm67-tdTomato were filmed. On the left are representative time series for each strain, and on the right are the corresponding countings synchronized in silico to the formation of two SPBs. Rts1 persists at kinetochores for an average time of 58 minutes in the wild-type and for 90 minutes in *spo13Δ* cells.

mutant, *spo13Δ mad2Δ* cells have an abnormal incidence of sister chromatids bi-orientation in meiosis I and fail to localize Mam1 to kinetochores. Hence, we can conclude that the monopolar attachment defect observed in *spo13Δ* cells is not a mere consequence of their delay in metaphase I but reflects a direct role of Spo13 in sister kinetochore mono-orientation.

By contrast, while our results confirm that the *spo13Δ* single mutant cleaves all the cohesin complexes during its single nuclear division (Figures 26 and 28) (Shonn et al., 2002; Katis et al., 2004b; Lee et al., 2004), *spo13Δ mad2Δ* cells do not display any defect in protecting centromeric cohesin (Figures 24, 25, 26, 27 and 28). Furthermore, *spo13Δ mam1Δ* cells that enter meiosis II also seem to retain sister chromatids cohesion until the second wave of APC/C activity (Figure 18). Indeed, *spo13Δ mam1Δ* cells that form four SPBs, only divide their nuclei once in meiosis II. Therefore, abrogating the metaphase I delay of *spo13Δ* cells restores the two-step cleavage of cohesin. Thus, the centromeric protection defect observed in *spo13Δ* single mutant is a consequence of its delay in metaphase I rather than a direct role of Spo13 in the centromeric protection machinery.

So far, we can conclude that *SPO13* deletion causes a moderate monopolar attachment defect. This defect causes the SAC to inhibit APC/C^{Cdc20} for a prolonged period. This prolonged arrest in metaphase causes meiosis II to be cut off. We already observed that cutting off the second division is not a mere consequence of the metaphase delay. Hence, Spo13 must be controlling a more fundamental aspect of the cell cycle machinery, which prevents a premature exit from meiosis when the first nuclear division is delayed. The fact that *spo13Δ* cells do not reassemble spindles after their single division strongly suggests that Cdk1 activity does not rise again after the first wave of APC/C activity. Therefore, the first wave of APC/C activity in *spo13Δ* seems to trigger the exit from meiosis. Katis et al. observed that Spo13 deletion abolished the metaphase I arrest of Cdc20 depleted cells (Katis et al., 2004b). Hence, we suspect that Spo13 might modulate the APC/C activity to avoid an inopportune exit from meiosis. We sought to understand which APC/C form triggers the division in *spo13Δ SCC1p-CDC20* double mutant and in *spo13Δ* single mutant.

2.4. Spo13 inhibits APC/C^{Ama1} in metaphase I

2.4.1. Spo13 deletion enables Ama1 to induce nuclear division in the absence of Cdc20

Budding yeast has three APC/C co-activators: Cdc20, Cdh1, which is required for mitotic exit but is inhibited during meiosis, and the meiosis-specific co-activator, Ama1. In wild-type cells, Cdc20 is essential for triggering anaphase and chromosome segregation. This is true for the mitotic division as well as for the two meiotic divisions. Therefore, cells in which Cdc20 is specifically depleted in meiosis remain arrested in metaphase I (Salah and Nasmyth, 2000). However, Katis et al. discovered that deleting *SPO13* in Cdc20-depleted cells triggers the escape from the metaphase I arrest and the formation of bi-nucleated spores (Katis et al., 2004b). We found that this escape from the metaphase I-arrest depends on APC/C^{Ama1} activity. Indeed, deleting Ama1 in the *spo13Δ SCC1p-Cdc20* background fully blocks cell cycle protein degradation as well as chromosomes segregation (Figure 29). We also checked whether Cdh1 could trigger the release from the metaphase I block in *spo13Δ SCC1p-CDC20* by specifically depleting Cdh1 in meiosis. However, *spo13Δ SCC1p-CDC20 HSL1p-CDH1* cells still escape the metaphase I arrest (Figure 30). Therefore, Ama1 is the sole APC/C co-activator triggering the release from metaphase I arrest in a *spo13Δ SCC1p-CDC20* background. In metaphase I, Ama1 is normally inhibited to avoid the premature loss of meiotic proteins (Okaz et al., 2012). Since Cdc20-depleted cells are able to escape their metaphase I-arrest in the absence of Spo13 and that this escape depends on Ama1, we conclude that Spo13 is required to maintain the metaphase I arrest in Cdc20-depleted cells by inhibiting Ama1. Hence, Spo13 might ensure that APC/C^{Ama1} remains inhibited until the second meiotic division.

2.4.2. The nuclear division in *spo13* mutant seems to be triggered by the two APC/C coactivator, Cdc20 and Ama1

Going back to the *spo13Δ* single mutant, the premature up-regulation of APC/C^{Ama1} might be required to trigger *spo13Δ* nuclear division. This could explain why the second meiotic division is "cut off" in *spo13Δ* cells as APC/C^{Ama1} is known to be required for the exit from meiosis and the formation of spores. However, *spo13Δ ama1Δ* cells also undergo a single nuclear division (Figure 31). We monitor the timing of nuclear division relative to entry into metaphase I in *spo13Δ*, *spo13Δ ama1Δ* and *spo13Δ SCC1p-CDC20* by live-cell imaging (Figure

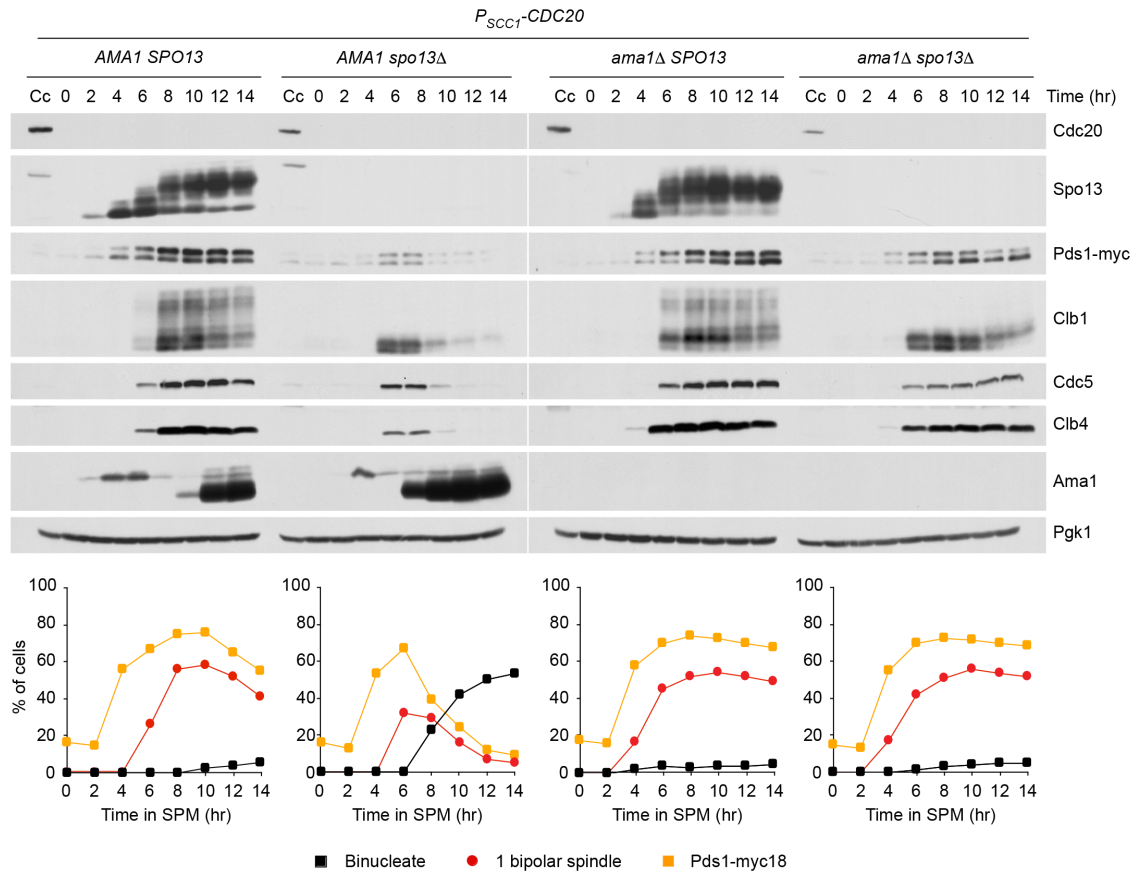


Figure 29: APC/C^{Ama1} triggers a meiotic division in *spo13Δ SCC1p-CDC20*.

Meiosis was induced in synchronized cultures of *SCC1p-CDC20* (Z18334), *ama1Δ SCC1p-CDC20* (Z18333), *spo13Δ SCC1p-CDC20* (Z18588), and *spo13Δ ama1Δ SCC1p-CDC20* (Z18589) cells. After transfer to sporulation medium (SPM), samples for immunofluorescence and TCA protein extraction were collected every 2 hours. On the upper part, immunoblot analysis of protein levels is shown. Cc stands for "cycling cells", these samples were collected from proliferating cells. On the lower part, immuno-fluorescence detection of securin (Pds1-myc), bipolar spindles (α -tubulin) and of the number of nuclei (DAPI) were quantifies. *SCC1p-CDC20* as well as *ama1Δ SCC1p-CDC20* strains arrest in metaphase I, as we can see from cell cycle proteins accumulation and IF cells remaining undivided with Pds1-myc nuclear signal and short bipolar spindle. *spo13Δ SCC1p-CDC20* strain degrades M-phase proteins, sign that the APC/C has been activated. IF cells lose Pds1-myc nuclear signal, divide their nuclei and disassemble their spindle. The deletion of Ama1 in *spo13Δ SCC1p-CDC20* restores the metaphase I arrest, suggesting that Ama1 activates the APC/C and triggers nuclear division in *spo13Δ SCC1p-CDC20* cells.

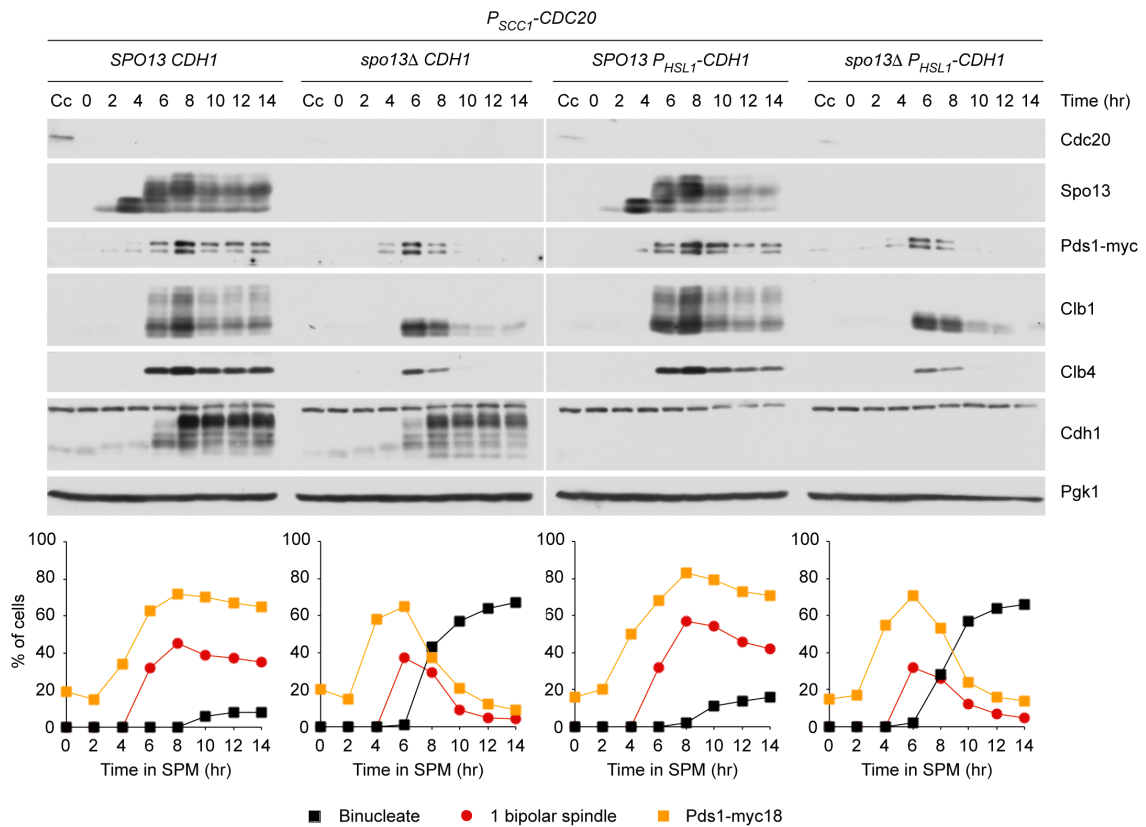


Figure 30: Cdh1 does not trigger the APC/C activation in *spo13Δ* SCC1p-CDC20.

Meiosis was induced in synchronized cultures of *SCC1p-CDC20* (Z32563), *HSL1p-CDH1 SCC1p-CDC20* (Z32561), *spo13Δ SCC1p-CDC20* (Z32562), and *spo13Δ HSL1-CDH1 SCC1p-CDC20* (Z32560) cells. After transfer to SPM, samples for immunofluorescence and TCA protein extraction were collected every 2 hours. On the upper part, immunoblot analysis of protein levels is shown. On the lower part, immuno-fluorescence detection of securin/Pds1-myc, bipolar spindles (α -tubulin) and divided nuclei were quantified. *SCC1p-CDC20* as well as *HSL1p-CDH1 SCC1p-CDC20* strains arrest in metaphase I, as we can see from cell cycle proteins accumulation and IF cells remaining undivided with Pds1-myc nuclear signal and short bipolar spindle. The *spo13Δ SCC1p-CDC20* strain degrades cell cycle markers, sign that the APC/C has been activated. IF cells lose Pds1-myc nuclear signal, divide their nuclei and disassemble their spindle. The depletion of Cdh1 in *spo13Δ SCC1p-CDC20* cells does not restore the metaphase I arrest.

31). While the *spo13Δ* mutant divides 80 minutes after metaphase I entry on average, *spo13Δ ama1Δ* and *spo13Δ SCC1p-CDC20* strains divide 110 minutes and 120 minutes after metaphase I onset, respectively. We hypothesize that Ama1 helps Cdc20 freeing itself from the SAC and that, in turn, Cdc20 amplifies Ama1 activity, therefore forming a positive feedback loop that efficiently triggers anaphase onset and the exit from meiosis in *spo13Δ* cells. This hypothesis could explain why the deletion of Ama1 is not sufficient to rescue the second meiotic division in *spo13Δ* cells.

2.4.3. The *CLB1* deletion also enables Ama1 to induce nuclear division in the absence of Cdc20

Okaz et al. identified Clb1 as an inhibitor of Ama1 in prophase arrested cells where Clb1 expression is induced (Okaz et al., 2012). Interestingly, Okaz et al. predicted that Ama1 should have another inhibitor in meiosis I and that this inhibitor needed to be a target of the transcription factor Ndt80 (Okaz et al., 2012). Furthermore, the deletion of *CLB1* in *SCC1p-CDC20* also leads to the release from the metaphase I arrest and to the formation of bi-nucleated cells (Argüello-Miranda, 2015). Hence, Clb1 and Spo13 are both enabling the release from the metaphase I arrest in Cdc20-depleted cells. We also noticed that while Clb1 is highly modified in metaphase I-arrested cells (Figure 29, *SCC1p-CDC20*), these modified forms disappear when we delete *SPO13* (Figure 29, *spo13Δ SCC1p-CDC20*). These results suggest that Spo13 is required for modifying Clb1 and that Clb1 and Spo13 might work in the same pathway to inhibit APC/C^{Ama1}. Therefore, we decided to investigate the mechanism of inhibition of Ama1 by Spo13 and Clb1.

2.4.4. Clb1 directly interacts with Ama1, independently of the interaction of Ama1 with the APC/C

To understand the mechanisms leading to Ama1 inhibition by Spo13 and Clb1, we analysed their physical interaction. While we did not detect an interaction between Spo13 and Ama1 (tested by immuno-precipitation, data not shown), Clb1 strongly interacts with APC/C^{Ama1} (Figure 32). We then sought to understand whether Clb1 binds directly to Ama1 or to the APC/C. The C-terminus portion of Ama1 is essential to its binding to the APC/C (Tan et al., 2011). Hence, while Ama1 tagged with Myc9 on the N-terminal side is functional and interacts with the APC/C, the C-terminally tagged version does not interact with the APC/C and, consequently, fails to sporulate (Oelschlaegel et al., 2005). Immuno-precipitation of Myc9-Ama1 and Ama1-myc9 shows that Clb1 interacts directly

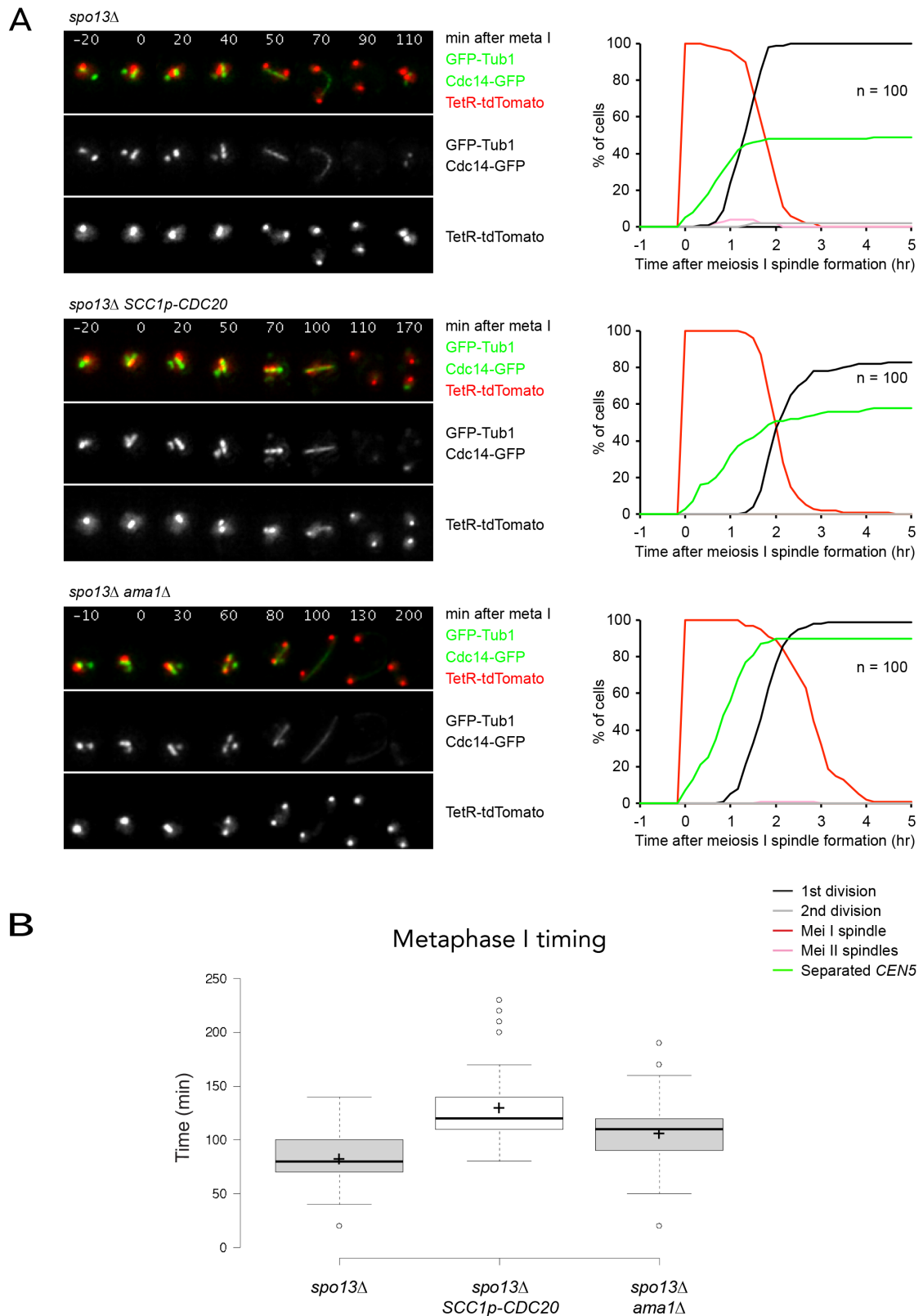


Figure 31: APC/C activation in *spo13Δ* can be triggered by Cdc20 or Ama1.

Life-cell imaging of *spo13Δ* (Z24862), *spo13Δ SCC1p-CDC20* (Z33049) and *spo13Δ ama1Δ* (Z33050) strains. (A) Representative time-lapse series and countings synchronized in-silico to the formation of the meiosis I spindle are displayed. (B) The duration of metaphase I (nuclear division time - metaphase I spindle formation time) in the 3 strains are compared. The median time of metaphase I is 82 ± 21 minutes for *spo13Δ*, 130 ± 32 minutes for *spo13Δ SCC1p-CDC20*, and 106 ± 27 minutes for *spo13Δ ama1Δ*.

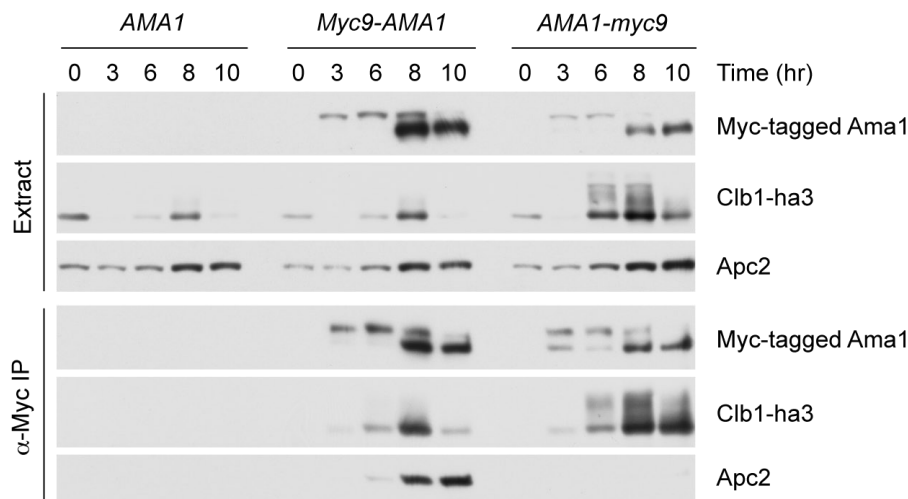


Figure 32: Clb1 interacts with myc9-Ama1 and with Ama1-myc9.

Anti-Myc immuno-precipitation from *CLB1-ha3* strains containing *AMA1* (Z31985), *myc9-AMA1* (Z31984) or *AMA1-myc9* (Z31983). The immuno-detection of whole cell extracts are displayed on top (Extracts) while the anti-Myc immuno-precipitates are displayed at the bottom (α -Myc IP). The untagged Ama1 allows controlling for unspecific binding. Myc9-Ama1 interacts with the APC/C subunit Apc2 while no binding was detected with Ama1-myc9. Clb1-ha3 binds similarly to Myc9-Ama1 and to Ama1-myc9.

with Ama1 regardless of Ama1's binding to the APC/C (Figure 32). Since Clb1 strongly interacts with Ama1 but Spo13 does not, Spo13's action on Ama1 might be indirect while Clb1 might directly inhibit Ama1 through their physical interaction. Spo13-dependent modification of Clb1 might be required for Clb1 inhibitory function on Ama1. Hence, the next part will focus on understanding how Spo13, which does not have a known enzymatic function, is involved in Clb1 modification.

2.4.5. The Spo13-Cdc5 complex phosphorylates Clb1

In metaphase I-arrested cells, Clb1 is highly modified (Figure 29). These slow-migrating forms are completely absent in *spo13* Δ cells. Spo13 is not an enzyme, it is therefore unlikely that it would directly modify Clb1. However, one of the main binding partner of Spo13 is the polo-like kinase, Cdc5 (Matos et al., 2008), which has a plethora of substrates during the cell cycle. We observe that in the absence of Cdc5 protein or kinase activity, Clb1 also runs as a single band while the slow migrating forms are undetectable (Figure 33). These results suggest that Spo13 mediates Clb1 phosphorylation by the Cdc5 kinase (Figure 33). To our knowledge, only few Cdc5 targets require the participation of Spo13, the other known case being the monopolin subunit, Lrs4 (Matos et al., 2008). For instance

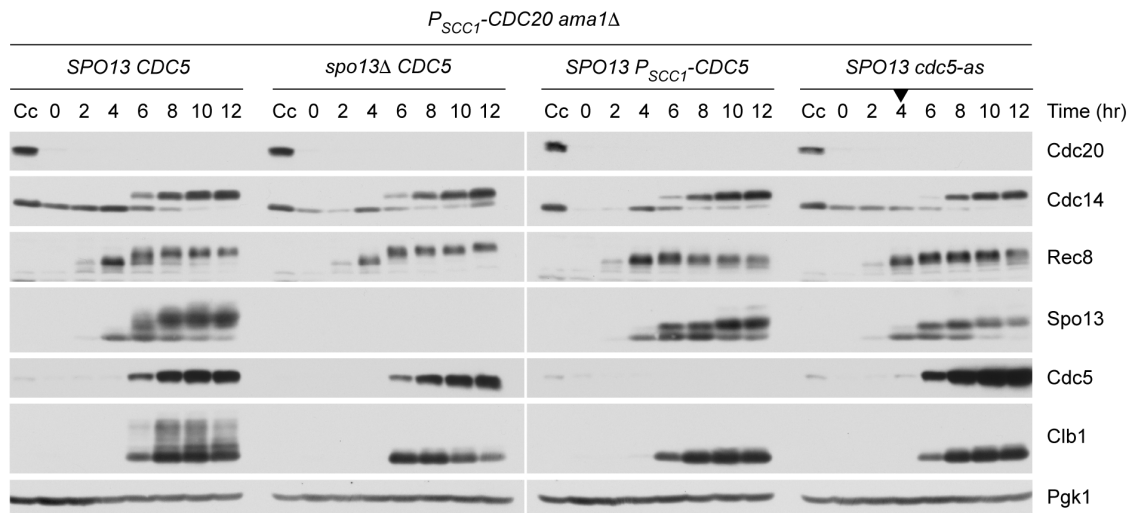


Figure 33: Clb1 modification depends on Spo13 and Cdc5.

Comparison of Clb1 modification state in metaphase I-arrested cells by western blotting. In order to have a comparable arrest in the wild-type and in *spo13Δ* cells, we used a *SCC1p-CDC20 ama1Δ* background. While Clb1 is highly modified in cells arrested in metaphase I (Z32845), it runs as a single band in *spo13Δ* (Z32846), in *SCC1P-CDC5* (Z32843) or in *cdc5-as* (Z32844) inhibited after 4 hours in SPM with 10 μ M of CMK inhibitor. Rec8 is also specifically modified by Cdc5 kinase activity, but its modification does not depend on Spo13.

Rec8 phosphorylation by Cdc5 does not depend on Spo13. Therefore, Cdc5 activity and specificity does not systematically require the participation of Spo13. A simple model would be that Spo13 would recruit Cdc5 to Clb1. We therefore checked whether Cdc5 interacts with Clb1 and whether this interaction depends on the presence of Spo13 by immuno-precipitating Cdc5-myc15 in a wild-type or in a *spo13Δ* strain (Figure 34). We observed that Cdc5 interacts with Clb1, however, this interaction is not disrupted by the deletion of *SPO13*. Hence, Spo13 must promote Clb1 phosphorylation in an other way.

2.4.6. Clb1 phosphorylation mapping

To confirm that the Clb1 slow-migrating forms we observe correspond to phosphorylations and that these modifications depend on both Spo13 and Cdc5, we performed affinity enrichment mass-spectrometry for Clb1-GFP in metaphase I-arrested cells and in the presence or absence of Spo13 or of Cdc5. More specifically, we use similar settings as the one used in Figure 33: we purified Clb1-GFP from *SCC1p-CDC20 ama1Δ*, *spo13Δ SCC1p-CDC20 ama1Δ* and *SCC1p-CDC5 SCC1p-CDC20 ama1Δ* strains. The *SCC1p-CDC20 ama1Δ* background was used to ensure that cells will be arrested in metaphase I in all strains, including in the absence of Spo13. Half of each sample was digested with trypsin while the other

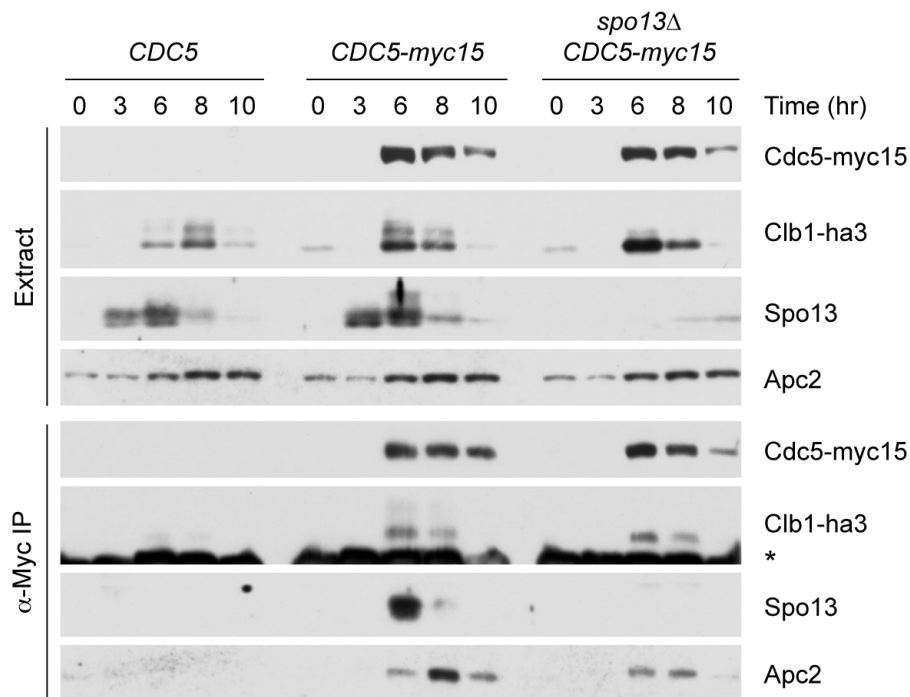


Figure 34: Cdc5-myc15 interacts with Clb1-ha3, this interaction is not affected by the deletion of SPO13.

Anti-myc immuno-precipitation in *CDC5* cells (Z32218, untag control), *CDC5-myc15* cells (Z32605) or *spo13* Δ *CDC5-myc15* cells (Z32604). The immuno-detection of whole cell extracts are displayed on top (Extracts) while the anti-Myc immuno-precipitates are displayed below (α -Myc IP). Clb1-ha3 interacts with Cdc5-myc15 in both a wild-type strain and *spo13* Δ background, showing that Spo13 is not required for Cdc5 recruitment to Clb1.

half was digested with lysC to ensure a maximum coverage of the Clb1 sequence. We used three biological replicates. Most phosphorylations are localized outside of the conserved cyclin-box domain (Figure 35). By comparing the intensity of each Clb1 phosphorylation in wild-type strain, *spo13Δ* and Cdc5-depletion, we can determine which amino acid is specifically phosphorylated depending on Spo13 and Cdc5 (Figure 36). We characterized six phosphorylation events that are significantly enriched only in the control strain (*SCC1p-CDC20 ama1Δ*) but not in *spo13Δ SCC1p-CDC20 ama1Δ* or *SCC1p-CDC5 SCC1p-CDC20 ama1Δ* strains. These phosphorylations are localized on S15, S84, S109, S137, S141 and S143 (Figure 36). We compared the sequences surrounding these phosphorylation sites to determine a potential phosphorylation motifs corresponding to Cdc5, but we did not detect any common features for the -10 to +10 amino acids above and below these six phosphorylated serines.

We mutated the six serines that are more phosphorylated in the wild-type to alanine to create a non-phosphorylatable mutant of Clb1. Since Spo13 is not expressed in mitosis and the Clb1 slow-migrating form is not visible, the six mutations integrated should not disturb Clb1 function in mitosis. While cells lacking either Clb2 or Clb1 are still able to complete mitosis, *clb1Δ clb2Δ* double mutant is not viable (Richardson et al., 1992; Fitch et al., 1992). Therefore, if *clb1-6A* mutant is functional, mitotic cells lacking Clb2 should be viable. Hence, we tested the functionality of the *clb1-6A* mutant by crossing *clb1-6A* haploid to a *clb2Δ* strain. The resulting diploid cells are sporulated and spores are dissected on a YPD plates (Figure 37). We looked at the growth of the haploids containing both *clb1-6A* and *CLB2* deletion and compare it to haploids containing *CLB1* and *CLB2* deletion. We observed no growth defect and concluded that *clb1-6A* is functional enough to carry out its mitotic function (Figure 37).

2.4.7. Clb1 non-phosphorylatable mutant fails to inhibit APC/C^{Ama1}

We then sought to determine whether the *clb1-6A* mutant is able to inhibit Ama1 in meiosis. The meiotic time course of *clb1-6A SCC1p-CDC20* cells shows that this strain escapes the metaphase I arrest normally observed in Cdc20-depleted cells and undergoes a single nuclear division similarly to *spo13Δ SCC1p-CDC20* and *clb1Δ SCC1p-CDC20* strains (Figure 38). The amount of bi-nucleated cells quantified in the *clb1-6A SCC1p-CDC20* strain is very close to what we observed in *spo13Δ SCC1p-CDC20* and slightly better than *clb1Δ SCC1p-CDC20* (Figures 29 and 38) (Argüello-Miranda, 2015). As expected, the metaphase I arrest is restored by deleting *AMA1* from the *clb1-6A SCC1p-CDC20* mutant (Figure 38). This

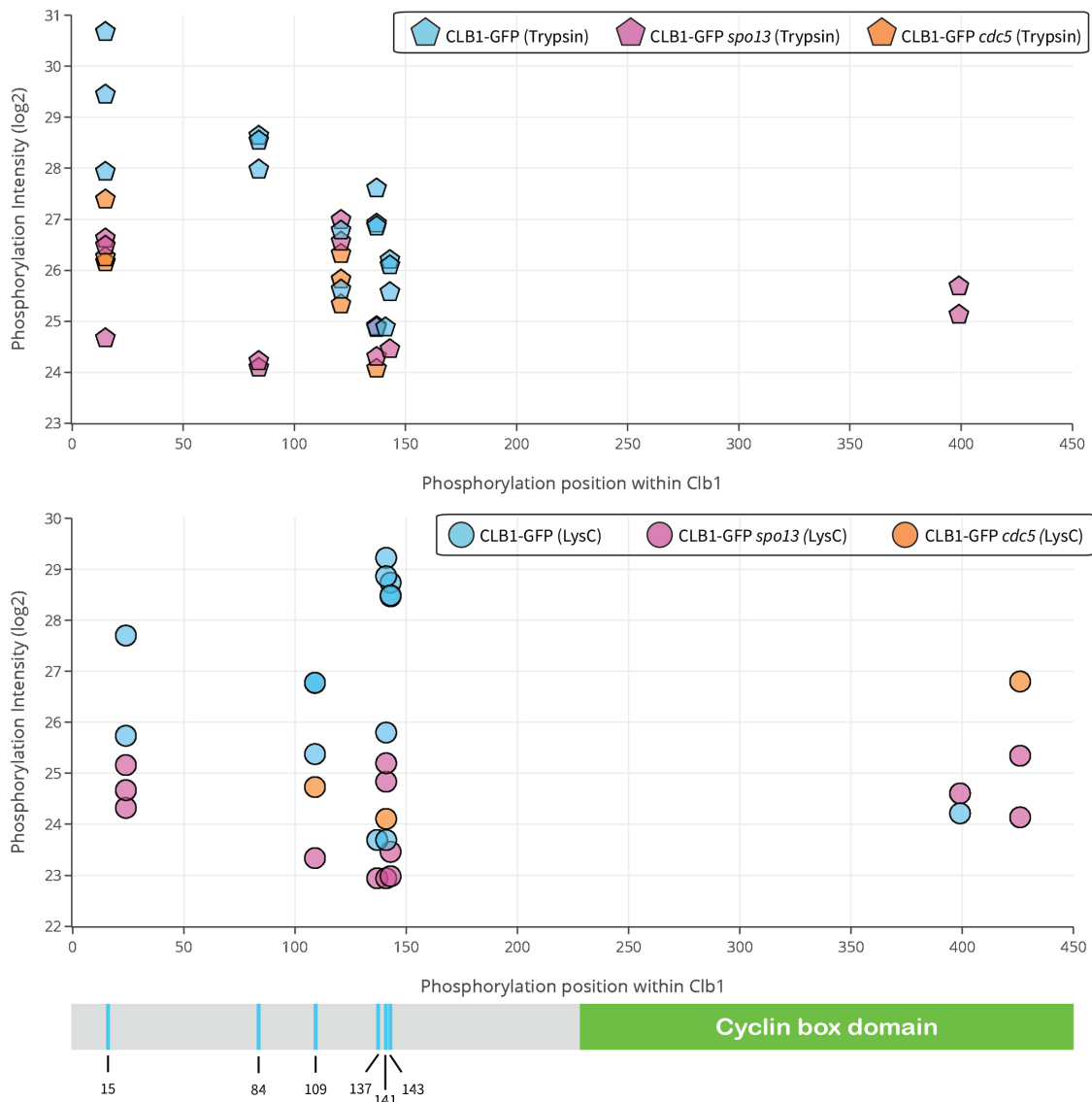


Figure 35: Several phosphorylation sites were identified in the N-terminus of CLB1. Clb1-GFP was immuno-precipitated from *CLB1-yeGFP SCC1p-CDC20 ama1Δ* (Z32114), *CLB1-yeGFP spo13Δ SCC1p-CDC20 ama1Δ* (Z32113) and *CLB1-yeGFP SCC1p-CDC5 SCC1p-CDC20 ama1Δ* (Z32112) to identify Clb1 phosphorylation sites and compare the phosphorylation intensity of each site in the 3 strains. Samples were digested either with trypsin (upper graph) or lysC (lower graph). The log₂ intensity values of each identified phosphorylated sites of Clb1 were normalized to the total Clb1 protein level measured for each sample. The normalized intensities were then plotted according to their position along the Clb1 amino acid sequence. Most phosphorylation sites identified and enriched in the wild-type (blue) are located in the N-terminal region, outside of the cyclin-box domain. The figure below (Figure 36) focuses on the N-terminus region of Clb1.

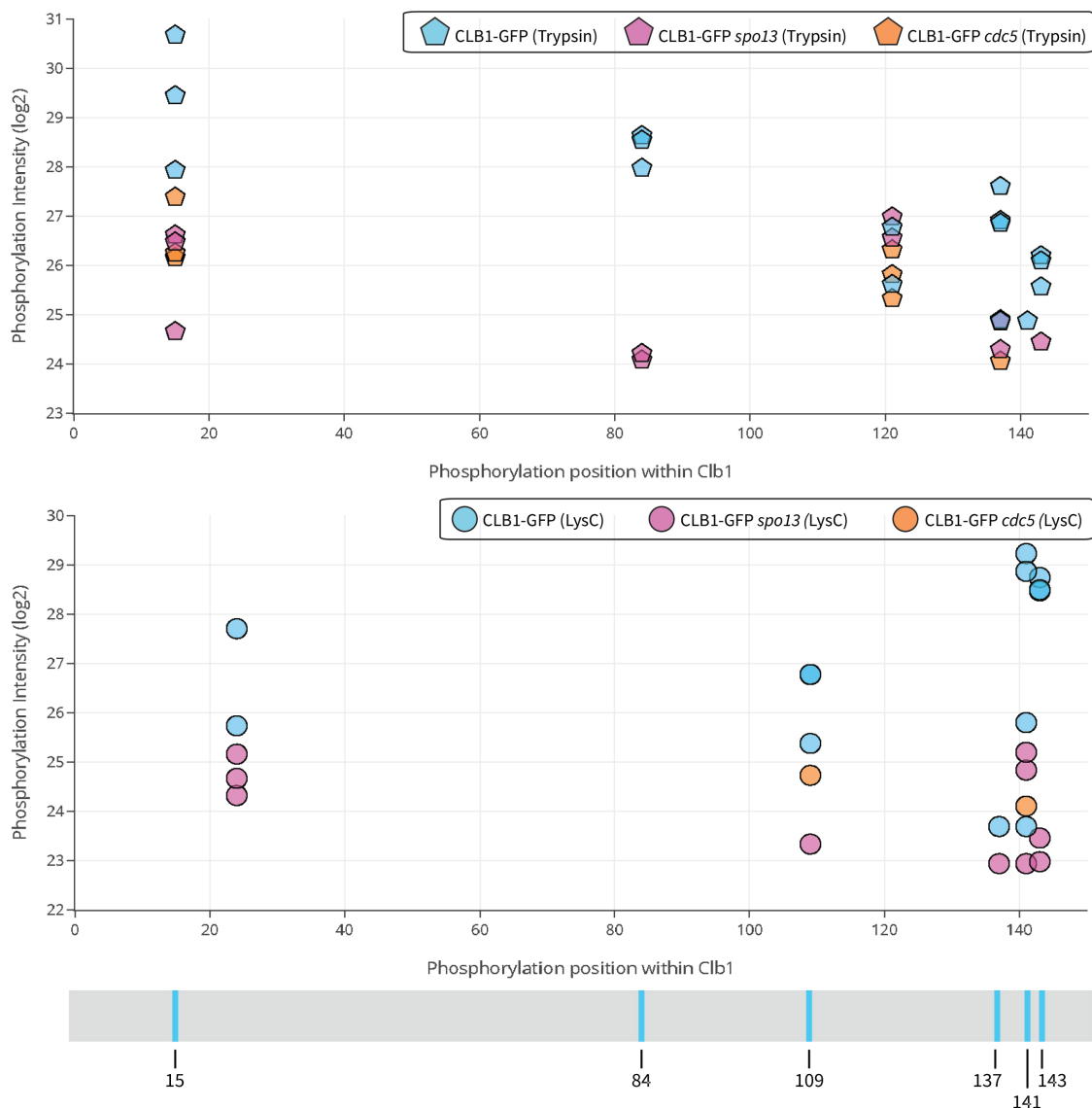


Figure 36: Clb1 phosphorylations are enriched in the wild-type compare to *spo13*Δ or Cdc5 depletion strains.

These graphs focus on the N-terminus sequence of Clb1 (from 0 to 160), from the experiment presented above (Figure 35). For both graphs, log₂ intensity values of each identified phosphorylated sites of Clb1 were normalized to the total Clb1 protein level measured for each sample. The normalized intensities were then plotted according to their position along the Clb1 amino acid sequence. Several phosphorylations are consistently higher in wild-type samples (blue) than in *spo13*Δ (pink) and *SCC1p-CDC20* replicates (orange). This data clearly shows that 6 phosphorylation sites in the N-terminal region of Clb1 are consistently more phosphorylated in the presence of Spo13 and Cdc5. These six sites are all serines and their precise location within Clb1 is indicated below the graphs.

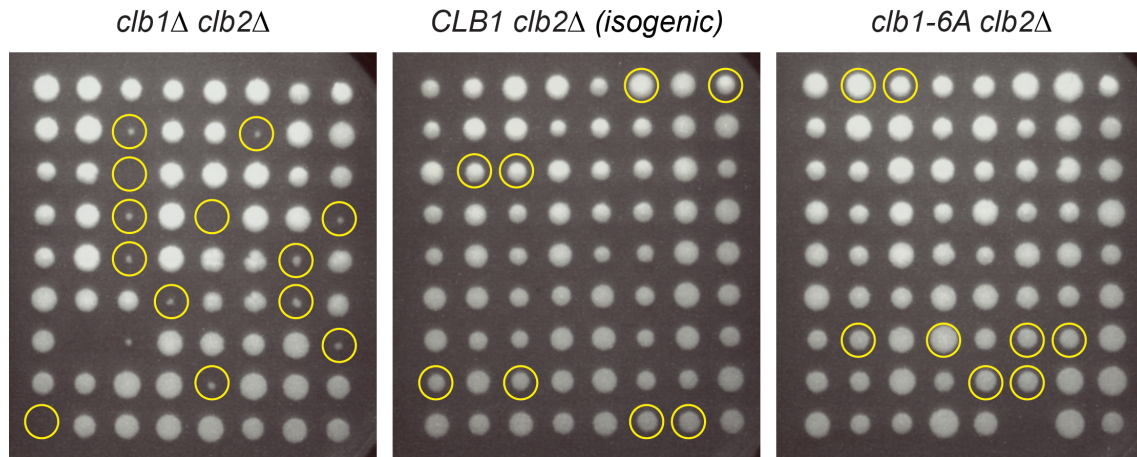


Figure 37: *clb1-6A clb2Δ* haploids are viable.

clb1Δ (Z31814), *clb1-6A* (Z32859), and *CLB1* isogenic control (Z32837) haploids were crossed to *clb2Δ* (Z3516) haploid cells. The resulting diploid cells were sporulated and 18 spores of each cross were dissected on a YPD plate. We looked at the growth of the haploids containing both *clb1-6A* and *CLB2* deletion and compared it to haploids containing *CLB1* (isogenic control) or *CLB1* deletion and *CLB2* deletion. While several spores from the *clb1Δ/clb2Δ* cross present obvious growth defects, all spores from the *clb1-6A/clb2Δ* are growing normally as all patches have comparable sizes.

result strongly suggests that the Clb1 phosphorylated form, rather than the unphosphorylated Clb1, is a potent inhibitor of Ama1. Our results show that Spo13 directs Cdc5 to phosphorylate Clb1 and that the phosphorylated Clb1 inhibits Ama1 during metaphase I. However, we cannot exclude that Spo13 could also inhibit Ama1 in a Clb1-independent fashion, additionally to its action on Clb1.

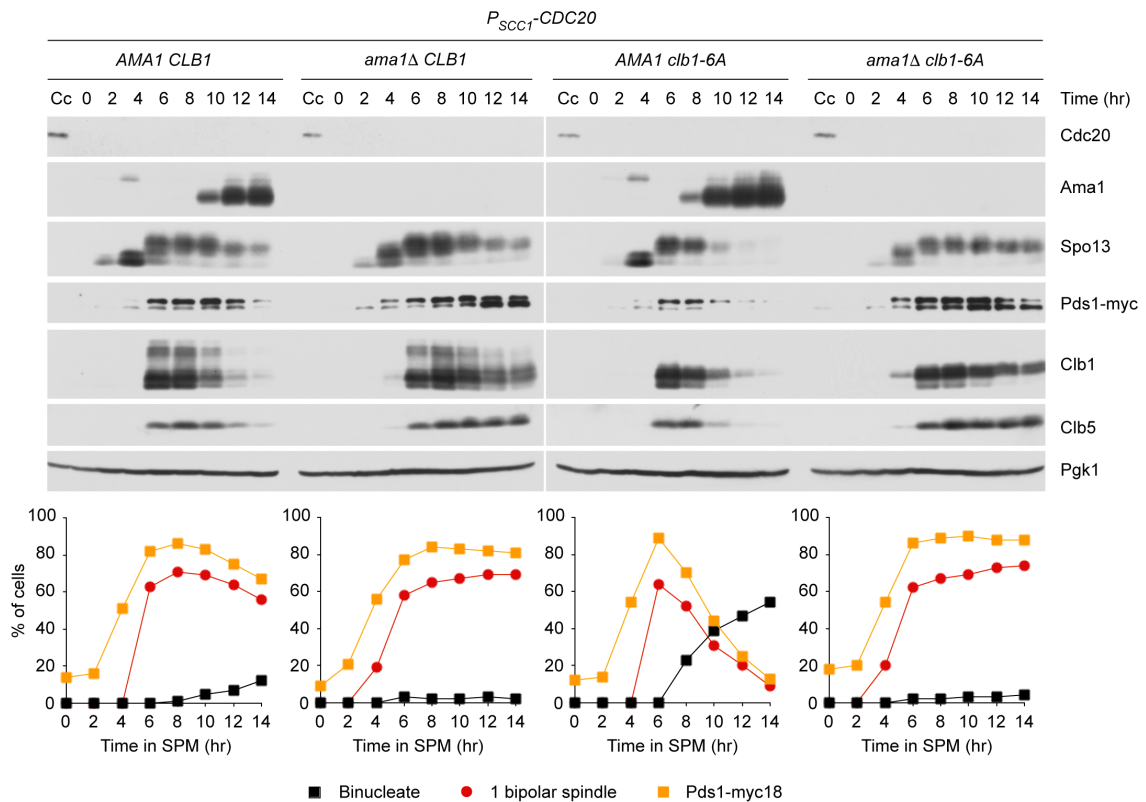


Figure 38: APC/C^{Ama1} triggers a meiotic division in *clb1-6A* *SCC1p-CDC20*.

Meiosis was induced in synchronized cultures of *CLB1* *SCC1p-CDC20* (Z32976), *CLB1 ama1Δ* *SCC1p-CDC20* (Z32975), *clb1-6A* *SCC1p-CDC20* (Z32978) and *clb1-6A ama1Δ* *SCC1p-CDC20* (Z32977) strains. After transfer to SPM, samples for immunofluorescence and TCA protein extraction were collected every 2 hours. On the upper part, immunoblot analysis of protein levels is shown. Cc stands for "cycling cells", these samples were collected from proliferating cells. On the lower part, immunofluorescence detection of securin (Pds1-myc), bipolar spindles (α -tubulin) and of the number of nuclei (DAPI) were quantifies. *CLB1* *SCC1p-CDC20* as well as *CLB1 ama1Δ* *SCC1p-CDC20* strains arrest in metaphase I, as we can see from M-phase proteins accumulation and IF cells remaining undivided with Pds1-myc nuclear signal and short bipolar spindle. The *clb1-6A* *SCC1p-CDC20* strain degrades cell cycle markers, indicating that the APC/C has been activated. 55% of IF cells loses Pds1-myc nuclear signal, divide their nuclei and disassemble their spindle by the end of the time-course. *clb1-6A ama1Δ* *SCC1p-CDC20* cells keep high levels of M-phase proteins through the whole time-course and IF shows that cells are arrested in metaphase I.

3 Discussion

For meiotic cells to undergo two successive nuclear divisions, they need to establish two waves of Cdk1 activity, controlled by two waves of APC/C activity. This is very different from mitosis where anaphase onset is coupled with the exit from mitosis. In the case of meiosis, cells re-built high Cdk1 kinase activity right after anaphase I to allow for a second division and the meiotic exit is coupled only to anaphase II. In *spo13Δ* cells, all landmarks of a second wave of Cdk1 activity are undetectable. Indeed, spindles do not reassemble after anaphase I and the second wave of Cdc14 release/capture is completely absent (Figure 9). Furthermore, the *spo13* mutant does not re-accumulate securin after anaphase (Katis et al., 2004b). Hence, it seems that *spo13Δ* cells exit meiosis immediately after their single division. *spo13Δ* cells are delayed in metaphase I by 40 minutes compared to wild-type cells (Figure 9). This metaphase I delay is responsible for the total absence of meiosis II in *spo13Δ* cells. Indeed, inactivating the SAC fully restores the second meiotic division in the absence of Spo13 (Figure 11). These results are consistent with the findings of Shonn et al. showing that the deletion of *MAD1* or *MAD2* could rescue the formation of tetrads in the absence of Spo13 (Shonn et al., 2002). A logical hypothesis is that the metaphase I delay in *spo13Δ* cells causes the second wave of Cdk1 activity and, subsequently, of APC/C activity to be "cut off". Reducing this metaphase I delay enables *spo13Δ* cells to undergo meiosis II before the exit from meiosis. This complex phenotype poses several questions:

1. Is this delay partly responsible for the monopolar attachment and centromeric cohesin protection defects previously reported for *spo13Δ* cells (Shonn et al., 2002; Katis et al., 2004b; Lee et al., 2004)?
2. What causes such a SAC response in *spo13Δ* cells?
3. Why is the second meiotic division "cut off" instead of being delayed according to the metaphase I delay?

3.1. Spo13 is directly required for monopolar attachment but not for centromeric cohesin protection

Several publications suggest that Spo13 is involved in two meiosis I-specific processes that are crucial for the proper segregation of chromosomes in meiosis. Namely, Spo13 seems to be required for the monopolar attachment of chromosomes and the protection of centromeric cohesin from separase during anaphase I (Katis et al., 2004b; Lee et al., 2004; Klein et al., 1999; Shonn et al., 2002). The combination of these two defects can explain how chromosomes are segregated in *spo13Δ* cells. Indeed, mutants defective for monopolar attachment fail to form two nuclei at anaphase I and only segregates DNA at the onset of anaphase II. By contrast, *spo13Δ* cells can segregate sister chromatids at anaphase I onset, suggesting that centromeric cohesin must be cleaved the first and only time separase gets activated. In favour of this model, several studies show that the retention of centromeric cohesin was at least partially affected in *spo13Δ* (Klein et al., 1999; Katis et al., 2004b; Shonn et al., 2002; Lee et al., 2004). Our results confirm that most cohesin complexes are cleaved at anaphase I onset. However, we and others observed that the protection machinery, Sgo1-PP2A, localizes properly at metaphase I in *spo13Δ* mutant (Lee et al., 2004) (Figure 28). Therefore, why are centromeric cohesin complexes cleaved at anaphase I in *spo13Δ* cells?

Although the combination of monopolar attachment defect and centromeric cohesin protection defect can explain chromosomes segregation pattern in the *spo13* mutant, it does not explain why the second round of Cdk1 and APC/C^{Cdc20} activity is cut off. Additionally, the delay of the *spo13* in metaphase I was never taken into account when assessing Spo13's potential roles in monopolar attachment and centromeric protection. This 40 minutes delay in metaphase I mean that *spo13Δ* cells undergo anaphase I at a timing that would normally correspond to anaphase II onset for wild-type cells (Figure 9). Hence, defects in these two meiosis I-specific processes could be due to the metaphase I delay of *spo13Δ* cells. To understand the real implication of Spo13 in these two processes, it is, therefore, crucial to assess *SPO13* deletion effects in cells that are not delayed at metaphase I and undergo a second meiotic division. Carefully re-analysing *spo13Δ mad2Δ* cells revealed that Spo13 is directly required for monopolar attachment but not for centromeric cohesin protection.

Spo13 is required for monopolar attachment

spo13Δ mad2Δ cells bi-orient sister chromatids significantly more frequently than *mad2* single mutants. Furthermore, the localization of the monopolin complex to kinetochores is strongly reduced in the absence of Spo13, as shown by Katis et al. and Lee et al. (Katis et al., 2004b; Lee et al., 2004). This defect is independent of the metaphase I delay observed in the *spo13* mutant. On the contrary, the mixture of sister chromatids bi-orientation and mono-orientation occurring in *spo13Δ* cells at metaphase I is, at least partially, responsible for the SAC-mediated delay in metaphase I. Indeed, "improving" the bi-orientation of sister chromatids in metaphase I shortens the SAC response and thus the length of metaphase I in *spo13* mutants. Additionally, the fact that deleting *MAM1* in *spo13* mutants increases the rate of sister-chromatids bi-orientation at meiosis I shows that some monopolin activity is retained in *SPO13* deletion, although strongly reduced (Katis et al., 2004b). Matos et al. then showed that all the subunits of the monopolin complex were still interacting with each other in the *spo13* mutant, indicating that the loading to kinetochores alone was impaired (Matos et al., 2008). How does Spo13 recruit or stabilize the monopolin complex to kinetochores is yet to be understood. It seems that Spo13's role in monopolar attachment depends on its interaction with the polo-like kinase, Cdc5. When Spo13's PBD-binding domain is mutated, its interaction with Cdc5 is almost fully abolished (Matos et al., 2008). While this mutant still undergoes two nuclear divisions and produces tetrad, *spo13-m2* cells fail to mono-orient sister-kinetochores efficiently during meiosis I. It was suggested that Cdc5 together with Spo13 phosphorylates Lrs4 (Katis et al., 2004b) but whether Lrs4 phosphorylation is required for the formation of the monopolin complex on kinetochores remains untested. Nevertheless, it is clear that Spo13-Cdc5 works upstream of the monopolin complex to establish monopolar attachment in meiosis I.

Except for closely related yeast, the budding yeast monopolin complex is not conserved and its equivalent in mammalian is yet to be identified (Rabitsch et al., 2003). However, it seems that Spo13's and Cdc5's role in monopolar attachment is conserved in fission yeast and mouse. Indeed, the functional homolog of Spo13 in *S. pombe*, Moa1 together with the polo-like kinase Plo1 participates in kinetochore monopolar attachment at meiosis I (Yokobayashi and Watanabe, 2005). The functional homolog of Spo13 in mouse, Meikin, is required for monopolar attachment of sister chromatids in mouse oocytes (Kim et al., 2015). As for fission yeast and budding yeast, Meikin mediates monopolar attachment together with the polo-like kinase Plk1. Spo13, Moa1, and Meikin have all been found to interact with kinetochores in meiosis I (Kim et al., 2015; Yokobayashi and Watanabe,

2005; Katis et al., 2004b). Additionally, the absence of Moa1 in fission yeast or Meikin in mouse oocyte affects the localization of the Polo-like-kinase to kinetochores. Spo13 might, therefore, recruit Cdc5 to kinetochores in order to promote monopolar attachment, probably by recruiting or stabilizing the monopolin complex to kinetochores. It is rather odd that while Spo13-Cdc5 function in monopolar attachment is conserved, a complex such as monopolin was not identified in other organisms. In fission yeast, for instance, Rec8 is required for establishing monopolar attachment and interacts directly with Moa1 (Yokobayashi and Watanabe, 2005). Therefore, in this organism, centromeric protection, and monopolar attachment seems to be directly coordinated. Such a link was not found in budding yeast where monopolar attachment and centromeric cohesin seem to be regulated by independent pathways (Tóth et al., 2000). In mammals, Meikin and Plk1 were the only proteins identified so far for playing a role in monopolar attachment (Kim et al., 2015). Further work is needed to understand the full implication of Spo13 and its functional orthologs for monopolar attachment of sister kinetochores in meiosis I.

Abolishing the metaphase I delay in *spo13*Δ cells rescues centromeric cohesin protection

We observed that in *spo13* mutants in which we restore the second meiotic division by reducing the metaphase I delay, most cells fail to segregate chromosomes at anaphase I onset. This phenotype strongly resembles the one of monopolin mutants in which sister chromatids are bi-oriented in meiosis I but remain physically linked until the removal of centromeric cohesin at anaphase II onset (Figure 22) (Tóth et al., 2000). This phenotype strongly suggests that centromeric cohesin blocks the division of sister chromatids at anaphase I. Impairing the centromeric protection machinery in those cells restores the nuclear division at anaphase I onset, thereby confirming that centromeric cohesin survives anaphase I onset in *spo13*Δ cells that undergo anaphase I without delay. Additionally, we observed that neither cohesin nor the centromeric protection machinery recruitment or removal was affected by the deletion of *SPO13* in *mad2*Δ cells (Figures 26, 27 and 28). Our results demonstrate that the centromeric protection defect observed in *spo13* mutants is due the delay in metaphase I triggered by the SAC. Because in the *spo13* mutant, anaphase I onset occurs at a time when wild-type cells undergo the second meiotic division, we propose that the coordination between the removal of the centromeric cohesin protection machinery and the second division is lost in *spo13*Δ cells. How is the centromeric protection removed specifically in meiosis II is still not well understood. Argüello et al. showed that the crucial step

for the cleavage of centromeric Rec8 in meiosis II was the removal of PP2A from centromeres and the subsequent phosphorylation of Rec8 by the Hrr25 kinase (Argüello-Miranda et al., 2017). However, how Sgo1-PP2A is removed from kinetochores specifically at anaphase II onset is still unclear. Although more research needs to be done to understand the timely removal of Sgo1-PP2A at anaphase II only, Spo13 seems somehow required to coordinate the second wave of APC/C activity with the de-protection of centromeric cohesin. Indeed, our results suggest that Spo13 is required to avoid the premature loss of centromeric cohesin only in case cells are delayed in meiosis I. Thus, some "timer" might define the timing of centromeric cohesin protection removal as well as the exit from meiosis independently of the waves of APC/C^{Cdc20} activity.

In the fission yeast *moa1Δ* mutant, the link between sister kinetochores is initially unimpaired but, as in budding yeast *spo13Δ* cells, centromeric cohesin is eventually cleaved at anaphase I and sister chromatids are segregated (Yokobayashi and Watanabe, 2005). And similarly to budding yeast *spo13Δ* cells, Sgo1 localization at centromeres is not affected (Yokobayashi and Watanabe, 2005). In mammals as well, *MEIKIN* deletion does not seem to affect the proper localization of the centromeric protection machinery Sgo2/PP2A. Centromeric protection is also not fully abolished in *Meikin*^{-/-} oocytes (Kim et al., 2015). Similarly to the *S. cerevisiae spo13Δ* mutant, *Meikin*^{-/-} oocytes are delayed in metaphase I by the SAC (Kim et al., 2015). Therefore, the premature loss of centromeric cohesin in *Meikin*^{-/-} might also be caused by the metaphase I delay rather than by a direct effect of Meikin on the centromeric protection machinery. The role of Spo13's orthologs for centromeric cohesin protection should be re-address while taking into account the delay caused by their inactivation.

In conclusion, our data show that Spo13, together with Cdc5, is directly required for sister kinetochores monopolar attachment in meiosis I, confirming the results published before (Lee et al., 2004; Katis et al., 2004b). This defect is independent of the extensive metaphase I delay observed in *spo13Δ* cells. In contrast, we showed that abolishing the metaphase I delay in *spo13Δ* cells fully rescues the centromeric cohesion defect that we and others observed (Shonn et al., 2002; Katis et al., 2004b; Lee et al., 2004). Therefore, Spo13 is not required for centromeric cohesin protection *per se*. Spo13 might, therefore, be required to coordinate centromeric cohesin deprotection with the second wave of APC/C activation.

3.2. *spo13* mutant's SAC response is triggered by a mixture of monopolar and bipolar attachment

The *spo13* Δ delay in metaphase I could be explained by the monopolar attachment defect. However, other known monopolar attachment mutants such as *mam1* Δ or *hrr25-zo* are only moderately delayed in metaphase I with the SAC staying active for 30 minutes (against 14 minutes in wild-type cells, Figure 16). Furthermore, this delay does not impair the normal completion of meiosis II (Figure 16). Since the *spo13* mutant segregates a mixture of sister chromatids and homologous chromosomes (Hugerat and Simchen, 1993), this mixed segregation pattern could be responsible for the extensive SAC response. Indeed, 68% of *mam1* Δ cells split centromeric dots in meiosis I (Figure 22) while only 54% of *spo13* Δ do so (Figure 9). Hence, improving either chromosomes mono-orientation or bi-orientation should diminish the metaphase I delay of *spo13* Δ cells. As anticipated, improving sister chromatids bi-orientation in metaphase I by deleting *MAM1* diminishes the SAC response and partially rescue the entry into meiosis II (Figure 17). This result matches the observation made by Katis et al. (Katis et al., 2004b). Moreover, abolishing the initiation of recombination in *spo13* Δ *mam1* Δ further improves bipolar attachment of sister chromatids and fully rescues the second wave of Cdk1 and APC/C^{Cdc20} activity (Figure 18). We could not rescue the monopolar attachment of sister chromatids in *spo13* Δ cells, as we failed to rescue the monopolin binding to kinetochores (data not shown). Nonetheless, our results clearly show that improving sister chromatid bi-orientation proportionally reduces the delay in metaphase I and, as a result, restores meiosis II. Therefore, our results strongly suggest that the metaphase I delay observed in *spo13* mutant is caused by a mixed segregation pattern that might fail to create sufficient tension to silence the SAC. This delay caused the cells to exit meiosis before undergoing meiosis II.

3.3. The SAC-dependent metaphase I delay alone does not recapitulate *spo13* Δ phenotype

Our results confirm that the metaphase I delay observed in *spo13* Δ cells is responsible for the loss of all hallmarks of meiosis II, as impairing the SAC fully rescues the second wave of Cdk1 activity and of APC/C activity. However, if *spo13* sole defect was its extensive delay in metaphase I, we should be able to recapitulate *spo13* Δ cells phenotype by triggering a similar SAC response in *SPO13* cells. But

when we compare *spo13Δ* to the recombination mutant, *spo11Δ* that activates the SAC even longer than *spo13Δ* cells (Figures 13 and 15), we observed that *spo11Δ* cells still undergo two nuclear divisions (Figure 13) (Shonn et al., 2000). So, despite the first wave of APC/C^{Cdc20} being strongly delayed, *spo11Δ* cells still reaccumulate Cdk1 activity to undergo a second nuclear division. Hence, a similar metaphase I delay fails to recapitulate the *spo13Δ* phenotype. Therefore, it seems that in the absence of Spo11, the second meiotic division and the exit from meiosis are delayed according to the delay in metaphase I. This is in sharp contrast with the *spo13* mutant in which the same metaphase I delay causes meiosis II to be 'cut off' as cells exit from meiosis with a timing resembling wild-type cells. It therefore seems that Spo13 is required to delay the exit from meiosis in case of delay in metaphase I. We hypothesize that, in the absence of Spo13, the coordination between chromosome segregation and the exit from meiosis is lost. Hence, we believe that Spo13 has an additional role in regulating progression through meiosis. And because the metaphase I arrest caused by Cdc20 depletion is rescued by the deletion of *SPO13* (Katis et al., 2004b), Spo13 is likely to regulate the APC/C during meiosis.

3.4. Spo13-Cdc5 and Clb1-Cdk1 inhibit APC/C^{Ama1} in metaphase I

Meiosis rely on the timely activation and down-regulation of both Clbs-Cdk1 and the APC/C (Okaz et al., 2012). Two forms of APC/C govern progression through meiosis: APC/C^{Cdc20} triggers anaphase I and anaphase II while APC/C^{Ama1} represses the mitotic program in prophase and is required at the end of meiosis for the sporulation program (Okaz et al., 2012). During the meiotic prophase, APC/C^{Ama1} actively degrades M-phase proteins, keeping the mitotic program off and making the entry into M-phase dependent of the Ndt80 transcription factor (Okaz et al., 2012). This system ensures that cells would not enter M-phase until recombination is completed. Ndt80 is inhibited by the recombination checkpoint; once recombination is completed, Ndt80 inhibition is relieved and Ndt80 triggers the expression of M-phase proteins including B-type cyclins and the polo-like kinase. In order to transit from prophase to metaphase I, APC/C^{Ama1} activity should be inhibited as cells enter metaphase I to enable the efficient accumulation of M-phase proteins (Okaz et al., 2012).

Clb1 and Spo13 are two meiosis I-specific inhibitors of APC/C^{Ama1}

Oelschlaegel et al. suggested that Cdk1 inhibits APC/C^{Ama1} in metaphase I to permit the accumulation of M-phase protein (Oelschlaegel et al., 2005). Okaz et al. found that Clb1-Cdk1 specifically inhibits APC/C^{Ama1} while the other B-type cyclins do not seem to have an inhibitory effect on APC/C^{Ama1} activity (Okaz et al., 2012). Katis et al. observed that deleting *SPO13* in *Cdc20* depleted cells could overcome the metaphase I arrest. Indeed, *spo13Δ SCC1p-CDC20* cells form bi-nucleated spores (Katis et al., 2004b). This result suggested that Spo13 might regulate APC/C activity in meiosis. We found that this division is carried out specifically by APC/C^{Ama1} activity. Indeed, the deletion of *AMA1* in *spo13Δ SCC1p-CDC20* cells restores the metaphase I arrest (Figure 29) while the depletion of *CDH1* does not (Figure 30). Therefore, Spo13 expression is required to maintain APC/C^{Ama1} inactive during metaphase I. Intriguingly, Spo13 is an early meiotic gene that starts to accumulate in prophase, when APC/C^{Ama1} is active. We therefore ought to understand how does Spo13 act as an inhibitor of Ama1 and whether its action is limited to metaphase I and how. An attractive model would be that Spo13 works together with Clb1-Cdk1, thereby restricting APC/C^{Ama1} inhibition to the accumulation of Clb1 at metaphase I onset. We therefore sought to investigate whether and how Clb1 and Spo13 work together to inhibit APC/C^{Ama1}.

Clb1 phosphorylation by Spo13-Cdc5 is essential for Clb1-mediated inhibition of Ama1

During metaphase I, Clb1 is strongly modified, but these slow running forms are completely absent in *SPO13* deletion cells (Figure 29). Spo13 having no enzymatic activity, Clb1 modification required the participation of a third party. As Spo13 was found to interact strongly with Cdc5 (Matos et al., 2008), we investigate whether the slow migrating form of Clb1 required the kinase activity of Cdc5. Indeed, we found that Spo13 directs the polo-like kinase Cdc5 to phosphorylate Clb1 (Figure 33). The analysis of Clb1-GFP protein by mass-spectrometry allowed us to identify several amino-acids that are specifically modified only in the presence of Spo13 and Cdc5. We identified six serines, all located in the N-terminus domain of Clb1, which are significantly more phosphorylated in wild-type cells than in *Cdc5*-depleted cells and *spo13Δ* (Figures 35 and 36). Those six phosphorylation sites are all outside of the conserved cyclin box. The cyclin-fold domain is conserved among cyclins and is dedicated to Cdk1 binding and

activation (Brown et al., 1995; Jeffrey et al., 1995). The N-terminus region, however, is highly divergent between cyclins and most likely play an important role for cyclins differential substrates recognition and specialized functions (reviewed in Morgan, 2006). The Clb1 meiosis-specific modifications we identified might, therefore, influence Clb1-Cdk1's substrates recognition or activity.

Mutating these six serines to alanines does not affect Clb1 function in mitosis (Figure 37). However, this non-phosphorylatable *clb1* mutant (*clb1-6A*) fails to maintain the metaphase I arrest in *Cdc20*-depleted cells (Figure 38). Thus, these six phosphorylations are crucial for Clb1's role as an inhibitor of APC/C^{Ama1}. Therefore, Spo13, together with Cdc5, modifies Clb1 to create a potent inhibitor of APC/C^{Ama1}. Hence, we found that a meiosis-specific protein can modify the function of a cyclin to tailor its function to its meiotic requirements. The expression of Cdc5 and Clb1 are both regulated by Ndt80, thus the inhibition of APC/C^{Ama1} is tightly restricted to the entry into metaphase I, carried out by the accumulation of Ndt80. The combined inhibition of Ama1 by Spo13, Cdc5, and Clb1-Cdk1 might ensure the rapid accumulation of M-phase protein at metaphase I onset by quickly inhibiting their targeted destruction by APC/C^{Ama1}.

Although our results show that Spo13-Cdc5 and Clb1-Cdk1 work together to maintain Ama1 inhibition during meiosis I, the precise inhibitory process remains elusive. Indeed, Spo13 absence does not seem to disrupt the interaction between Clb1 and Ama1 or between Ama1 and the APC/C (data not shown). Furthermore, the phosphorylation state of Clb1 does not seem to alter its binding to Ama1 either. The phosphorylation state of Clb1 must, therefore, affect its inhibitory effect on APC/C^{Ama1} in a more subtle way. The structure of Ama1 and its binding to the APC/C has been much less studied than Cdc20 or Cdh1 and further work is required to fully understand its regulation. Similarly to Cdh1 that is inhibited by Cdk1 phosphorylation, Ama1 phosphorylation state might influence APC/C^{Ama1} activity. Ama1 possesses several Cdk1 consensus sites that might be specifically phosphorylated by Clb1-Cdk1 to inhibit the activation of the APC/C by Ama1 during the meiosis M-phase. In favour of that model, mutating the eight Cdk1 consensus sites found in *AMA1* ORF results in a more active APC/C^{Ama1} version that bypasses the *CDC20* depletion metaphase I arrest (Orlando Argüello-Miranda, unpublished, Oelschlaegel et al., 2005). Further work would nonetheless be needed to confirm that Ama1 phosphorylation inhibits APC/C^{Ama1} and to determine whether the phosphorylation of Clb1 by Spo13-Cdc5 influences Clb1-Cdk1 activity and Ama1 modification.

Model for APC/C regulation in meiosis

While Clb1 has no major role in mitosis, it is the most important cyclin in meiosis (Dahmann and Futcher, 1995). Its importance for the meiotic program is not fully understood. However, its role as a key regulator of the meiosis-specific form of APC/C, APC/C^{Ama1}, could explain this (Okaz et al., 2012). Additionally to their inhibitory effect on Ama1, both Clb1 and Cdc5 have been described as activators of APC/C^{Cdc20} in mitosis for yeast and mammals, although this was not tested in meiosis (Lahav-Baratz et al., 1995; Rudner et al., 2000; Rudner and Murray, 2000; Golan et al., 2002; Kraft et al., 2003; Rahal and Amon, 2008). It therefore seems that Cdk1 and polo-like kinase have antagonistic roles in regulating APC/C^{Cdc20} and APC/C^{Ama1}: the phosphorylation of APC/C subunits by Cdk1 and Cdc5 being required for the activation of APC/C by Cdc20 while Cdc5 together with Spo13 and Clb1-Cdk1 inhibits APC/C^{Ama1}. This system strongly resemble the timely regulation of APC/C^{Cdc20} and APC/C^{Cdh1} in mitotic cells where Cdk1 promotes APC/C^{Cdc20} activation by phosphorylating several APC/C subunits while the phosphorylation of Cdh1 by Clbs-Cdk1 hinders its binding to the APC/C, thereby efficiently inhibiting APC/C^{Cdh1}. This system offers a model for the orderly APC/C activation by Cdc20 and Cdh1 (Kramer et al., 2000): The rise of Cdk1 activity promotes APC/C^{Cdc20} while repressing APC/C^{Cdh1}. The activation of APC/C^{Cdc20} at anaphase I triggers the destruction of the cyclins and, consequently, the down-regulation of Cdk1 kinase activity, as well as the release of the Cdc14 phosphatase that removes the phosphorylation on Cdk1 substrates. Cdh1 is therefore dephosphorylated and free to bind and activates the APC/C (reviewed in Alfieri et al., 2017). Similarly, the Cdk1-dependent inhibition of Ama1 might ensure that APC/C^{Ama1} does not get activated before APC/C^{Cdc20}, therefore avoiding the premature exit from meiosis. However, Spo13 being degraded at anaphase I onset, it is unclear why APC/C^{Ama1} does not get active until anaphase II onset. Ama1 might have additional inhibitors that survive the first wave of APC/C^{Cdc20} degradation and might delay APC/C^{Ama1} activity until anaphase II. The activation of APC/C^{Ama1} might depend on a balance between its inhibitors and Ama1 protein level. It would, therefore, be crucial to understand how is Ama1's protein level increase precisely "set up" for the end of the second meiotic division. The regulation of Ama1 protein level is most likely based at the transcriptional level. Indeed, while *AMA1* mRNA level remains constant during early meiosis, it drastically increases towards the end the meiosis (Chu and Herskowitz, 1998; Primig et al., 2000). However, recent work by Cheng et al. suggests that translation control play a much bigger role in controlling the timely accumulation of proteins

during yeast meiosis than previously expected (Cheng et al., 2018). More work would be required to investigate whether Ama1 protein levels are also regulated at a transcriptional level. As a conclusion, our results offer a model for Ama1 inhibition during meiosis I but might not be sufficient to explain how is Ama1 inhibited in metaphase II. Understanding the transcriptional regulation of Ama1 at the end of meiosis might be crucial to understand APC/C^{Ama1} precise timing of up-regulation for the meiotic exit.

3.5. Concluding remarks

Spo13 plays a crucial role in chromosomes orientation in meiosis I by promoting monopolar attachment. However, Spo13 does not directly regulate centromeric cohesin protection but rather ensures that the removal of the centromeric protection machinery is coordinated with the second meiotic division in case cells are delayed in metaphase I. Therefore, Spo13 seems to ensure that meiosis II specific event such as centromeric cohesin deprotection only occur after the first wave of APC/C^{Cdc20} activity, which degrades Spo13. Spo13 might coordinate these events with meiosis II by inhibiting APC/C^{Ama1}. We showed that Spo13 together with the polo-like kinase phosphorylate Clb1 to create a potent Ama1 inhibitor. We propose that this Spo13 function is crucial to avoid the premature exit from meiosis when cells are delayed in metaphase I. However, Spo13 mediated inhibition of Ama1 cannot be the only pathway to control APC/C^{Ama1} activity. If it was, *spo13Δ* cells would not be able to accumulate M-phase proteins at metaphase I entry. The transcriptional control of Ama1 and additional inhibitors are most likely to play an important role for the timely activation of APC/C^{Ama1}. Spo13's function in monopolar attachment and Ama1 inhibition could easily explain the complex phenotype of *spo13Δ* cells. The rather mild monopolar attachment defect triggers a robust SAC response that strongly delays *spo13Δ* cells in metaphase I. And, as Ama1 protein levels increase, in the absence of enough Ama1 inhibitory power, APC/C^{Ama1} activity drives *spo13Δ* cells out of meiosis before the completion of the second meiotic division. In favour of this model, we observed that nuclear division in *spo13Δ* was delayed in the absence of Ama1 or Cdc20 (Figure 31). We therefore believe that APC/C^{Ama1} initiates M-phase protein degradation, thus weakening the SAC inhibitory effect on Cdc20 and helping APC/C^{Cdc20} up-regulation. APC/C^{Cdc20} can, in turn, target its substrates for degradation and "speed up" the completion of the meiotic division and exit in *spo13Δ* cells. A network summarizing Spo13's roles in meiosis I is depicted in Figure 39.

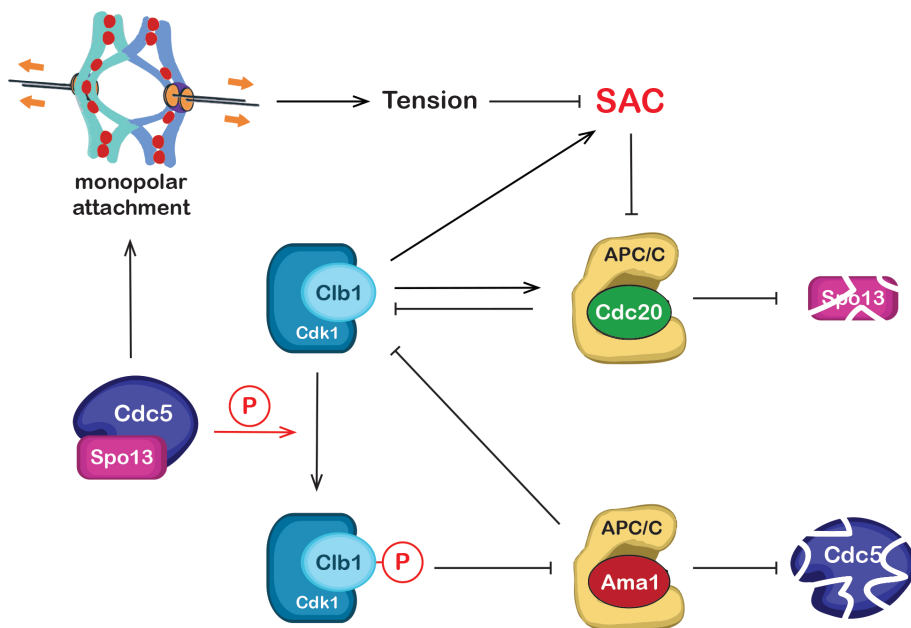


Figure 39: Model for Spo13 function in meiosis I

Spo13-Cdc5 promotes, on one hand, monopolar attachment of sister kinetochores and, on the other hand, the phosphorylation of Clb1. The Clb1 phosphorylated form inhibits APC/C^{Ama1} activity.

4 Materials and Methods

4.1. Yeast Strains

All experiments were performed with diploid *Saccharomyces cerevisiae* strains of the fast-sporulating SK1 genetic background (*ho::LYS2 lys2 ade2!::hisG trp1::hisG leu2::hisG his3!::hisG ura3*) (Kane and Roth, 1974). Diploid strains were obtained by mating a *MATa* and a *MAT α* haploid strains bearing the appropriate genotypes. Unless stated otherwise, mutations in diploid strains are homozygous. The genotype of the yeast strains used in this work are listed in the Table 1. The following alleles were previously described: *clb2::LEU2* (Richardson et al., 1992), *spo13::HIS3MX6* (Katis et al., 2004b), *mad1::URA3* (Hardwick and Murray, 1995), *mad2::KIURA3* (Chen et al., 1999), *mam1::HIS3* (Buonomo et al., 2003), *spo11::hisG-URA3-hisG* (Cha et al., 2000), *hrr25-zo-HIS3::hrr25::NatMX4* (Petronczki et al., 2006), *CLB2p-SGO1* (Katis et al., 2010), *CNM67-tdTomato* and *TetR-tdTomato* (Matos et al., 2008), the *cdc5* analog-sensitive mutant, *cdc5L158G* and *clb1::NatMX4* (Okaz et al., 2012), *Rec8-18SD* and *REC8* isogenic control (Argüello-Miranda et al., 2017), *ama1 Δ* , *myc18-AMA1*, *PDS1-myc18* (Oelschlaegel et al., 2005). To suppress *CDC20* expression in meiotic cells, the endogenous *CDC20* promoter was replaced by the mitosis-specific promoter of either *CLB2* (Lee and Amon, 2003) or *SCC1* genes (Clyne et al., 2003). Likewise, *CDC5* expression was suppressed during meiosis by replacing the endogenous *CDC5* promoter with the promoter of *SCC1* (Clyne et al., 2003).

4.1.1. Construction of plasmids and yeast strains

To visualize their behavior during meiosis by live-cell imaging, several proteins were tagged with the red fluorescent proteins (RFP) mCherry or tdTomato (Shaner et al., 2004) or with a green fluorescent protein (GFP): either yeGFP (Janke et al., 2004), eGFP (Knop et al., 1999) or mNeonGreen (Shaner et al., 2013) on their C-termini by one step PCR tagging (Knop et al., 1999) as indicated in the strains table (Table 1). GFP-tubulin was expressed from his own promoter, integrated at the *URA3* locus. To visualize Rec8 by live-cell imaging, YIplac128 carrying SK1 *REC8* (-333 to +2212), C-terminally tagged with mNeonGreen

(Shaner et al., 2013) was integrated into the promoter of the *rec8::KanMX4* locus (Buonomo et al., 2000). *spo13::BleMX4*, *clb1::BleMX4* and *spo11::BleMX4* were obtained by replacing the marker by one step PCR marker in *spo13::HIS3MX6*, *clb1::NatMX4* and *spo11::HIS3MX6*, respectively. Mad2 and Mad1 were tagged at the C-terminus with mNeonGreen using one-step PCR tagging (Knop et al., 1999). Tagged proteins are functional as judged from normal proliferation and sporulation of homozygous diploids. The *mps1-as1* allele (Jones et al., 2005) was backcrossed > 7 times to SK1 strain (Argüello-Miranda et al., 2017). To restrict *AMA1* expression to early meiosis, *AMA1* promoter was replaced by the early meiotic gene promoter, *DMC1p* (-340 to -1) and *DMC1p-AMA1* was integrated into the *leu2* locus (Argüello-Miranda et al., 2017). To deplete *CDH1* in meiotic cells, the *CDH1* promoter was replaced by the promoter of the mitosis-specific protein, *HSL1*. To create the *clb1-6A* mutant, the N-terminus fragment of *CLB1* (from -82 to 795 bp) containing the following mutations (the number correspond to the amino acid position within the protein): S15A, S84A, S109A, S137A, S141A and S143A, was synthesized by the company GeneArt (ThermoFisher Scientific). This fragment replaced the wild-type sequence into the *YIplac128-CLB1* plasmid to create the *YIplac128-clb1-6A*. Both plasmids were integrated into *clb1::BleMX4* strain to obtain *clb1-6A* mutant and the *CLB1* isogenic control.

Table 1: *S. cerevisiae* SK1 strains used in this study

Figures	Strain	Genotype
37	Z3516	<i>MATα clb2::LEU2</i>
12	Z23072	<i>MATa/MATα mad1::URA3 MAD2-neonGreen::TRP1 CNM67-tdTomato-NatMX4</i>
12, 13, 15, 16	Z23073	<i>MATa/MATα MAD2-neonGreen::TRP1 CNM67-tdTomato-NatMX4</i>
15	Z23074	<i>MATa/MATα spo13::HIS3MX6 MAD2-neonGreen::TRP1 CNM67-tdTomato-NatMX4</i>
16	Z23477	<i>MATa/MATα mam1::HIS3 MAD2-neonGreen::TRP1 CNM67-tdTomato-NatMX4</i>
13	Z23549	<i>MATa/MATα spo11::hisG-URA3-hisG MAD2-neonGreen::TRP1 CNM67-tdTomato-NatMX4</i>
16	Z23586	<i>MATa/MATα hrr25-zo-HIS3::hrr25::NatMX4 MAD2-neonGreen::TRP1 CNM67-tdTomato-NatMX4</i>

10	Z23604	<i>MATa/MATα MAD1ha3::NatMX4 PDS1myc18::KITRP1</i>
10	Z23605	<i>MATa/MATα spo13::HIS3MX6 MAD1ha3::NatMX4 PDS1myc18::KITRP1</i>
23	Z24519	<i>MATa/MATα mad2::KIURA3 MAM1-yeGFP::KITRP1 MTW1-mCherry::HphMX4</i>
17	Z24687	<i>MATa/MATα mam1::HIS3 spo13::HIS3MX6 CNM67-tdTomato-NatMX4 HTB1/HTB1-EGFP-KanMX4</i>
17	Z24688	<i>MATa/MATα mam1::HIS3 CNM67-tdTomato-NatMX4 HTB1/HTB1-EGFP-KanMX4</i>
17	Z24689	<i>MATa/MATα spo13::HIS3MX6 CNM67-tdTomato-NatMX4 HTB1/HTB1-EGFP-KanMX4</i>
17	Z24690	<i>MATa/MATα CNM67-tdTomato-NatMX4 HTB1/HTB1-EGFP-KanMX4</i>
11, 20, 21	Z24861	<i>MATa/MATα spo13::HIS3MX6 mad2::KIURA3 CDC14/CDC14-GFP-LEU2 ura3/ura3::tub1p-yEGFP-TUB1-URA3 tetOx224-HIS3 (integrated 1.4 kb left of CENV) leu2::URA3p-tetR-tdTomato::LEU2</i>
9, 20, 21, 31	Z24862	<i>MATa/MATα spo13::HIS3MX6 CDC14/CDC14-GFP-LEU2 ura3/ura3::tub1p-yEGFP-TUB1-URA3 his3/tetOx224-HIS3 (integrated 1.4 kb left of CENV) leu2/leu2::URA3p-tetR-tdTomato::LEU2</i>
11, 20, 21	Z24863	<i>MATa/MATα mad2::KIURA3 CDC14/CDC14-GFP-LEU2 ura3/ura3::tub1p-yEGFP-TUB1-URA3 his3/tetOx224-HIS3 (integrated 1.4 kb left of CENV) leu2/leu2::URA3p-tetR-tdTomato::LEU2</i>
9, 22	Z24864	<i>MATa/MATα CDC14/CDC14-GFP-LEU2 ura3/ura3::tub1p-yEGFP-TUB1-URA3 his3/tetOx224-HIS3 (integrated 1.4 kb left of CENV) leu2/leu2::URA3p-tetR-tdTomato::LEU2</i>
23	Z25101	<i>MATa/MATα mad2::KIURA3 spo13::HIS3MX6 MAM1-yeGFP::KITRP1 MTW1-mCherry::HphMX4</i>

26	Z25866	<i>MATa/MATα mad2::KIURA3 spo13::HIS3MX6 REC8-neongreen-LEU2::rec8::KanMX4 CNM67-tdTomato-NatMX4</i>
26	Z25867	<i>MATa/MATα spo13::HIS3MX6 REC8-neongreen-LEU2::rec8::KanMX4 CNM67-tdTomato-NatMX4</i>
26	Z25868	<i>MATa/MATα mad2::KIURA3 REC8-neongreen-LEU2::rec8::KanMX4 CNM67-tdTomato-NatMX4</i>
26	Z25869	<i>MATa/MATα REC8-neongreen-LEU2::rec8::KanMX4 CNM67-tdTomato-NatMX4</i>
24	Z25956	<i>MATa/MATα spo13::HIS3MX6 mad2::KIURA3 spo11::hisG-URA3-hisG/spo11::NatMX4 sgo1::NatMX4::CLB2p-HA3-SGO1/sgo1::KanMX6::CLB2p- HA3-SGO1 SPC42/SPC42-GFP-HphMX4 his3/tetOx224-HIS3 (integrated 1.4 kb left of CENV) leu2/leu2::URA3p-tetR-tdTomato::LEU2</i>
24	Z25957	<i>MATa/MATα spo13::HIS3MX6 mad2::KIURA3 spo11::hisG-URA3-hisG/spo11::NatMX4 SPC42-GFP-HphMX4 his3/tetOx224-HIS3 (integrated 1.4 kb left of CENV) leu2/leu2::URA3p-tetR-tdTomato::LEU2</i>
24	Z25958	<i>MATa/MATα spo13::HIS3MX6 mad2::KIURA3 SPC42/SPC42-GFP-HphMX4 his3/tetOx224-HIS3 (integrated 1.4 kb left of CENV) leu2/leu2::URA3p-tetR-tdTomato::LEU2</i>
19	Z26963	<i>MATa/MATα spo13::BleMX4 mam1::HIS3 cdc20::SCC1p-CDC20::KanMX6 ama1::CaURA3 MAD2-neonGreen::TRP1 leu2::URA3p-tetR- tdTomato::LEU2/leu2::DMC1p-AMA1cDNA-LEU2 his3/tetOx224-HIS3 (integrated 1.4 kb left of CENV)</i>
19	Z26965	<i>MATa/MATα spo13::BleMX4 cdc20::SCC1p-CDC20::KanMX6 ama1::CaURA3 MAD2-neonGreen::TRP1 leu2::URA3p-tetR- tdTomato::LEU2/leu2::DMC1p-AMA1cDNA-LEU2 his3/tetOx224-HIS3 (integrated 1.4 kb left of CENV)</i>

14	Z27294	MATa/MAT α rec8-18SD-ha3-LEU2::rec8::KanMX4 MAD2-neonGreen::TRP1 CNM67-tdTomato-NatMX4
14	Z27295	MATa/MAT α REC8ha3-LEU2::rec8::KanMX4 MAD2-neonGreen::TRP1 CNM67-tdTomato-NatMX4
19	Z29307	MATa/MAT α spo11::hisG-URA3-hisG spo13::BleMX4 mam1::HIS3 cdc20::SCC1p-CDC20::KanMX6 ama1::CaURA3 MAD2-neonGreen::TRP1 leu2::DMC1p- AMA1cDNA-LEU2/leu2::URA3p-tetR-tdTomato::LEU2 his3/tetOx224-HIS3 (integrated 1.4 kb left of CENV)
19	Z29310	MATa/MAT α cdc20::SCC1p-CDC20::KanMX6 ama1::CaURA3 MAD2-neonGreen::TRP1 leu2::DMC1p- AMA1cDNA-LEU2/leu2::URA3p-tetR-tdTomato::LEU2 his3/tetOx224-HIS3 (integrated 1.4 kb left of CENV)
37	Z31814	MATa clb1::BleMX4
22	Z31843	MATa/MAT α mam1::HIS3 CDC14/CDC14-GFP-LEU2 ura3/ura3::tub1p-yEGFP-TUB1-URA3 his3/tetOx224-HIS3 (integrated 1.4 kb left of CENV) leu2/leu2::URA3p-tetR-tdTomato::LEU2
32	Z31983	MATa/MAT α CLB1ha3::URA3 AMA1myc9-KITRP1
32	Z31984	MATa/MAT α CLB1ha3::URA3 AMA1myc9-KITRP1
32	Z31985	MATa/MAT α CLB1ha3::URA3
35, 36	Z32112	MATa/MAT α cdc5::SCC1p-CDC5-KanMX4 Clb1-yeGFP-KITRP ama1::NatMX4 cdc20::SCC1pCDC20::HphMX4
35, 36	Z32113	MATa/MAT α spo13::BleMX4 Clb1-yeGFP-KITRP ama1::NatMX4 cdc20::SCC1pCDC20::HphMX5
35, 36	Z32114	MATa/MAT α Clb1-yeGFP-KITRP ama1::NatMX4 cdc20::SCC1pCDC20::HphMX4
34	Z32218	MATa/MAT α CLB1ha3::URA3
27	Z32302	MATa/MAT α sgo1::NatMX4::CLB2p-HA3-SGO1 mad2::KIURA3 spo13::HIS3MX6 REC8-neongreen-LEU2::rec8::KanMX4 CNM67-tdTomato-NatMX4

27	Z32304	<i>MATa/MATα mad2::KIURA3 spo13::HIS3MX6 REC8-neongreen-LEU2::rec8::KanMX4 CNM67-tdTomato-NatMX4</i>
30	Z32560	<i>MATa/MATα spo13::HIS3MX6 cdc20::SCC1p-CDC20::KanMX6 CDH1::HSL1p-CDH1-HphMX4 PDS1myc18::KITRP1</i>
30	Z32561	<i>MATa/MATα cdc20::SCC1p-CDC20::KanMX6 CDH1::HSL1p-CDH1-HphMX4 PDS1myc18::KITRP1</i>
30	Z32562	<i>MATa/MATα spo13::HIS3MX6 cdc20::SCC1p-CDC20::KanMX6 PDS1myc18::KITRP1</i>
30	Z32563	<i>MATa/MATα cdc20::SCC1p-CDC20::KanMX6 PDS1myc18::KITRP1</i>
34	Z32604	<i>MATa/MATα CLB1ha3::URA3 CDC5myc15::URA3 spo13::HIS3MX6</i>
34	Z32605	<i>MATa/MATα CLB1ha3::URA3 CDC5myc15::URA3</i>
37	Z32837	<i>MATa clb1::BleMX4::CLB1::LEU2 PDS1myc18::KITRP1</i>
33	Z32843	<i>MATa/MATα cdc20::SCC1p-CDC20::KanMX6 cdc5::SCC1p-CDC5-KanMX4 ama1::NatMX4 PDS1myc18::KITRP1</i>
33	Z32844	<i>MATa/MATα cdc5L158G-HphMX4 cdc20::SCC1p-CDC20::KanMX6 ama1::NatMX4 PDS1myc18::KITRP1</i>
33	Z32845	<i>MATa/MATα cdc20::SCC1p-CDC20::KanMX6 ama1::NatMX4 PDS1myc18::KITRP1</i>
33	Z32846	<i>MATa/MATα spo13::HIS3MX6 cdc20::SCC1p-CDC20::KanMX6 ama1::NatMX4 PDS1myc18::KITRP1</i>
37	Z32859	<i>MATa clb1::BleMX4::CLB1-6A::LEU2 PDS1myc18::KITRP1</i>

25	Z32950	<i>MATa/MATα rec8-18SD-ha3-LEU2::rec8::KanMX4 spo13::HIS3MX6 mad2::KIURA3 spo11::hisG-URA3-hisG/spo11::NatMX4 his3/tetOx224-HIS3 (integrated 1.4 kb left of CENV) leu2/leu2::URA3p-tetR-tdTomato::LEU2 SPC42/SPC42-GFP-HphMX4</i>
25	Z32951	<i>MATa/MATα spo13::HIS3MX6 mad2::KIURA3 spo11::hisG-URA3-hisG/spo11::NatMX4 his3/tetOx224-HIS3 (integrated 1.4 kb left of CENV) leu2/leu2::URA3p-tetR-tdTomato::LEU2 SPC42/SPC42-GFP-HphMX4</i>
38	Z32975	<i>MATa/MATα ama1::KanMX4 clb1::BleMX4::CLB1::LEU2 cdc20::SCC1p-CDC20::KanMX6 PDS1myc18::KITRP1</i>
38	Z32976	<i>MATa/MATα clb1::BleMX4::CLB1::LEU2 cdc20::SCC1p-CDC20::KanMX6 PDS1myc18::KITRP1</i>
38	Z32977	<i>MATa/MATα ama1::KanMX4 clb1::BleMX4::CLB1-6A::LEU2 cdc20::SCC1p-CDC20::KanMX6 PDS1myc18::KITRP1</i>
38	Z32978	<i>MATa/MATα clb1::BleMX4::CLB1-6A::LEU2 cdc20::SCC1p-CDC20::KanMX6 PDS1myc18::KITRP1</i>
20, 21	Z33012	<i>MATa/MATα mam1::HIS3 mad2::KIURA3 CDC14/CDC14-GFP-LEU2 ura3/ura3::tub1p-yEGFP-TUB1-URA3 his3/tetOx224-HIS3 (integrated 1.4 kb left of CENV) leu2/leu2::URA3p-tetR-tdTomato::LEU2</i>
31	Z33049	<i>MATa/MATα cdc20::SCC1p-CDC20::KanMX6 spo13::HIS3MX6 his3/tetOx224-HIS3 (integrated 1.4 kb left of CENV) leu2/leu2::URA3p-tetR-tdTomato::LEU2 CDC14/CDC14-GFP-LEU2 ura3/ura3::tub1p-yEGFP-TUB1-URA3</i>
31	Z33050	<i>MATa/MATα ama1::NatMX4 spo13::HIS3MX6 heterozygous for: his3/tetOx224-HIS3 (integrated 1.4 kb left of CENV) leu2/leu2::URA3p-tetR-tdTomato::LEU2 CDC14/CDC14-GFP-LEU2 ura3/ura3::tub1p-yEGFP-TUB1-URA3</i>

28	Z33195	<i>MATa/MATα mad2::KIURA3 spo13::HIS3MX6 CNM67-tdTomato-NatMX4 RTS1-neonGreen::TRP1</i>
28	Z33196	<i>MATa/MATα mad2::KIURA3 CNM67-tdTomato-NatMX4 RTS1-neonGreen::TRP1</i>
28	Z33197	<i>MATa/MATα spo13::HIS3MX6 CNM67-tdTomato-NatMX4 RTS1-neonGreen::TRP1</i>
28	Z33198	<i>MATa/MATα CNM67-tdTomato-NatMX4 RTS1-neonGreen::TRP1</i>
18	Z33585	<i>MATa/MATα spo13::BleMX4 spo11::hisG-URA3-hisG mam1::HIS3 CNM67-tdTomato-NatMX4 HTB1/HTB1-EGFP-KanMX4</i>
18	Z33587	<i>MATa/MATα spo13::BleMX4 mam1::HIS3 CNM67-tdTomato-NatMX4 HTB1/HTB1-EGFP-KanMX4</i>

4.2. Meiotic time course

Meiotic time courses were prepared and carried out at 30 °C. Diploid strains were obtained by mating two haploid stains, from the proper genotype, of opposite mating types. The crossing mixture was then streaked to single colonies on glycerol plates (YPG). After 40 hours, single colonies were transferred onto yeast extract peptone dextrose (YPD) plates. 23 hours later, each resulting patch was plated to a thin, homogeneous layer of cells on a YPD plate. Simultaneously, a loop-full of the patch was put on a sporulation plate (SPM, 2% K-acetate). No more than 24 hours later, the meiotic proficiency of each diploid on the sporulation plate was evaluated by looking at the cells on a phase-contrast microscope. The best diploid for each strain was then inoculated into 250 ml of YEPA medium (YP plus 2% K-acetate) in a 2.8 l flask to an OD₆₀₀ of 0.3. The cultures were then shaken at 200 rpm for 11.5 hours at 30 °C on an orbital shaker. At the end of this period, the cultures generally reached an OD₆₀₀ of 1.5 to 1.7 and most cells are arrested in G1, with less than 15% budded cells. The cultures are then pelleted by centrifugation at 3500 rpm for 3 min, washed once with 150 ml of SPM medium, centrifuged once again, and finally resuspended in 100 ml of SPM media, resulting in a final OD₆₀₀ of 3 - 3.5. At the time points indicated on each figure (generally, every 2 hours, from 0 to 12 hours), samples were collected for trichloroacetic

acid (TCA) protein extracts and immuno-fluorescence. Whenever the estradiol-inducible system was used, the expression of proteins under the control of the *GAL1* promoter was triggered with 5 μ M β -estradiol (Sigma).

4.3. TCA extraction

8 to 10 ml of meiotic culture were centrifuged (4000 rpm, 2 min, 4 °C), resuspended in 1 ml of 10% TCA and transferred to a 1.5 ml safe-lock Eppendorf tube. The samples were centrifuged again at 8000 rpm for 2 min at 4 °C. The pellets were then frozen in liquid nitrogen and stored at -80 °C until further processing. For TCA extraction, pellets were put on ice. 200 μ l of zirconium beads (of diameter 0.5 mm) and 300 μ l of 10 % TCA were added to each sample. Cells were then disrupted at 30 Hertz, 5 min, in the cold room, with a mixer mill (MM400, Retsch). After breakage, tubes are immediately transferred on ice and 700 μ l of 10% TCA was added to each sample. The supernatant was transferred, without the beads, to a new, cold, safe-lock Eppendorf tube and spun at 3000 rpm, 4°C, for 10 min. The pellets were quickly resuspended in 200 μ l of 2x Laemmli buffer (62.5 mM Tris-HCl pH 6.8, 10% glycerol, 2% SDS, 0.01% bromophenol blue) with 33 μ l β -mercaptoethanol freshly added. The acid was neutralized by adding 100 μ l of 1 M Tris Base. Samples were then mixed thoroughly and boiled for 10 min at 95°C. Finally, we spun the samples 10 min at 13000 rpm. Protein concentration of the TCA extracts was measured with the Bradford protein assay (BioRad) and 60 μ g of protein was loaded on 8% SDS-Polyacrylamide gels. For Spo13, Mad2 and Pgc1 protein detection, we used a 10% SDS polyacrylamide gels instead.

4.4. Western Blotting and protein detection

To transfer proteins from the SDS-polyacrylamide gel to PVDF membranes (Immobilon P, Millipore), we used semi-dry western blotting at 0.45 mA/cm² for 1 hour. Membranes were then blocked for 1 hour in phosphate-buffer saline (PBS) buffer containing 0.1% Tween 20 (PBS-T) and 4% non-fat milk powder (PBS-T/milk). PVDF membranes were then incubated in primary antibodies at room temperature. The time of incubation for primary and secondary antibodies is specified in the table 2. Primary antibodies were diluted in fresh PBS-T/milk with 0.01% sodium azide and aliquot were conserved at -20°C to be re-used. Dilutions are specified in the antibodies table (Table 2). Membranes were then washed four times 5 min with PBS-T/milk before incubation in the secondary antibody corresponding to the primary antibody used, conjugated with horseradish peroxidase

and diluted at 1:5000 in PBS-T/milk. The timings of incubation of the secondary antibodies are also indicated in Table 2. After four washes with PBS-T, the membranes were incubated 20 seconds with ECL reagents (ECL detection system, GE Healthcare), exposed to x-ray film and developed using an x-ray film processor machine (Optimax 2010, Protec).

Table 2: Antibodies specifications and incubation time.

Protein detected	Antibody type	Incubation time of primary	Incubation time of secondary	Dilution	Producer
Ama1	Rabbit polyclonal	45 min	45 min	1:2000	(Oelschlaegel et al., 2005)
Apc2	Rabbit polyclonal	1 hour	1 hour	1:2000	(Camasses et al., 2003)
Cdc14	Goat polyclonal	3 hours	3 hours or overnight at 4°C	1:1000	Santa Cruz (sc-12045)
Cdc20	Rabbit polyclonal	1.5 hours	1.5 hours	1:5000	(Camasses et al., 2003)
Cdc5	Rabbit polyclonal	45 min	45 min	1:5000	(Matos et al., 2008)
Cdh1	Rabbit polyclonal	1 hour	1 hour	1:5000	Zachariae Lab
Clb1	Goat polyclonal	3 hours	3 hours or overnight at 4°C	1:300	Santa Cruz (sc-7647)
Clb4	Goat polyclonal	2 hours	2 hours or overnight at 4°C	1:400	Santa Cruz (sc-6702)

Clb5	Goat polyclonal	2 hours	2 hours or overnight at 4°C	1:100	Santa Cruz (sc-6704)
Dbf4	Rabbit polyclonal	1 hour	1 hour	1:5000	(Matos et al., 2008)
Ha (12CA5)	Mouse monoclonal	1 hour	1 hour	1:100	
Ha	Rat monoclonal	1 hour	1 hour	1:500	Roche (3F10)
Myc (9E10)	Mouse monoclonal	1 hour	1 hour	1:150	(Evan et al., 1985)
Myc (A-14)	Rabbit polyclonal	1 hour	1 hour	1:500	Santa Cruz (sc-789)
Pgk1	Mouse monoclonal	30 min	30 min	1:40000	Molecular Probe (A-6457)
Rec8	Rabbit polyclonal	1 hour	1 hour	1:5000	(Katis et al., 2010)
Spo13	Rabbit polyclonal	45 min	45 min	1:5000	(Matos et al., 2008)
Tub2	Rabbit polyclonal	45 min	45 min	1:20000	Wolfgang Seufert

4.5. Immuno-fluorescence

Samples for immuno-fluorescence were collected every two hours by harvesting 900 μ l of meiotic culture and fixed by immediately adding 100 μ l of 35% formaldehyde. The samples were then fixed overnight at 4 °C. The next day, samples were washed three times with 1 ml of 0.1 M potassium phosphate buffer

pH 6.4, one time with 1 ml spheroplasting buffer (1.2 M sorbitol, 0.1M potassium phosphate buffer pH 7.4, 0.5 mM MgCl₂) and finally resuspended in 400 μ l of spheroplasting buffer. The samples were then split in two, 200 μ l is frozen as a backup, while we proceed with spheroplasting with the remaining 200 μ l. 4 μ l of a freshly prepared 10% solution of β -mercaptoethanol was added to each sample before incubation at 30 °C, 700 rpm, for 15 min. Samples were then incubated with 10 μ l of zymolase solution (zymolyase 100T from amsbio, 1 mg/ml in spheroplasting buffer) at 30 °C, 700 rpm. Every 5-10 min, we assessed the appearance of the cells through a phase-contrast microscope. When about 75% of the fixed cells looked dark with fuzzy contours, the digestion was stopped by adding 1 ml of ice-cold spheroplasting buffer and kept on ice. After centrifugation at 2500 rpm for 3 min, the spheroplasts are resuspended in 100 μ l of spheroplasting buffer. For each time point, a drop of spheroplasted cells is deposited on a well of a 15-wells slide coated with poly-lysine. Spheroplasted cells are let 5 min to adhere to the surface. The excess volume is removed and the cells were dehydrated by incubating the slides 3 min in methanol and 10 seconds in acetone, both at -20 °C. Slides were let to dry for 2 min. Cells were then re-hydrated by incubating each well with 10 μ l of filtered PBS per well, and then blocked with PBS containing 1% bovine serum albumin (PBS-BSA, filtered) for one hour. The slides were incubated with primary antibodies (1:5 mouse monoclonal anti-myc, 1:300 Rat monoclonal anti- α -tubulin, Serotec, diluted in PBS-BSA) for at least one hour. Wells were then washed at least four times with PBS-BSA for a total washing period of 30 min. Secondary antibodies (1:200 Alexa Fluor 488 donkey anti-rat IgG, life technology ref A21208 and 1:100 Cy3 goat pre-absorbed to mouse IgG, Abacam ab97035, diluted in PBS-BSA) were incubated for one hour and then washed at least four times with PBS. The wells are covered with 5 μ l of mounting medium (100 mg p-phenylenediamine, 0.05 μ g/ml DAPI in glycerol) and the cover slip was carefully applied to avoid the formation of bubbles and to spread the mounting media uniformly. The slides and the cover slips were sealed together with nail polish.

4.6. Immuno-precipitation

For immuno-precipitation, 40 ml of meiotic culture were harvested at the indicated time points, immediately treated with 2 mM PMSF and washed with 2 mM PMSF in cold water. The cell pellets were then snap-frozen in liquid nitrogen until further processing. Cells were resuspended in 400 μ l of B70 breakage buffer (70

mM KOAc, 50 mM Hepes/KOH pH 7.4, 40 mM β -Glycerophosphate, 10% Glycerol, 0.1% Triton X-100, 2.5 mM MgOAc) containing protease inhibitors (5 mM Pefabloc, 2 mM PMSF and 1 Complete, EDTA free, protease tablet from Roche for 15 ml B70), phosphatase inhibitor (1 PhosSTOP tablet for 15ml, Roche) and 1 mM DTT. Cells breakage was performed using 200 μ l zirconium beads (of diameter 0.5 mm) and disrupted 4 times 4 min at 30 Hertz with a mixer mill (MM400, Retsch) and with 4 min in ice between each run. The cell extract is then separated from the beads and centrifuged 30 min at 14.000 rpm. The clear extract was carefully separated from cell debris. The protein concentration of each sample was measured and samples were adjusted to the same concentrations. Extracts were pre-cleared with 150 μ l of protein-A-agarose beads (Roche) for 30 min. The clear extract was then separated from the beads. 30 μ l of the extract was mixed with 30 μ l hot 2 x Laemmli buffer for whole cells extract samples and frozen. For immuno-precipitation, 20 μ l of monoclonal mouse antibodies to Myc (9E11) or Ha (12CA5) were added to the remaining extract and incubated on ice for 1 hour. 30 μ l of protein-A-agarose beads previously blocked in BSA-B70 was added to each sample and incubated for 1 hour on a rotating wheel. Beads were then washed to remove unbound proteins with 1 ml of the following buffers: 2 times 5 min in B70 containing 1 mg/ml BSA, 5 min in B150 (150 mM KOAc, 50 mM Hepes/KOH pH 7.4, 40 mM β -Glycerophosphate, 10% Glycerol, 0.1% Triton X-100, 2.5 mM MgOAc), 5 min in B200 (200 mM KOAc, 50 mM Hepes/KOH pH 7.4, 40 mM β -glycerophosphate, 10% Glycerol, 0.1% Triton X-100, 2.5 mM MgOAc) and 2 times 3 min in B70. All the wash buffers contain protease inhibitors (Complete EDTA-free proteases inhibitor tablet, Pefabloc and 2 mM PMSF) and 1 mM DTT. After washes completion, the beads were resuspended in 20 μ l hot Laemmli buffer and boiled at 95 °C. Beads were filtered out and protein samples were loaded on an 8% or 10% SDS-polyacrylamide gel. Proteins were detected by following the usual protocol (see above, Western Blotting and protein detection).

4.7. Affinity-enrichment mass spectrometry of Clb1-GFP

4.7.1. Large-scale meiotic culture

This protocol was adapted from Martin Schwickart's work (Schwickart, 2005; Schwickart et al., 2004). All the large-scale meiotic cultures were prepared and carried out at 30 °C. As for classical meiotic time courses, healthy diploid strains

are obtained by mating two haploid stains, from the proper genotype, of opposite mating types. The mating mixture was then streaked to single colonies on YPG. After 40 hours, healthy single colonies are transferred onto YPD plates and grew for 23 hours. We then select the best diploid for each strain and plate them homogeneously on 12 plates for each diploid. 24 hours later, the cells from the YPD plates are collected and inoculated in 8 l YEPA medium containing 1:1000 of antifoam SE-15 (Sigma-Aldrich) to an OD_{600} of 0.3. Prior to inoculation, the 8 l of YEPA contained in a 15 l glass beaker was pre-heated in a 30 °C water bath. The cultures are aerated with pressurized humidified air brought to the culture by a tubing system connected to large air-stones disk (diameter of 120 mm) for aquarium. The air flow was sufficient to stir the culture and keep the cell suspension homogeneous. The temperature was kept constant by keeping the cultures immersed in the 30 °C water-bath. After 11 hours, the cells, now mostly arrested in G1, were washed and transfer to approximately 4 l of SPM medium. The volume of SPM media was calculated to get a final OD_{600} of 3. Cells were harvested after 8 hours in SPM, when most the cells were arrested in metaphase I. To quickly cool down the samples, the cultures were poured through a funnel filled with crushed ice. We immediately proceeded to the immuno-precipitation for mass spectrometry protocol without freezing the cell pellets.

4.7.2. Immuno-precipitation for mass spectrometry

All steps were carried out on ice and in the cold room. Cells pellets from the large-scale meiotic culture protocol were washed with 1 l of ice-cold water containing 2 mM of PMSF, spun, and resuspended in 15 ml breakage buffer (70 mM KOAc, 50 mM Hepes/KOH pH 7.4, 40 mM β -glycerophosphate, 10% glycerol, 0.1% Triton X-100, 2.5 mM MgOAc) containing proteases inhibitors (5 mM Pefabloc, 2 mM PMSF and 1 Complete, EDTA free, proteases inhibitor tablet from Roche for 15 ml B70), phosphatase inhibitor (1 PhosSTOP tablet from Roche) and 1 mM DTT. Cells breakage was performed using 15 ml glass beads (of diameter 0.5 mm) and disrupted 4 times 4 min at 30 Hertz with a mixer mill (MM400, Retsch) and with 4 min in ice between runs. The supernatant was separated from the beads and spun 45 min at 18000 rpm. The clear extract is then carefully separated from cell debris, the protein concentration of each sample was measured and samples were adjusted to the same concentrations. Extracts were pre-cleared with 15 ml of Sepharose 4B beads for 30 min (GE Healthcare). The beads were filtered out by running the extract through an empty chromatography column. For the immuno-precipitation, we added to the extract 500 μ l of 50% slurry of anti-GFP nanobodies coupled to agarose beads (GFP-Trap, Chromotek). The extract with

beads is rotated 1 hour on a wheel. Beads are then washed to remove unbound proteins with 45 ml of the following buffers: 2 times 5 min in B70 containing 1mg/ml BSA, 5 min in B150 (150 mM KOAc, 50 mM Hepes/KOH pH 7.4, 40 mM β -glycerophosphate, 10% glycerol, 0.1% Triton X-100, 2.5 mM MgOAc), 5 min in B200 (200 mM KOAc, 50 mM Hepes/KOH pH 7.4, 40 mM β -glycerophosphate, 10% glycerol, 0.1% Triton X-100, 2.5 mM MgOAc). All the washing buffers contained Complete Protease inhibitors, Pefabloc, 1 mM DTT and 2 mM PMSF. Two additional washes in Tris/HCl buffer (50 mM Tris/HCl pH 7.5, 70 mM NaCl, 5% glycerol) were performed for 5 min each in order to remove detergents and to prepare the processing of the sample for mass spectrometry. In order to reach an optimal peptide coverage of Clb1 sequence, each sample was split in two: half was digested with trypsin and the other half, with lysC. The next steps were adapted from the Keilhauer et al. protocol for on-bead digestion of proteins (Keilhauer et al., 2015). The beads were transferred to a small empty chromatography column and spun dry. At room temperature, the column bottom opening was plugged and beads were incubated with 250 μ l elution buffer (50 mM Tris/HCl pH 7.5, 2 M urea, 1 mM DTT) containing either 5 ng/ μ l trypsin (sequencing grade modified trypsin, Promega) or 5 ng/ μ l lysC enzyme (RLys-C, mass spec grade, Promega) for 40 min with short vortexing every 5 min. The column were placed in fresh 2 ml eppendorf tubes and spun at 6000 rpm for 30 sec. The beads were washed 2 times with 125 μ l elution buffer containing 5.5 mM iodoacetamide and spun. Eluates from the two washes were combined with the first eluate. The resulting partial digestion product was left overnight at room temperature for the completion of the trypsin/lysC digestion. The digestion was stopped by adding 11% of the total volume of 10% trifluoroacetic acid (TFA). The affinity-enrichment mass spectrometry (AE-MS) experiment consists of three biological replicates that were processed on different days. The peptides mixtures were kept frozen until all the replicates were ready. The next steps were performed by the mass-spectrometry core facility of the Max Planck Institute of Biochemistry. The peptide samples were cleaned-up by loading them on StageTips to remove salts (Rappsilber et al., 2007). The eluates were analysed by liquid chromatography tandem mass spectrometry (LC-MS/MS) on a Q Exactive HF (Orbitrap) instrument from Thermo Fisher using data-dependent acquisition strategies.

4.8. Mass spectrometry: protein enrichment and post transcriptional modifications analysis

4.8.1. Raw data processing

The raw files provided by the mass-spectrometry core facility were analysed together using the MaxQuant Software (Cox and Mann, 2008)(version 1.6.0.16). The derived peak list was searched with the built-in Andromeda search engine against the reference yeast proteome downloaded in September 2016 from Ensembl (<https://www.ensembl.org/>), and a file containing 247 frequently observed contaminants, such as human keratins, bovine serum proteins, and proteases. Samples digested with trypsin and those digested with lysC were analysed separately. All settings remained the same between these groups except for the enzyme specified. Strict trypsin or lysC specificity was required with C-terminal cleavage after K or R, allowing up to two missed cleavages. The minimum and maximum required peptide length was set to 7 and 25 amino acids, respectively. Phosphorylation of serine, threonine or tyrosine, acetylation of proteins on the N-terminus and oxidation of methionine were set as variable modifications. Carbamidomethylation of cysteine was set as a fixed modification. The maximum number of modifications per peptide was set to five. As no labelling was performed, multiplicity was set to 1. The "match between runs" option was enabled with a match time window of 0.5 min and an alignment time window of 20 min. The label-free quantification algorithm integrated into MaxQuant was used to quantify relative protein intensity between each sample with the following parameters (Cox et al., 2014): the minimum ratio count was set to 2, the FastLFQ option was enabled, LFQ minimum number of neighbours was set to 3, and the LFQ average number of neighbours to 6, as per default. The default settings of MaxQuant for Orbitrap instruments and for identification were used. More specifically, peptide tolerance was set to 4.5 ppm, the isotope match tolerance was set to 2 ppm and the centroid match tolerance was set to 8 ppm. The peptide-to-spectrum match and protein identifications were filtered using a target-decoy approach at a false discovery rate (FDR) of 1%.

4.8.2. Data analysis

The data analysis was carried out using Perseus software (Tyanova et al., 2016) (version 1.6.2.1) and a custom python script. The "proteinGroups.txt" and the "Phospho(STY)Sites.txt" files produced by MaxQuant were loaded into Perseus.

In both case, we independently analysed the sample sets digested with trypsin and with lysC, as the MaxQuant search was also performed independently. The "proteinGroups.txt" file contains all the proteins identified, and we use the LFQ intensity for the analysis protein enrichment between our different conditions. The "Phospho(STY)Sites.txt" file contains the identified phosphorylation sites and is used to map Clb1 phosphorylations and compare Clb1 phosphorylation states in wild-type cells and *spo13Δ* or Cdc5 depleted cells. For both files, hits to the reverse database and contaminants were eliminated.

Protein enrichment analysis

The LFQ intensities were log-transformed (log₂) and samples were grouped in triplicates. Identified proteins were filtered for hits having at least two valid values in at least one group. After this, missing values were imputed with values representing a normal distribution around the detection limit of the mass spectrometer (width of 0.3 and down shift of 1.5). We checked that the distribution of log₂ (LFQ intensity) is roughly normal and comparable between samples, and that missing values imputation does not disturb the overall distribution by plotting histograms of intensities in Perseus.

Phosphorylation analysis and mapping

First, identified phosphorylation sites with a localization probability of less than 0.75 were filtered out. The intensities were log-transformed (log₂) and rows with no valid values were filtered out. We then search for Clb1 phosphorylation sites in both lysC and trypsin digested sets and exported these data for further analysis with python. The intensities for each site is normalized to Clb1 protein intensity obtained in the "proteinGroups.txt", in order to account for the slight variation in the total amount of Clb1-GFP pulled down. Variations were, however, minimal and did not significantly influence the outcome of the analysis. The normalized intensities obtained with lysC and trypsin digestion were then plotted separately with python-plotly (y axis) according to the position within the proteins (x axis). We checked the peptide coverages of Clb1 for each sample to confirm that the variation of phosphorylation intensities was not due to variations in peptides coverage. The coverage was around 73% in trypsin samples and 48% in lysC samples and was very consistent across conditions and replicates. The combined coverage for trypsin and lysC digestions was around 75%.

4.9. Live-cell imaging

4.9.1. Image acquisition

Strains were prepared as described above for a classical meiotic time-course and identically transfer in SPM media (for an OD₆₀₀ around 3) after 11 hours in YEPA. Cultures were then incubated for 3 to 4 hours at 30 °C before starting imaging. Cultures were then diluted to OD⁶⁰⁰ \ 0.2 by adding 30 µl of culture to 300 µl SPM media previously added into a µ-slide 8 wells Ibidi chamber coated with Concanavalin A (Sigma, 0.5 mg/ml in PBS). Imaging was performed in the Imaging Facility of the Max Planck Institute of Biochemistry (MPIB-IF) on a DeltaVision Elite (GE Healthcare) system based on an Olympus IX-71 inverted microscope equipped with an Olympus 100X/1.40NA/oil UPLSAPO objective and a PCO sCMOS 5.5 camera. The microscope is controlled by the SoftWoRx 5.0 software (GE Healthcare). Cells were kept at 30 ° with an environmental chamber. 8 positions were selected per strain with 20-30 cells per field of view. Images were acquired in the green and the red channel every 10 min for 12 hours using a 10% neutral density filter and exposure times of 50 to 200 ms. For proteins tagged with tdTomato, we used the DAPI-FITC-TRITC filter set. For proteins tagged with mCherry, we used the DAPI-FITC-mCh filter set. For each time point, 8 Z-sections, 1 µm apart, were acquired. Z-stacks were automatically deconvolved at the end of the time-course (Additive algorithm supplied by the SoftWoRx program) and projected to a single 2D-image (SoftWoRx, standard projection). Acquisitions were subsequently analysed via imageJ as described in the next section.

4.9.2. Data Analysis and figures

Cells counting and figures preparation were both made in ImageJ (W. S. Rasband, U. S. NIH, Bethesda, MD, <http://imagej.nih.gov/ij/>). For data analysis, we followed each cell individually through time and manually record the observed timing of the events quantified using Microsoft Excel. The events quantified are plotted (y-axis) over time (x-axis) As the events followed vary depending on the proteins and processes accessed, the counting details are provided for each figure. For each strain, 100 cells are quantified. Representative cells for each strain were cut out from the image file to make a figure. Brightness and contrast were adjusted for each channel to reach an optimal display of the events quantified. A merge of the red and green channel was obtained using the "RGB color merge" tool. Stacks of the merged channel and individual red and green channels were combined vertically using the "Stack Combiner" plugin. The acquisition times

were displayed on the upper part of the stacks using the "Time Stamper" tool. Time point $t = 0$ was set to a specific event, such as entry into metaphase I, indicated in each figure legend. Selected frames were combined horizontally to create a representative picture of the meiotic progression for each strain using the "Montage" tool.

Bibliography

Abrieu, A., Magnaghi-Jaulin, L., Kahana, J. A., Peter, M., Castro, A., Vigneron, S., Lorca, T., Cleveland, D. W., and Labbé, J.-C. (2001). "Mps1 is a kinetochore-associated kinase essential for the vertebrate mitotic checkpoint". *Cell* 106.1, 83–93.

Alexandru, G., Uhlmann, F., Mechtler, K., Poupart, M.-A., and Nasmyth, K. (2001). "Phosphorylation of the cohesin subunit Scc1 by Polo/Cdc5 kinase regulates sister chromatid separation in yeast". *Cell* 105.4, 459–472.

Alfieri, C., Zhang, S., and Barford, D. (2017). "Visualizing the complex functions and mechanisms of the anaphase promoting complex/cyclosome (APC/C)". *Open biology* 7.11, 170204.

Anghileri, P., Branduardi, P., Sternieri, F., Monti, P., Visintin, R., Bevilacqua, A., Alberghina, L., Martegani, E., and Baroni, M. D. (1999). "Chromosome separation and exit from mitosis in budding yeast: dependence on growth revealed by cAMP-mediated inhibition". *Experimental cell research* 250.2, 510–523.

Argüello-Miranda, O., Zagoriy, I., Mengoli, V., Rojas, J., Jonak, K., Oz, T., Graf, P., and Zachariae, W. (2017). "Casein kinase 1 coordinates cohesin cleavage, gametogenesis, and exit from M phase in meiosis II". *Developmental cell* 40.1, 37–52.

Argüello-Miranda, O. (2015). "The regulatory network controlling the transition from prophase I into metaphase I". PhD thesis. Fakultät Mathematik und Naturwissenschaften der Technischen Universität ät Dresden Dresden.

Asakawa, H, Kitamura, K, and Shimoda, C (2001). "A novel Cdc20-related WD-repeat protein, Fzr1, is required for spore formation in *Schizosaccharomyces pombe*". *Molecular Genetics and Genomics* 265.3, 424–435.

Biggins, S. and Murray, A. W. (2001). "The budding yeast protein kinase Ipl1/Aurora allows the absence of tension to activate the spindle checkpoint". *Genes & development* 15.23, 3118–3129.

- Blanco, M. A., Pelloquin, L., and Moreno, S. (2001). "Fission yeast *mfr1* activates APC and coordinates meiotic nuclear division with sporulation". *Journal of cell science* 114.11, 2135–2143.
- Bloom, J. and Cross, F. R. (2007). "Multiple levels of cyclin specificity in cell-cycle control". *Nature reviews Molecular cell biology* 8.2, 149.
- Braunstein, I., Miniowitz, S., Moshe, Y., and Hershko, A. (2007). "Inhibitory factors associated with anaphase-promoting complex/cylosome in mitotic checkpoint". *Proceedings of the National Academy of Sciences* 104.12, 4870–4875.
- Brown, N., Noble, M., Endicott, J., Garman, E., Wakatsuki, S, Mitchell, E, Rasmussen, B, Hunt, T, and Johnson, L. (1995). "The crystal structure of cyclin A". *Structure* 3.11, 1235–1247.
- Buckingham, L. E., Wang, H., Elder, R. T., McCarroll, R. M., Slater, M. R., and Esposito, R. (1990). "Nucleotide sequence and promoter analysis of SPO13, a meiosis-specific gene of *Saccharomyces cerevisiae*." *Proceedings of the National Academy of Sciences* 87.23, 9406–9410.
- Buonomo, S. B., Clyne, R. K., Fuchs, J., Loidl, J., Uhlmann, F., and Nasmyth, K. (2000). "Disjunction of homologous chromosomes in meiosis I depends on proteolytic cleavage of the meiotic cohesin Rec8 by separin". *Cell* 103.3, 387–398.
- Buonomo, S. B., Rabitsch, K. P., Fuchs, J., Gruber, S., Sullivan, M., Uhlmann, F., Petronczki, M., Tóth, A., and Nasmyth, K. (2003). "Division of the nucleolus and its release of CDC14 during anaphase of meiosis I depends on separase, SPO12, and SLK19". *Developmental cell* 4.5, 727–739.
- Burton, J. L. and Solomon, M. J. (2007). "Mad3p, a pseudosubstrate inhibitor of APCCdc20 in the spindle assembly checkpoint". *Genes & development* 21.6, 655–667.
- Camasses, A., Bogdanova, A., Shevchenko, A., and Zachariae, W. (2003). "The CCT chaperonin promotes activation of the anaphase-promoting complex through the generation of functional Cdc20". *Molecular cell* 12.1, 87–100.
- Campbell, L. and Hardwick, K. G. (2003). "Analysis of Bub3 spindle checkpoint function in *Xenopus* egg extracts". *Journal of cell science* 116.4, 617–628.
- Carlile, T. M. and Amon, A. (2008). "Meiosis I is established through division-specific translational control of a cyclin". *Cell* 133.2, 280–291.

- Carmena, M., Wheelock, M., Funabiki, H., and Earnshaw, W. C. (2012). "The chromosomal passenger complex (CPC): from easy rider to the godfather of mitosis". *Nature reviews Molecular cell biology* 13.12, 789.
- Cha, R. S., Weiner, B. M., Keeney, S., Dekker, J., and Kleckner, N. (2000). "Progression of meiotic DNA replication is modulated by interchromosomal interaction proteins, negatively by Spo11p and positively by Rec8p". *Genes & development* 14.4, 493–503.
- Chang, L., Zhang, Z., Yang, J., McLaughlin, S. H., and Barford, D. (2014). "Molecular architecture and mechanism of the anaphase-promoting complex". *Nature* 513.7518, 388.
- (2015). "Atomic structure of the APC/C and its mechanism of protein ubiquitination". *Nature* 522.7557, 450.
- Chao, W. C., Kulkarni, K., Zhang, Z., Kong, E. H., and Barford, D. (2012). "Structure of the mitotic checkpoint complex". *Nature* 484.7393, 208.
- Cheeseman, I. M., Chappie, J. S., Wilson-Kubalek, E. M., and Desai, A. (2006). "The conserved KMN network constitutes the core microtubule-binding site of the kinetochore". *Cell* 127.5, 983–997.
- Chen, R.-H., Waters, J. C., Salmon, E., and Murray, A. W. (1996). "Association of spindle assembly checkpoint component XMad2 with unattached kinetochores". *Science* 274.5285, 242.
- Chen, R.-H., Shevchenko, A., Mann, M., and Murray, A. W. (1998). "Spindle checkpoint protein Xmad1 recruits Xmad2 to unattached kinetochores". *The Journal of cell biology* 143.2, 283–295.
- Chen, R.-H., Brady, D. M., Smith, D., Murray, A. W., and Hardwick, K. G. (1999). "The spindle checkpoint of budding yeast depends on a tight complex between the Mad1 and Mad2 proteins". *Molecular biology of the cell* 10.8, 2607–2618.
- Cheng, Z., Otto, G. M., Powers, E. N., Keskin, A., Mertins, P., Carr, S. A., Ivanovic, M., and Brar, G. A. (2018). "Pervasive, coordinated protein-level changes driven by transcript isoform switching during meiosis". *Cell* 172.5, 910–923.
- Chu, S. and Herskowitz, I. (1998). "Gametogenesis in yeast is regulated by a transcriptional cascade dependent on Ndt80". *Molecular cell* 1.5, 685–696.
- Ciosk, R., Zachariae, W., Michaelis, C., Shevchenko, A., Mann, M., and Nasmyth, K. (1998). "An ESP1/PDS1 complex regulates loss of sister chromatid cohesion at the metaphase to anaphase transition in yeast". *Cell* 93.6, 1067–1076.

- Cleveland, D. W., Mao, Y., and Sullivan, K. F. (2003). "Centromeres and kinetochores: from epigenetics to mitotic checkpoint signaling". *Cell* 112.4, 407–421.
- Clyne, R. K., Katis, V. L., Jessop, L., Benjamin, K. R., Herskowitz, I., Lichten, M., and Nasmyth, K. (2003). "Polo-like kinase Cdc5 promotes chiasmata formation and cosegregation of sister centromeres at meiosis I". *Nature Cell Biology* 5.5, 480.
- Cohen-Fix, O., Peters, J.-M., Kirschner, M. W., and Koshland, D. (1996). "Anaphase initiation in *Saccharomyces cerevisiae* is controlled by the APC-dependent degradation of the anaphase inhibitor Pds1p." *Genes & development* 10.24, 3081–3093.
- Cooper, K. F. and Strich, R. (2011). "Meiotic control of the APC/C: similarities & differences from mitosis". *Cell division* 6.1, 16.
- Cooper, K. F., Mallory, M. J., Egeland, D. B., Jarnik, M., and Strich, R. (2000). "Ama1p is a meiosis-specific regulator of the anaphase promoting complex/cyclosome in yeast". *Proceedings of the National Academy of Sciences* 97.26, 14548–14553.
- Corbett, K. D. and Harrison, S. C. (2012). "Molecular architecture of the yeast monopolin complex". *Cell reports* 1.6, 583–589.
- Cox, J. and Mann, M. (2008). "MaxQuant enables high peptide identification rates, individualized ppb-range mass accuracies and proteome-wide protein quantification". *Nature biotechnology* 26.12, 1367.
- Cox, J., Hein, M. Y., Lubner, C. A., Paron, I., Nagaraj, N., and Mann, M. (2014). "MaxLFQ allows accurate proteome-wide label-free quantification by delayed normalization and maximal peptide ratio extraction". *Molecular & cellular proteomics*, mcp–M113.
- Dahmann, C. and Futcher, B. (1995). "Specialization of B-type cyclins for mitosis or meiosis in *S. cerevisiae*." *Genetics* 140.3, 957–963.
- Davis, B. K. (1971). "Genetic analysis of a meiotic mutant resulting in precocious sister-centromere separation in *Drosophila melanogaster*". *Molecular and General Genetics MGG* 113.3, 251–272.
- De Antoni, A., Pearson, C. G., Cimini, D., Canman, J. C., Sala, V., Nezi, L., Mapelli, M., Sironi, L., Faretta, M., Salmon, E. D., et al. (2005). "The Mad1/Mad2 complex as a template for Mad2 activation in the spindle assembly checkpoint". *Current Biology* 15.3, 214–225.

- DeLuca, K. F., Lens, S. M., and DeLuca, J. G. (2011). "Temporal changes in Hec1 phosphorylation control kinetochore–microtubule attachment stability during mitosis". *J Cell Sci* 124.4, 622–634.
- Ditchfield, C., Johnson, V. L., Tighe, A., Ellston, R., Haworth, C., Johnson, T., Mortlock, A., Keen, N., and Taylor, S. S. (2003). "Aurora B couples chromosome alignment with anaphase by targeting BubR1, Mad2, and Cenp-E to kinetochores". *J Cell Biol* 161.2, 267–280.
- Evan, G. I., Lewis, G. K., Ramsay, G., and Bishop, J. M. (1985). "Isolation of monoclonal antibodies specific for human c-myc proto-oncogene product." *Molecular and cellular biology* 5.12, 3610–3616.
- Fang, G., Yu, H., and Kirschner, M. W. (1998). "The checkpoint protein MAD2 and the mitotic regulator CDC20 form a ternary complex with the anaphase-promoting complex to control anaphase initiation". *Genes & development* 12.12, 1871–1883.
- Fitch, I, Dahmann, C, Surana, U, Amon, A, Nasmyth, K, Goetsch, L, Byers, B, and Futcher, B (1992). "Characterization of four B-type cyclin genes of the budding yeast *Saccharomyces cerevisiae*." *Molecular biology of the cell* 3.7, 805–818.
- Funabiki, H., Yamano, H., Kumada, K., Nagao, K., Hunt, T., and Yanagida, M. (1996). "Cut2 proteolysis required for sister-chromatid separation in fission yeast". *Nature* 381.6581, 438.
- Furuta, T., Tuck, S., Kirchner, J., Koch, B., Auty, R., Kitagawa, R., Rose, A. M., and Greenstein, D. (2000). "EMB-30: an APC4 homologue required for metaphase-to-anaphase transitions during meiosis and mitosis in *Caenorhabditis elegans*". *Molecular biology of the cell* 11.4, 1401–1419.
- Futcher, B. (2008). "Cyclins in meiosis: lost in translation". *Developmental cell* 14.5, 644–645.
- Gillett, E. S., Espelin, C. W., and Sorger, P. K. (2004). "Spindle checkpoint proteins and chromosome–microtubule attachment in budding yeast". *J Cell Biol* 164.4, 535–546.
- Golan, A., Yudkovsky, Y., and Hershko, A. (2002). "The cyclin-ubiquitin ligase activity of cyclosome/APC is jointly activated by protein kinases Cdk1-cyclin B and Plk". *Journal of biological chemistry* 277.18, 15552–15557.
- Goldstein, L. S. (1980). "Mechanisms of chromosome orientation revealed by two meiotic mutants in *Drosophila melanogaster*". *Chromosoma* 78.1, 79–111.

- Goldstein, L. S. (1981). "Kinetochore structure and its role in chromosome orientation during the first meiotic division in male *D. melanogaster*". *Cell* 25.3, 591–602.
- Gorbsky, G. J., Kallio, M., Daum, J. R., and Topper, L. M. (1999). "Protein dynamics at the kinetochore: cell cycle regulation of the metaphase to anaphase transition". *The FASEB Journal* 13.9002, s231–S234.
- Grandin, N. and Reed, S. I. (1993). "Differential function and expression of *Saccharomyces cerevisiae* B-type cyclins in mitosis and meiosis." *Molecular and cellular biology* 13.4, 2113–2125.
- Gruber, S., Haering, C. H., and Nasmyth, K. (2003). "Chromosomal cohesin forms a ring". *Cell* 112.6, 765–777.
- Haering, C. H., Löwe, J., Hochwagen, A., and Nasmyth, K. (2002). "Molecular architecture of SMC proteins and the yeast cohesin complex". *Molecular cell* 9.4, 773–788.
- Haering, C. H., Farcas, A.-M., Arumugam, P., Metson, J., and Nasmyth, K. (2008). "The cohesin ring concatenates sister DNA molecules". *Nature* 454.7202, 297.
- Hardwick, K. G. and Murray, A. W. (1995). "Mad1p, a phosphoprotein component of the spindle assembly checkpoint in budding yeast." *The Journal of cell biology* 131.3, 709–720.
- Hardwick, K. G., Weiss, E., Luca, F. C., Winey, M., and Murray, A. W. (1996). "Activation of the budding yeast spindle assembly checkpoint without mitotic spindle disruption". *Science* 273.5277, 953–956.
- Hardwick, K. G., Johnston, R. C., Smith, D. L., and Murray, A. W. (2000). "MAD3 encodes a novel component of the spindle checkpoint which interacts with Bub3p, Cdc20p, and Mad2p". *The Journal of cell biology* 148.5, 871–882.
- Hassold, T. and Hunt, P. (2001). "To err (meiotically) is human: the genesis of human aneuploidy". *Nature Reviews Genetics* 2.4, 280.
- Hauf, S., Waizenegger, I. C., and Peters, J.-M. (2001). "Cohesin cleavage by separase required for anaphase and cytokinesis in human cells". *Science* 293.5533, 1320–1323.

- Hauf, S., Cole, R. W., LaTerra, S., Zimmer, C., Schnapp, G., Walter, R., Heckel, A., Van Meel, J., Rieder, C. L., and Peters, J.-M. (2003). "The small molecule Hesperadin reveals a role for Aurora B in correcting kinetochore–microtubule attachment and in maintaining the spindle assembly checkpoint". *J Cell Biol* 161.2, 281–294.
- Hauf, S., Roitinger, E., Koch, B., Dittrich, C. M., Mechtler, K., and Peters, J.-M. (2005). "Dissociation of cohesin from chromosome arms and loss of arm cohesion during early mitosis depends on phosphorylation of SA2". *PLoS biology* 3.3, e69.
- Hepworth, S. R., Friesen, H., and Segall, J. (1998). "NDT80 and the meiotic recombination checkpoint regulate expression of middle sporulation-specific genes in *Saccharomyces cerevisiae*". *Molecular and cellular biology* 18.10, 5750–5761.
- Herzog, F., Primorac, I., Dube, P., Lenart, P., Sander, B., Mechtler, K., Stark, H., and Peters, J.-M. (2009). "Structure of the anaphase-promoting complex/cyclosome interacting with a mitotic checkpoint complex". *Science* 323.5920, 1477–1481.
- Hornig, N. C. and Uhlmann, F. (2004). "Preferential cleavage of chromatin-bound cohesin after targeted phosphorylation by Polo-like kinase". *The EMBO journal* 23.15, 3144–3153.
- Howell, B., McEwen, B., Canman, J., Hoffman, D., Farrar, E., Rieder, C., and Salmon, E. (2001). "Cytoplasmic dynein/dynactin drives kinetochore protein transport to the spindle poles and has a role in mitotic spindle checkpoint inactivation". *J Cell Biol* 155.7, 1159–1172.
- Howell, B. J., Moree, B., Farrar, E. M., Stewart, S., Fang, G., and Salmon, E. (2004). "Spindle checkpoint protein dynamics at kinetochores in living cells". *Current biology* 14.11, 953–964.
- Hoyt, M. A., Totis, L., and Roberts, B. T. (1991). "*S. cerevisiae* genes required for cell cycle arrest in response to loss of microtubule function". *Cell* 66.3, 507–517.
- Hugerat, Y. and Simchen, G. (1993). "Mixed segregation and recombination of chromosomes and YACs during single-division meiosis in *spo13* strains of *Saccharomyces cerevisiae*." *Genetics* 135.2, 297–308.
- Hwang, L. H., Lau, L. F., Smith, D. L., Mistrot, C. A., Hardwick, K. G., Hwang, E. S., Amon, A., and Murray, A. W. (1998). "Budding yeast Cdc20: a target of the spindle checkpoint". *Science* 279.5353, 1041–1044.

- Iouk, T., Kerscher, O., Scott, R. J., Basrai, M. A., and Wozniak, R. W. (2002). "The yeast nuclear pore complex functionally interacts with components of the spindle assembly checkpoint". *J Cell Biol* 159.5, 807–819.
- Irniger, S., Piatti, S., Michaelis, C., and Nasmyth, K. (1995). "Genes involved in sister chromatid separation are needed for B-type cyclin proteolysis in budding yeast". *Cell* 81.2, 269–277.
- Ishiguro, T., Tanaka, K., Sakuno, T., and Watanabe, Y. (2010). "Shugoshin–PP2A counteracts casein-kinase-1-dependent cleavage of Rec8 by separase". *Nature cell biology* 12.5, 500.
- Janke, C., Magiera, M. M., Rathfelder, N., Taxis, C., Reber, S., Maekawa, H., Moreno-Borchart, A., Doenges, G., Schwob, E., Schiebel, E., et al. (2004). "A versatile toolbox for PCR-based tagging of yeast genes: new fluorescent proteins, more markers and promoter substitution cassettes". *Yeast* 21.11, 947–962.
- Jaspersen, S. L. and Winey, M. (2004). "The budding yeast spindle pole body: structure, duplication, and function". *Annu. Rev. Cell Dev. Biol.* 20, 1–28.
- Jaspersen, S. L., Charles, J. F., and Morgan, D. O. (1999). "Inhibitory phosphorylation of the APC regulator Hct1 is controlled by the kinase Cdc28 and the phosphatase Cdc14". *Current Biology* 9.5, 227–236.
- Jeffrey, P. D., Russo, A. A., Polyak, K., Gibbs, E., Hurwitz, J., Massagué, J., and Pavletich, N. P. (1995). "Mechanism of CDK activation revealed by the structure of a cyclinA-CDK2 complex". *Nature* 376.6538, 313.
- Jones, M. H., Huneycutt, B. J., Pearson, C. G., Zhang, C., Morgan, G., Shokat, K., Bloom, K., and Winey, M. (2005). "Chemical genetics reveals a role for Mps1 kinase in kinetochore attachment during mitosis". *Current Biology* 15.2, 160–165.
- Kallio, M., Weinstein, J., Daum, J. R., Burke, D. J., and Gorbsky, G. J. (1998). "Mammalian p55CDC mediates association of the spindle checkpoint protein Mad2 with the cyclosome/anaphase-promoting complex, and is involved in regulating anaphase onset and late mitotic events". *The Journal of cell biology* 141.6, 1393–1406.
- Kallio, M. J., McClelland, M. L., Stukenberg, P. T., and Gorbsky, G. J. (2002). "Inhibition of aurora B kinase blocks chromosome segregation, overrides the spindle checkpoint, and perturbs microtubule dynamics in mitosis". *Current Biology* 12.11, 900–905.

- Kane, S. M. and Roth, R. (1974). "Carbohydrate metabolism during ascospore development in yeast". *Journal of Bacteriology* 118.1, 8–14.
- Katis, V. L., Galova, M., Rabitsch, K. P., Gregan, J., and Nasmyth, K. (2004a). "Maintenance of cohesin at centromeres after meiosis I in budding yeast requires a kinetochore-associated protein related to MEI-S332". *Current Biology* 14.7, 560–572.
- Katis, V. L., Matos, J., Mori, S., Shirahige, K., Zachariae, W., and Nasmyth, K. (2004b). "Spo13 facilitates monopolin recruitment to kinetochores and regulates maintenance of centromeric cohesion during yeast meiosis". *Current Biology* 14.24, 2183–2196.
- Katis, V. L., Lipp, J. J., Imre, R., Bogdanova, A., Okaz, E., Habermann, B., Mechtler, K., Nasmyth, K., and Zachariae, W. (2010). "Rec8 phosphorylation by casein kinase 1 and Cdc7-Dbf4 kinase regulates cohesin cleavage by separase during meiosis". *Developmental cell* 18.3, 397–409.
- Keeney, S., Giroux, C. N., and Kleckner, N. (1997). "Meiosis-specific DNA double-strand breaks are catalyzed by Spo11, a member of a widely conserved protein family". *Cell* 88.3, 375–384.
- Keilhauer, E. C., Hein, M. Y., and Mann, M. (2015). "Accurate protein complex retrieval by affinity enrichment mass spectrometry (AE-MS) rather than affinity purification mass spectrometry (AP-MS)". *Molecular & Cellular Proteomics* 14.1, 120–135.
- Kelly, A. E. and Funabiki, H. (2009). "Correcting aberrant kinetochore microtubule attachments: an Aurora B-centric view". *Current opinion in cell biology* 21.1, 51–58.
- Kerrebrock, A. W., Moore, D. P., Wu, J. S., and Orr-Weaver, T. L. (1995). "Mei-S332, a Drosophila protein required for sister-chromatid cohesion, can localize to meiotic centromere regions". *Cell* 83.2, 247–256.
- Kerrebrock, A., Miyazaki, W., Birnby, D, and Orr-Weaver, T. (1992). "The Drosophila mei-S332 gene promotes sister-chromatid cohesion in meiosis following kinetochore differentiation." *Genetics* 130.4, 827–841.
- Kim, J., Ishiguro, K.-i., Nambu, A., Akiyoshi, B., Yokobayashi, S., Kagami, A., Ishiguro, T., Pendas, A. M., Takeda, N., Sakakibara, Y., et al. (2015). "Meikin is a conserved regulator of meiosis-I-specific kinetochore function". *Nature* 517.7535, 466.

- Kim, S. H., Lin, D. P., Matsumoto, S., Kitazono, A., and Matsumoto, T. (1998). "Fission yeast Slp1: an effector of the Mad2-dependent spindle checkpoint". *Science* 279.5353, 1045–1047.
- Kitajima, T. S., Miyazaki, Y., Yamamoto, M., and Watanabe, Y. (2003). "Rec8 cleavage by separase is required for meiotic nuclear divisions in fission yeast". *The EMBO journal* 22.20, 5643–5653.
- Kitajima, T. S., Kawashima, S. A., and Watanabe, Y. (2004). "The conserved kinetochore protein shugoshin protects centromeric cohesion during meiosis". *Nature* 427.6974, 510.
- Kitajima, T. S., Sakuno, T., Ishiguro, K.-i., Iemura, S.-i., Natsume, T., Kawashima, S. A., and Watanabe, Y. (2006). "Shugoshin collaborates with protein phosphatase 2A to protect cohesin". *Nature* 441.7089, 46.
- Klapholz, S. and Esposito, R. E. (1980a). "Isolation of SPO12–1 and SPO13–1 from a natural variant of yeast that undergoes a single meiotic division". *Genetics* 96.3, 567–588.
- (1980b). "Recombination and chromosome segregation during the single division meiosis in SPO12–1 and SPO13–1 diploids". *Genetics* 96.3, 589–611.
- Klapholz, S., Waddell, C. S., and Esposito, R. E. (1985). "The role of the SPO11 gene in meiotic recombination in yeast". *Genetics* 110.2, 187–216.
- Klein, F., Mahr, P., Galova, M., Buonomo, S. B., Michaelis, C., Nairz, K., and Nasmyth, K. (1999). "A central role for cohesins in sister chromatid cohesion, formation of axial elements, and recombination during yeast meiosis". *Cell* 98.1, 91–103.
- Knop, M., Siegers, K., Pereira, G., Zachariae, W., Winsor, B., Nasmyth, K., and Schiebel, E. (1999). "Epitope tagging of yeast genes using a PCR-based strategy: more tags and improved practical routines". *Yeast* 15.10B, 963–972.
- Kraft, C., Herzog, F., Gieffers, C., Mechtler, K., Hagting, A., Pines, J., and Peters, J.-M. (2003). "Mitotic regulation of the human anaphase-promoting complex by phosphorylation". *The EMBO journal* 22.24, 6598–6609.
- Kramer, E. R., Scheuringer, N., Podtelejnikov, A. V., Mann, M., and Peters, J.-M. (2000). "Mitotic regulation of the APC activator proteins CDC20 and CDH1". *Molecular biology of the cell* 11.5, 1555–1569.

- Lahav-Baratz, S., Sudakin, V., Ruderman, J. V., and Hershko, A. (1995). "Reversible phosphorylation controls the activity of cyclosome-associated cyclin-ubiquitin ligase". *Proceedings of the National Academy of Sciences* 92.20, 9303–9307.
- Lampson, M. A. and Cheeseman, I. M. (2011). "Sensing centromere tension: Aurora B and the regulation of kinetochore function". *Trends in cell biology* 21.3, 133–140.
- Lampson, M. A., Renduchitala, K., Khodjakov, A., and Kapoor, T. M. (2004). "Correcting improper chromosome–spindle attachments during cell division". *Nature cell biology* 6.3, 232.
- Langan, T., Gautier, J, Lohka, M, Hollingsworth, R, Moreno, S, Nurse, P, Maller, J, and Sclafani, R. (1989). "Mammalian growth-associated H1 histone kinase: a homolog of cdc2+/CDC28 protein kinases controlling mitotic entry in yeast and frog cells." *Molecular and Cellular Biology* 9.9, 3860–3868.
- Lee, B. H. and Amon, A. (2003). "Role of Polo-like kinase CDC5 in programming meiosis I chromosome segregation". *Science* 300.5618, 482–486.
- Lee, B. H., Kiburz, B. M., and Amon, A. (2004). "Spo13 maintains centromeric cohesion and kinetochore coorientation during meiosis I". *Current biology* 14.24, 2168–2182.
- Li, R. and Murray, A. W. (1991). "Feedback control of mitosis in budding yeast". *Cell* 66.3, 519–531.
- Li, X. and Dawe, R. K. (2009). "Fused sister kinetochores initiate the reductional division in meiosis I". *Nature cell biology* 11.9, 1103.
- Lindon, C. (2008). *Control of mitotic exit and cytokinesis by the APC/C*.
- Liu, D., Vleugel, M., Backer, C. B., Hori, T., Fukagawa, T., Cheeseman, I. M., and Lampson, M. A. (2010). "Regulated targeting of protein phosphatase 1 to the outer kinetochore by KNL1 opposes Aurora B kinase". *The Journal of cell biology* 188.6, 809–820.
- Luo, X. and Yu, H. (2008). "Protein metamorphosis: the two-state behavior of Mad2". *Structure* 16.11, 1616–1625.
- Luo, X., Tang, Z., Rizo, J., and Yu, H. (2002). "The Mad2 spindle checkpoint protein undergoes similar major conformational changes upon binding to either Mad1 or Cdc20". *Molecular cell* 9.1, 59–71.

- Luo, X., Tang, Z., Xia, G., Wassmann, K., Matsumoto, T., Rizo, J., and Yu, H. (2004). "The Mad2 spindle checkpoint protein has two distinct natively folded states". *Nature Structural and Molecular Biology* 11.4, 338.
- Maiato, H., DeLuca, J., Salmon, E., and Earnshaw, W. C. (2004). "The dynamic kinetochore-microtubule interface". *Journal of cell science* 117.23, 5461–5477.
- Mapelli, M. and Musacchio, A. (2007). "MAD contortions: conformational dimerization boosts spindle checkpoint signaling". *Current opinion in structural biology* 17.6, 716–725.
- Maresca, T. J. and Salmon, E. (2010). "Welcome to a new kind of tension: translating kinetochore mechanics into a wait-anaphase signal". *J Cell Sci* 123.6, 825–835.
- Marston, A. L. and Amon, A. (2004). "Meiosis: cell-cycle controls shuffle and deal". *Nature Reviews Molecular Cell Biology* 5.12, 983–997.
- Marston, A. L., Tham, W.-H., Shah, H., and Amon, A. (2004). "A genome-wide screen identifies genes required for centromeric cohesion". *Science* 303.5662, 1367–1370.
- Matos, J., Lipp, J. J., Bogdanova, A., Guillot, S., Okaz, E., Junqueira, M., Shevchenko, A., and Zachariae, W. (2008). "Dbf4-dependent CDC7 kinase links DNA replication to the segregation of homologous chromosomes in meiosis I". *Cell* 135.4, 662–678.
- McGuinness, B. E., Hirota, T., Kudo, N. R., Peters, J.-M., and Nasmyth, K. (2005). "Shugoshin prevents dissociation of cohesin from centromeres during mitosis in vertebrate cells". *PLoS biology* 3.3, e86.
- Mitchell, A. P. (1994). "Control of meiotic gene expression in *Saccharomyces cerevisiae*." *Microbiological reviews* 58.1, 56–70.
- Morgan, D. O. (2006). *The cell cycle: principles of control*. New Science Press.
- Musacchio, A. (2015). "The molecular biology of spindle assembly checkpoint signaling dynamics". *Current biology* 25.20, R1002–R1018.
- Musacchio, A. and Hardwick, K. G. (2002). "The spindle checkpoint: structural insights into dynamic signalling". *Nature reviews Molecular cell biology* 3.10, 731–741.
- Musacchio, A. and Salmon, E. D. (2007). "The spindle-assembly checkpoint in space and time". *Nature reviews Molecular cell biology* 8.5, 379.

- Nasmyth, K. (1996). "At the heart of the budding yeast cell cycle". *Trends in Genetics* 12.10, 405–412.
- Nasmyth, K. and Haering, C. H. (2005). "The structure and function of SMC and kleisin complexes". *Annu. Rev. Biochem.* 74, 595–648.
- (2009). "Cohesin: its roles and mechanisms". *Annual review of genetics* 43, 525–558.
- Nicklas, R. B. (1997). "How cells get the right chromosomes". *Science* 275.5300, 632–637.
- Nicklas, R. B. and Ward, S. C. (1994). "Elements of error correction in mitosis: microtubule capture, release, and tension." *The Journal of cell biology* 126.5, 1241–1253.
- Nicklas, R. B., Waters, J. C., Salmon, E., and Ward, S. C. (2001). "Checkpoint signals in grasshopper meiosis are sensitive to microtubule attachment, but tension is still essential". *Journal of cell science* 114.23, 4173–4183.
- Oelschlaegel, T., Schwickart, M., Matos, J., Bogdanova, A., Camasses, A., Havlis, J., Shevchenko, A., and Zachariae, W. (2005). "The yeast APC/C subunit Mnd2 prevents premature sister chromatid separation triggered by the meiosis-specific APC/C-Ama1". *Cell* 120.6, 773–788.
- Okaz, E., Argüello-Miranda, O., Bogdanova, A., Vinod, P., Lipp, J. J., Markova, Z., Zagoriy, I., Novak, B., and Zachariae, W. (2012). "Meiotic prophase requires proteolysis of M phase regulators mediated by the meiosis-specific APC/C Ama1". *Cell* 151.3, 603–618.
- Östergren, G. (1951). "The mechanism of co-orientation in bivalents and multivalents". *Hereditas* 37.1-2, 85–156.
- Pesin, J. A. and Orr-Weaver, T. L. (2008). "Regulation of APC/C activators in mitosis and meiosis". *Annual review of cell and developmental biology* 24, 475–499.
- Peters, J.-M. (2006). "The anaphase promoting complex/cyclosome: a machine designed to destroy". *Nature reviews Molecular cell biology* 7.9, 644.
- Petronczki, M., Siomos, M. F., and Nasmyth, K. (2003). "Un menage a quatre: the molecular biology of chromosome segregation in meiosis". *Cell* 112.4, 423–440.
- Petronczki, M., Matos, J., Mori, S., Gregan, J., Bogdanova, A., Schwickart, M., Mechtler, K., Shirahige, K., Zachariae, W., and Nasmyth, K. (2006). "Monopolar

attachment of sister kinetochores at meiosis I requires casein kinase 1". *Cell* 126.6, 1049–1064.

Primig, M., Williams, R. M., Winzeler, E. A., Tevzadze, G. G., Conway, A. R., Hwang, S. Y., Davis, R. W., and Esposito, R. E. (2000). "The core meiotic transcriptome in budding yeasts". *Nature genetics* 26.4, 415.

Rabitsch, K. P., Petronczki, M., Javerzat, J.-P., Genier, S., Chwalla, B., Schleiffer, A., Tanaka, T. U., and Nasmyth, K. (2003). "Kinetochores recruitment of two nucleolar proteins is required for homolog segregation in meiosis I". *Developmental cell* 4.4, 535–548.

Rabitsch, K. P., Gregan, J., Schleiffer, A., Javerzat, J.-P., Eisenhaber, F., and Nasmyth, K. (2004). "Two fission yeast homologs of *Drosophila* Mei-S332 are required for chromosome segregation during meiosis I and II". *Current Biology* 14.4, 287–301.

Rahal, R. and Amon, A. (2008). "Mitotic CDKs control the metaphase–anaphase transition and trigger spindle elongation". *Genes & development* 22.11, 1534–1548.

Rappsilber, J., Mann, M., and Ishihama, Y. (2007). "Protocol for micro-purification, enrichment, pre-fractionation and storage of peptides for proteomics using StageTips". *Nature protocols* 2.8, 1896.

Rattani, A., Vinod, P., Godwin, J., Tachibana-Konwalski, K., Wolna, M., Malumbres, M., Novák, B., and Nasmyth, K. (2014). "Dependency of the spindle assembly checkpoint on Cdk1 renders the anaphase transition irreversible". *Current Biology* 24.6, 630–637.

Richardson, H., Lew, D. J., Henze, M., Sugimoto, K., and Reed, S. I. (1992). "Cyclin-B homologs in *Saccharomyces cerevisiae* function in S phase and in G2". *Genes & development* 6.11, 2021–2034.

Riedel, C. G., Katis, V. L., Katou, Y., Mori, S., Itoh, T., Helmhart, W., Gálová, M., Petronczki, M., Gregan, J., Cetin, B., et al. (2006). "Protein phosphatase 2A protects centromeric sister chromatid cohesion during meiosis I". *Nature* 441.7089, 53.

Rieder, C. L., Cole, R. W., Khodjakov, A., and Sluder, G. (1995). "The checkpoint delaying anaphase in response to chromosome monoorientation is mediated by an inhibitory signal produced by unattached kinetochores." *The Journal of cell biology* 130.4, 941–948.

- Rieder, C. L., Schultz, A., Cole, R., and Sluder, G. (1994). "Anaphase onset in vertebrate somatic cells is controlled by a checkpoint that monitors sister kinetochore attachment to the spindle." *The Journal of cell biology* 127.5, 1301–1310.
- Rock, J. M. and Amon, A. (2009). "The FEAR network". *Current Biology* 19.23, R1063–R1068.
- Roeder, G. S. (1995). "Sex and the single cell: meiosis in yeast". *Proceedings of the National Academy of Sciences* 92.23, 10450–10456.
- Ruchaud, S., Carmena, M., and Earnshaw, W. C. (2007). "Chromosomal passengers: conducting cell division". *Nature reviews Molecular cell biology* 8.10, 798.
- Rudner, A. D. and Murray, A. W. (2000). "Phosphorylation by Cdc28 activates the Cdc20-dependent activity of the anaphase-promoting complex". *The Journal of cell biology* 149.7, 1377–1390.
- Rudner, A. D., Hardwick, K. G., and Murray, A. W. (2000). "Cdc28 activates exit from mitosis in budding yeast". *The Journal of cell biology* 149.7, 1361–1376.
- Salah, S.-M. and Nasmyth, K. (2000). "Destruction of the securin Pds1p occurs at the onset of anaphase during both meiotic divisions in yeast". *Chromosoma* 109.1-2, 27–34.
- Salic, A., Waters, J. C., and Mitchison, T. J. (2004). "Vertebrate shugoshin links sister centromere cohesion and kinetochore microtubule stability in mitosis". *Cell* 118.5, 567–578.
- Salimian, K. J., Ballister, E. R., Smoak, E. M., Wood, S., Panchenko, T., Lampson, M. A., and Black, B. E. (2011). "Feedback control in sensing chromosome biorientation by the Aurora B kinase". *Current Biology* 21.13, 1158–1165.
- Sarkar, S., Shenoy, R. T., Dalgaard, J. Z., Newnham, L., Hoffmann, E., Millar, J. B., and Arumugam, P. (2013). "Monopolin subunit Csm1 associates with MIND complex to establish monopolar attachment of sister kinetochores at meiosis I". *PLoS genetics* 9.7, e1003610.
- Schwab, M., Lutum, A. S., and Seufert, W. (1997). "Yeast Hct1 is a regulator of Clb2 cyclin proteolysis". *Cell* 90.4, 683–693.
- Schwickart, M. (2005). "Molecular analysis of novel subunits of the anaphase-promoting complex (APC/C) in yeast". PhD thesis. Technische Universität Dresden Dresden.

- Schwickart, M., Havlis, J., Habermann, B., Bogdanova, A., Camasses, A., Oelschlaegel, T., Shevchenko, A., and Zachariae, W. (2004). "Swm1/Apc13 is an evolutionarily conserved subunit of the anaphase-promoting complex stabilizing the association of Cdc16 and Cdc27". *Molecular and cellular biology* 24.8, 3562–3576.
- Sczaniecka, M., Feoktistova, A., May, K. M., Chen, J.-S., Blyth, J., Gould, K. L., and Hardwick, K. G. (2008). "The spindle checkpoint functions of Mad3 and Mad2 depend on a Mad3 KEN box-mediated interaction with Cdc20-anaphase-promoting complex (APC/C)". *Journal of Biological Chemistry* 283.34, 23039–23047.
- Shah, J. V., Botvinick, E., Bonday, Z., Furnari, F., Berns, M., and Cleveland, D. W. (2004). "Dynamics of centromere and kinetochore proteins: implications for checkpoint signaling and silencing". *Current biology* 14.11, 942–952.
- Shaner, N. C., Campbell, R. E., Steinbach, P. A., Giepmans, B. N., Palmer, A. E., and Tsien, R. Y. (2004). "Improved monomeric red, orange and yellow fluorescent proteins derived from *Discosoma* sp. red fluorescent protein". *Nature biotechnology* 22.12, 1567.
- Shaner, N. C., Lambert, G. G., Chamma, A., Ni, Y., Cranfill, P. J., Baird, M. A., Sell, B. R., Allen, J. R., Day, R. N., Israelsson, M., et al. (2013). "A bright monomeric green fluorescent protein derived from *Branchiostoma lanceolatum*". *Nature methods* 10.5, 407.
- Shenoy, S., Choi, J.-K., Bagrodia, S., Copeland, T. D., Maller, J. L., and Shalloway, D. (1989). "Purified maturation promoting factor phosphorylates pp60c-src at the sites phosphorylated during fibroblast mitosis". *Cell* 57.5, 763–774.
- Shonn, M. A., McCarroll, R., and Murray, A. W. (2000). "Requirement of the spindle checkpoint for proper chromosome segregation in budding yeast meiosis". *Science* 289.5477, 300–303.
- (2002). "Spo13 protects meiotic cohesin at centromeres in meiosis I". *Genes & development* 16.13, 1659–1671.
- Simonetta, M., Manzoni, R., Mosca, R., Mapelli, M., Massimiliano, L., Vink, M., Novak, B., Musacchio, A., and Ciliberto, A. (2009). "The influence of catalysis on mad2 activation dynamics". *PLoS biology* 7.1, e1000010.

- Sironi, L., Mapelli, M., Knapp, S., De Antoni, A., Jeang, K.-T., and Musacchio, A. (2002). "Crystal structure of the tetrameric Mad1–Mad2 core complex: implications of a 'safety belt' binding mechanism for the spindle checkpoint". *The EMBO journal* 21.10, 2496–2506.
- Skoufias, D. A., Andreassen, P. R., Lacroix, F. B., Wilson, L., and Margolis, R. L. (2001). "Mammalian mad2 and bub1/bubR1 recognize distinct spindle-attachment and kinetochore-tension checkpoints". *Proceedings of the National Academy of Sciences* 98.8, 4492–4497.
- Sobel, S. G. (1997). "Mini review: mitosis and the spindle pole body in *Saccharomyces cerevisiae*". *Journal of Experimental Zoology* 277.2, 120–138.
- Sudakin, V., Chan, G. K., and Yen, T. J. (2001). "Checkpoint inhibition of the APC/C in HeLa cells is mediated by a complex of BUBR1, BUB3, CDC20, and MAD2". *The Journal of cell biology* 154.5, 925–936.
- Sullivan, M. and Morgan, D. O. (2007). "A novel destruction sequence targets the meiotic regulator Spo13 for anaphase-promoting complex-dependent degradation in anaphase I". *Journal of Biological Chemistry* 282.27, 19710–19715.
- Sun, S.-C. and Kim, N.-H. (2011). "Spindle assembly checkpoint and its regulators in meiosis". *Human reproduction update* 18.1, 60–72.
- Tan, G. S., Magurno, J., and Cooper, K. F. (2011). "Ama1p-activated anaphase-promoting complex regulates the destruction of Cdc20p during meiosis II". *Molecular biology of the cell* 22.3, 315–326.
- Tanaka, T. U., Rachidi, N., Janke, C., Pereira, G., Galova, M., Schiebel, E., Stark, M. J., and Nasmyth, K. (2002). "Evidence that the Ipl1-Sli15 (Aurora kinase-INCENP) complex promotes chromosome bi-orientation by altering kinetochore-spindle pole connections". *Cell* 108.3, 317–329.
- Tang, Z., Shu, H., Qi, W., Mahmood, N. A., Mumby, M. C., and Yu, H. (2006). "PP2A is required for centromeric localization of Sgo1 and proper chromosome segregation". *Developmental cell* 10.5, 575–585.
- Taylor, S. S., Hussein, D., Wang, Y., Elderkin, S., and Morrow, C. J. (2001). "Kinetochore localisation and phosphorylation of the mitotic checkpoint components Bub1 and BubR1 are differentially regulated by spindle events in human cells". *Journal of cell science* 114.24, 4385–4395.

Tóth, A., Rabitsch, K. P., Gálová, M., Schleiffer, A., Buonomo, S. B., and Nasmyth, K. (2000). "Functional genomics identifies monopolin: a kinetochore protein required for segregation of homologs during meiosis I". *Cell* 103.7, 1155–1168.

Tung, K.-S., Hong, E.-J. E., and Roeder, G. S. (2000). "The pachytene checkpoint prevents accumulation and phosphorylation of the meiosis-specific transcription factor Ndt80". *Proceedings of the National Academy of Sciences* 97.22, 12187–12192.

Tyanova, S., Temu, T., Sinitcyn, P., Carlson, A., Hein, M. Y., Geiger, T., Mann, M., and Cox, J. (2016). "The Perseus computational platform for comprehensive analysis of (prote) omics data". *Nature methods* 13.9, 731.

Uhlmann, F. and Nasmyth, K. (1998). "Cohesion between sister chromatids must be established during DNA replication". *Current Biology* 8.20, 1095–1102.

Uhlmann, F., Lottspeich, F., and Nasmyth, K. (1999). "Sister-chromatid separation at anaphase onset is promoted by cleavage of the cohesin subunit Scc1". *Nature* 400.6739, 37.

Uhlmann, F., Wernic, D., Poupart, M.-A., Koonin, E. V., and Nasmyth, K. (2000). "Cleavage of cohesin by the CD clan protease separin triggers anaphase in yeast". *Cell* 103.3, 375–386.

Vigneron, S., Prieto, S., Bernis, C., Labbé, J.-C., Castro, A., and Lorca, T. (2004). "Kinetochore localization of spindle checkpoint proteins: who controls whom?" *Molecular biology of the cell* 15.10, 4584–4596.

Vink, M., Simonetta, M., Transidico, P., Ferrari, K., Mapelli, M., De Antoni, A., Massimiliano, L., Ciliberto, A., Faretta, M., Salmon, E. D., et al. (2006). "In vitro FRAP identifies the minimal requirements for Mad2 kinetochore dynamics". *Current Biology* 16.8, 755–766.

Visintin, R., Prinz, S., and Amon, A. (1997). "CDC20 and CDH1: a family of substrate-specific activators of APC-dependent proteolysis". *Science* 278.5337, 460–463.

Visintin, R., Craig, K., Hwang, E. S., Prinz, S., Tyers, M., and Amon, A. (1998). "The phosphatase Cdc14 triggers mitotic exit by reversal of Cdk-dependent phosphorylation". *Molecular cell* 2.6, 709–718.

Waal, M. S. van der, Hengeveld, R. C., Horst, A. van der, and Lens, S. M. (2012). "Cell division control by the Chromosomal Passenger Complex". *Experimental cell research* 318.12, 1407–1420.

- Wassmann, K. and Benezra, R. (1998). "Mad2 transiently associates with an APC/p55Cdc complex during mitosis". *Proceedings of the National Academy of Sciences* 95.19, 11193–11198.
- Watanabe, Y. (2005). "Shugoshin: guardian spirit at the centromere". *Current opinion in cell biology* 17.6, 590–595.
- Waters, J. C., Chen, R.-H., Murray, A. W., and Salmon, E. (1998). "Localization of Mad2 to kinetochores depends on microtubule attachment, not tension". *The Journal of cell biology* 141.5, 1181–1191.
- Weiss, E. and Winey, M. (1996). "The *Saccharomyces cerevisiae* spindle pole body duplication gene MPS1 is part of a mitotic checkpoint." *The Journal of cell biology* 132.1, 111–123.
- Welburn, J. P., Vleugel, M., Liu, D., Yates, J. R., Lampson, M. A., Fukagawa, T., and Cheeseman, I. M. (2010). "Aurora B phosphorylates spatially distinct targets to differentially regulate the kinetochore-microtubule interface". *Molecular cell* 38.3, 383–392.
- Ye, Q., Ur, S. N., Su, T. Y., and Corbett, K. D. (2016). "Structure of the *Saccharomyces cerevisiae* Hrr25: Mam1 monopolin subcomplex reveals a novel kinase regulator". *The EMBO journal*, e201694082.
- Yokobayashi, S. and Watanabe, Y. (2005). "The kinetochore protein Moa1 enables cohesion-mediated monopolar attachment at meiosis I". *Cell* 123.5, 803–817.
- Zachariae, W. and Nasmyth, K. (1999). "Whose end is destruction: cell division and the anaphase-promoting complex". *Genes & development* 13.16, 2039–2058.
- Zachariae, W., Schwab, M., Nasmyth, K., and Seufert, W. (1998). "Control of cyclin ubiquitination by CDK-regulated binding of Hct1 to the anaphase promoting complex". *Science* 282.5394, 1721–1724.

Contributions

The immuno-precipitation presented in Figure 32 was realized together with Katarzyna Jonak. The rest of this work was my own.

Acknowledgements

Above all, I would like to thank my supervisor Dr. Wolfgang Zachariae for welcoming me into his lab and for his outstanding scientific training. This whole project wouldn't have started without the impulse of Dr. Orlando Argüello-Miranda that tested out a great deal of hypothesis about the control of Ams1 and Spo13. I am grateful for his constant support, scientific expertise and inspiring scientific discussions. I would like to thank all the Zachariae lab members, past and present, for making the lab such a fun place to be, for their support and for all the stimulating scientific discussion we had. I'm very grateful to our amazing technicians Isabella Mathes, Alben Bergsoy and Anja Wehner, for their technical support. I would like to thank Dr. Nagarjuna Nagaraj, head of the Core Facility of Mass Spectrometry, for his excellent technical advice and scientific support. I would like to thank Prof. Barbara Conradt and Dr. Stephan Gruber for their scientific expertise and support as part of my thesis advisory committee. I thank the members of my thesis advisory committee, Prof. Barbara Conradt, Prof. Peter Becker, Prof. Nicolas Gompel, Prof. Marc Bramkamp, Prof. Christof Osman and Prof. Jochen Wolf for reviewing this work. I am really grateful to my family for their endless support, and for even trying to understand all the subtleties of the meiotic divisions. I would like to address a special thanks to my husband, Pavel Sinitcyn, whose critical scientific mind is a constant source of inspiration. I owe him for helping me getting started with Perseus and MaxQuant software as well as python. He also endlessly motivated me to write this thesis. Last but not least, I would like to thank my friends from the Max Planck Institute for making these years so enjoyable.

Curriculum vitae

Education

- 2008-2011 Bachelor Degree of Science and Technology, Speciality Cell Biology. University Aix-Marseille II, Marseille, France.
- 2010-2011 One year of undergraduate studies in Biology has been completed at the University of East Anglia, Norwich, United Kingdom, as part of the Erasmus Program.
- 2011-2012 Master Degree in Molecular and Cellular Biology, Development and Stem Cells. UPMC, Paris, France.

Workshops and Conferences

- 4-7/09/2015 Cell Cycle EMBO workshop, poster presentation.
- 25-29/04/2016 BioBash Python Workshop
- 25-29/06/2016 Chromosome segregation and Aneuploidy EMBO workshop, poster presentation
- 25-26/11/2016 BioVoxxel, Image processing and analysis Workshop.
- 02/2017 Quantitative Biology Workshop, MITx, edX.
- 8-13/07/2018 MaxQuant Summer School on Computational Mass Spectrometry-Based Proteomics.
- 2018-2019 Introduction to computer science, CS50, Harvard, edX

Publications

1. Argüello-Miranda, O., Zagoriy, I., Mengoli, V., **Rojas, J.**, Jonak, K., Oz, T., Graf, P. and Zachariae, W., 2017. Casein kinase 1 coordinates cohesin cleavage, gametogenesis, and exit from M phase in meiosis II. *Developmental cell*.
2. Jonak, K., Zagoriy, I., Oz, T., Graf, P., **Rojas, J.**, Mengoli, V. and Zachariae, W., 2017. APC/C-Cdc20 mediates deprotection of centromeric cohesin at meiosis II in yeast. *Cell Cycle*.

Award

- 2010 Erasmus Scholarship